

UNIVERSIDADE DE LISBOA INSTITUTO SUPERIOR TÉCNICO

Geostatistical Modelling for Reservoir Characterization at Early Exploration Stages

Ângela Maria Soares Pereira

Supervisor: Doctor Amílcar de Oliveira Soares

Thesis approved in public session to obtain the PhD Degree in Petroleum Engineering

Jury final classification: Pass with Distinction



UNIVERSIDADE DE LISBOA INSTITUTO SUPERIOR TÉCNICO

Geostatistical Modelling for Reservoir Characterization at Early Exploration Stages

Ângela Maria Soares Pereira

Supervisor: Doctor Amílcar de Oliveira Soares

Thesis approved in public session to obtain the PhD Degree in

Petroleum Engineering

Jury final classification: Pass with Distinction

Jury

Chairperson: Doctor Francisco Manuel da Silva Lemos, Instituto Superior Técnico, Universidade de Lisboa

Members of the Committee:

Doctor Amílcar de Oliveira Soares, Instituto Superior Técnico, Universidade de Lisboa Doctor José António de Almeida, Faculdade de Ciências e Tecnologia, Universidade Nova de Lisboa

Doctor Leonardo Azevedo Guerra Raposo Pereira, Instituto Superior Técnico, Universidade de Lisboa

Doctor Davide Alexandre da Costa Gamboa, Universidade de Aveiro

Funding Institutions

Fundação para a Ciência e a Tecnologia Universidade de Lisboa

Resumo

A modelação geoestatística é utilizada na caracterização sísmica de reservatórios, para estimar modelos quantitativos de distribuição espacial das propriedades das rochas subterrâneas. A inversão sísmica é um método utilizado para gerar modelos de alta resolução dessas propriedades e quantificar a incerteza associada. Para isso, são utilizados dados sísmicos, que têm grande cobertura espacial e podem ser relacionados com as propriedades das rochas. São utilizados também, dados de poços que são medições diretas das propriedades das rochas, geralmente escassos ou inexistentes em fases iniciais de exploração. A distribuição espacial das propriedades das rochas está associada à geometria das estruturas geológicas e fácies. Em ambientes geológicos complexos, os padrões de continuidade espacial podem ser bastante heterogéneos, o que torna a sua estimação num desafio. A inversão sísmica geoestatística é um método iterativo, que utiliza a simulação sequencial estocástica, como método de perturbação e atualização dos modelos, juntamente com um optimizador global para guiar a convergência do método, com base na correspondência entre a sísmica observada e sintética. Na presente tese, são propostos métodos de inversão geoestatística que visam melhorar a estimação dos modelos de propriedades das rochas subterrâneas, tornando-os geologicamente mais consistentes e credíveis. Inicialmente, é apresentada a integração de análogos geológicos juntamente com um modelo regionalizado, no procedimento de inversão sísmica geoestatística, para ultrapassar a ausência de dados em fase iniciais de exploração, permitindo a avaliação da incerteza. Para além disso é proposta a integração na inversão sísmica geoestatística de um procedimento baseado nos dados, para estimar e atualizar as anisotropias locais diretamente a partir de dados sísmicos, com vista a caracterizar padrões espaciais não estacionários. Por último, é proposta a integração de atributos sísmicos na função objetivo do procedimento de inversão, para ajudar a condicionar a convergência do método. Os métodos propostos foram aplicados a casos de estudo, tendo resultado em melhorias nos modelos gerados.

Palavras-chave: modelação geoestatística, inversão sísmica, anisotropias locais, padrões de continuidade espacial, fases iniciais de exploração.

Abstract

Geostatistical modeling is used in the seismic reservoir characterization, to build quantitative spatial distribution models of the subsurface rock properties. Seismic inversion is a method used to build high-resolution models of those rock properties and quantify the associated uncertainty. For this is used seismic reflection data, as have large spatial coverage and can be related with subsurface rock properties. Well-log data, which are direct measurements of subsurface rock properties, are also used. However, in early exploration stages, well-log data can be sparse or absent. The spatial distribution of subsurface rock properties is linked to the geometry of geological structures and facies. In complex geological environments, these spatial continuity patterns can be highly heterogeneous, which makes their prediction a challenge. Geostatistical seismic inversion is an iterative process, which uses stochastic sequential simulation algorithm as model perturbation and update technique, together with a global optimizer to guide the convergence of the inversion procedure, based on match between observed seismic reflection data and the synthetic seismic. In this thesis, are proposed geostatistical seismic inversion methods to improve the prediction of subsurface rock property models, making them more geologically consistent and reliable. Initially, is presented the integration of geological analogues and a regionalized model in the geostatistical seismic inversion, to overcome the lack of well-log data at early exploration stages, allowing for uncertainty assessment. Furthermore, is proposed the integration in the geostatistical seismic inversion of a data-driven procedure, to estimate and update local anisotropies directly from seismic data, aiming characterize non-stationary spatial patterns. Finally, is proposed the integration of seismic attributes in the objective function of the geostatistical seismic inversion procedure, to help conditioning the convergence of the seismic inversion method. The proposed methods were applied to case studies, resulting in improvements of the subsurface rock property models.

Keywords: geostatistical modelling, seismic inversion, local anisotropies, spatial continuity patterns, early exploration stages.

Acknowledgements | Agradecimentos

Ao meu orientador, o Professor Amílcar Soares, um profundo agradecimento por todo o seu apoio e motivação, pelo conhecimento que partilhou comigo, pela oportunidade que me deu, pela sua amizade e enorme compreensão.

Ao Professor Leonardo Azevedo, um forte agradecimento pelo seu apoio, por todo o conhecimento que partilhou comigo, pela sua energia e enorme paciência.

À Fundação para a Ciência e a Tecnologia (Bolsa SFRH/BD/136316/2018) e à Universidade de Lisboa (BD2015), um agradecimento pelo apoio financeiro a esta tese.

À Partex Oil & Gas, Repsol e DGEG por fornecerem parte dos dados que permitiram realizar esta tese. À Schlumberger pela doação do software Petrel e à CGG pela doação do software Hampson-Russel.

À Professora Maria João Pereira, ao CERENA e todas as pessoas que nele trabalham, agradeço o acolhimento ao longo deste tempo.

Ao Rúben Nunes, quero agradecer o companheirismo, a boa disposição e o conhecimento partilhado.

À Alzira Ramos e à Catarina Marques, agradeço a sua amizade e boas vibrações partilhadas ao longo deste tempo.

A todos os colegas, um agradecimento pelo companheirismo, pela troca de ideias e conhecimentos, pela ajuda e pelos almoços animados.

Ao Professor Pedro Terrinha, agradeço a sua amizade e a liberdade que me deu.

À Ana Cláudia, um enorme agradecimento pela sua ajuda, valiosos comentário e sugestões e por toda a sua amizade.

Agradeço à minha família e aos meus amigos todo o apoio e motivação.

Um enorme agradecimento ao Bruno, pelo carinho e amizade, pelo apoio, pela motivação e pela paciência de me acompanhar neste percurso.

Um profundo agradecimento aos meus pais e à minha irmã, pelo apoio incondicional, pelo carinho, pela disponibilidade sem fim e por toda a motivação.

Table of Contents

1.		Intro	duct	tion	1
	1.	1.	Sco	pe and Motivation	1
	1.	2.	Obje	ectives	3
	1.	3.	The	sis Structure	3
2.		Geo	stati	stical Modelling for Subsurface Geology	5
	2.	1.	Stoc	chastic Sequential Simulation Methods	7
		2.1.	1.	Direct Sequential Simulation	9
		2.1.	2.	Direct Sequential Co-Simulation with Joint Probability Distributions	12
		2.1.	3.	Spatial Characterization of Non-Stationary Patterns	13
		2.1.4 Fun		Direct Sequential Simulation and Co-simulation with Multi-local Dis	
3.		Geo	stati	stical Seismic Reservoir Modelling	19
	3.	1.	Seis	smic Inversion for Reservoir Characterization	19
	3.	2.	Ove	rview of Seismic Inversion Methods	21
	3.	3.	Geo	statistical Seismic Inversion Methods	26
		3.3.	1.	Trace-by-trace geostatistical seismic inversion	26
		3.3.	2.	Global Stochastic Seismic Inversion	28
4.		Geo	stati	stical seismic inversion for frontier exploration	33
	4.	1.	Intro	oduction	33
	4.	2.	Metl	hodology	35
		4.2.	1.	Geostatistical seismic inversion using geological analogues	36
	4.	3.	Cas	e Study	39
		4.3.	1.	Geological Setting - Stratigraphy	40
		4.3.	2.	Dataset Description	43
	4.	4.	Res	ults	47
	4.	5.	Disc	cussion	51
	4.	6.	Con	clusion	52
		•		g Local Anisotropies with Template Matching during Geostatistical	
111					
	5.			tract	
	5	/	intro	oduction	56

	5.3.	Met	hodology	. 58	
	5.3	.1.	Geostatistical Seismic Inversion		59
	5.3	.2.	Geostatistical Seismic Inversion with Self-Update Local Anisotropies		60
	5.3	.3.	Templates Matching and Local Anisotropy Estimation		62
	5.4.	App	olication Examples	. 63	
	5.4	.1.	Synthetic Case Application		64
	5.4	.2.	Real Case Application		70
	5.5.	Disc	cussion	. 75	
	5.6.	Cor	nclusion	. 76	
6.	Sei	smic	inversion integrating seismic attributes to enhance geological models		79
	6.1.	Intro	oduction	. 79	
	6.2.	Met	hodology	. 80	
	6.3.	App	lication Examples	. 82	
	6.3	.1.	Synthetic Case Application		82
	6.3	.2.	Real Case Application		93
	6.4.	Disc	cussion	. 95	
	6.5.	Cor	nclusion	. 96	
7.	Fin	al rer	marks		97
8.	Re	feren	ces		99

List of Figures

Figure 1 – Representation of the relation between the variogram γh and the covariance Ch
(adapted from Azevedo and Soares 2017)6
Figure 2 – Sampling process in DSS. The global cdf of Fzz is sampled by intervals defined by
the local mean and variance of zxu : The value $y(xu)*$ corresponds to the local
estimate $zxu*$. The $Gyxu*$, $\sigma sk2xu$ define the interval of Fzz from where the simulated
value $zxu*$ is drawn (adapted from Soares 2001)10
Figure 3 - Representation of a geological non-stacionary pattern from a meandriform
channel. The local anisotropy variation is represented by the ellipses with different
orientations (Θ) and axis ratio ($a b$). The spatial distribution of the rock properties will be
affected by the curvilinear shape of the channel13
Figure 4 - Representation of the search radius for standard DSS and DSS-LA (adapted from
Horta et al. 2010)15
Figure 5 - Relation between the forward modeling and seismic inversion (adapted from
Barclay et al. 2008)20
Figure 6 - Schematic representation of reflection coefficient and its relation with acoustic
impedance and lithological interfaces (adapted from Simm and Bacon 2014)21
Figure 7 - Schematic representation of geostatistical modelling workflow to derive
petrophysical rock properties from acoustic impedance (elastic model) resulting from seismic
inversion (adapted from Azevedo and Soares 2017)21
Figure 8 – Schematic representation with the differences in bandwidth extension of inverted
models from deterministic and stochastic inversion (adapted from Azevedo and Soares
2017)23
Figure 9 - Schematic representation of the trace-by-trace geostatistical seismic inversion
workflow (Bortoli et al. 1992, Haas and Dubrule 1994). In the first step the red dots represent
the well-log data and the blue dot the first location of the random path (dashed line) where a
set of Ns acoustic impedance traces will be simulated (adapted from Azevedo and Soares
2017)27
Figure 10 - General workflow of iterative global stochastic seismic inversion methods
(adapted from Azevedo and Soares 2017)29
Figure 11 - Global stochastic seismic inversion (GSI) workflow (adapted from Azevedo and
Soares 2017)30
Figure 12 – Calculus of the mismatch between synthetic and real seismic data in a trace-by-
trace basis. The objective function can be defined as the Pearson's correlation coefficient,
but other equations may be applied (adapted from Caetano 2009)31

Figure 13 – Creation of the auxiliary volumes creation (Best CC and Best AI), from the traces
with highest correlation coefficient and corresponding Ip traces (adapted from Caetano
2009)31
Figure 14 – General workflow of geostatistical seismic inversion for frontier exploration using
geological analogues37
Figure 15 - Map with the location of the Algarve basin in the southwestern Iberian margin
(adapted from Matias et al. 2011)40
Figure 16 – Simplified Tectostratigraphy of the Algarve basin (adapted from Ramos et al. 2016)41
Figure 17 - Lithostratigraphy of the offshore wells from the Algarve Basin by Roque (2007)
(adapted from Roque 2007)42
Figure 18 – Map view with the location of the available data. The grid represents the seismic
data and the area of study is highlight in gray. The location of the wells used as analogs (W1,
W2, W3), is outside the seismic grid area43
Figure 19 - Ip well-logs of the geological analogues wells, from where the initial a priori
probability distributions function was extract, to be used as conditioning data in the seismic
inversion procedure43
Figure 20 -Vertical section with the seismic interpretation of the three main seismo-
stratigraphic units used to define the regional geological model. In region 2 it is possible to
visualize the turbidite sequences (M – Miocene; P – Pliocene)44
Figure 21 - [Left] 3D volume and [Right] Vertical section of the regional model with the three
main seismic units: Region 1 – overburden region; Region 2 – reservoir region; Region 3 –
underburden region44
Figure 22 - Seismic reflection data for the area of interest: (a) seismic volume, (b) vertical
section and (c) time slice from region 2 showing the turbidite channels45
Figure 23 - Initial probability distributions functions of acoustic impedance for each region,
obtained from well-logs analogues46
Figure 24 - Variogram models for each geological region: [Top] horizontal main direction,
[Middle] horizontal minor direction, [Bottom] vertical direction46
Figure 25 - Evolution of the correlation coefficient over the iterative process of seismic
inversion. The convergence of the method occurs in iteration 647
Figure 26 - Crossplot between the real seismic and the synthetic seismic at the end of the
inversion procedure. The correlation coefficient for the: [Top left] entire volume is 0.85; [Top
right] for Region 1 (overburden) is 0.80; [Bottom left] for Region 2 (reservoir) is 0.89; [Bottom
right] Region 3 (underburden) is 0.7048

Figure 27 - Synthetic seismic computed from the acoustic impedance best-fit model in the
last iteration: (a) synthetic seismic volume, (b) vertical section and (c) time slice from region 2
showing the turbidite channels49
Figure 28 - [Left] Vertical section of the residuals between real seismic data and the
synthetic seismic and; [Right] corresponding distribution function49
Figure 29 –Best-fit inverse model of acoustic impedance from 6th iteration: (a) Best Ip
volume, (b) vertical section and (c) time slice from region 2 showing the turbidite channels.
The lower Ip values (purple) are associated to turbidite channels. (d) Probability distribution
function (pdf) of the Best-fit Ip model, reproducing the initial Ip pdf50
Figure 30 - Vertica section of variance computed from the 32 realizations of Ip models from
the last iteration. Higher variance areas are associated with a higher uncertainty in the
estimate Ip values50
Figure 31 - Schematic representation of the iterative geostatistical seismic inversion with
self-update local anisotropies (GSI-LA-Self-Update)59
Figure 32 – Ensemble of pre-defined elliptical templates Tk , mimicking different local
variogram models with different parameters (direction, main (La) and minor ratios (Lb)). The
templates set corresponds to all possible combinations between these three parameters62
Figure 33 - Example of templates matching the true image and creation of the auxiliary
anisotropy model expressed by the local variogram parameters obtained from the selected
template63
Figure $34 - a$ True fullstack vertical seismic section; b True acoustic impedance model. The
vertical black lines represent the location of the wells used as conditioning data in the
geostatistical seismic inversion64
Figure 35 – Evolution of the local spatial continuity models estimated with template matching
at the end of each iteration and used in GSI-LA-Self-Update for the next iteration: ${f a}$ - ${f e}$ 1st
iteration to 5 th iteration, respectively65
Figure 36 – Local spatial continuity model used in GSI-LA66
Figure 37 – Comparison of global similarity (S) evolution for the three geostatistical inversion
methods considered66
Figure 38 - Synthetic fullstack seismic vertical section calculated from the Ip mean model
with: a GSI; b GSI-LA; c GSI-LA-Self-Update67
Figure 39 - Vertical sections of Ip mean models from last iteration for the three tested
methods: a GSI; b GSI-LA; c GSI-LA-Self-Update. The lower Ip values correspond to
meandriform sand-rich channels, and the high Ip values to mud-rich sedimentary sequences.
Black arrows point to low Ip values, related to sand channel facies, highlighting the
improvement introduced with the proposed method67

Figure 40 - Vertical sections of facies true model and most likely facies model from last
iteration for the three tested methods: ${\bf a}$ Ip true model; ${\bf b}$ GSI; ${\bf c}$ GSI-LA; ${\bf d}$ GSI-LA-Self-
Update. Sand (Ip \leq 8500, in yellow) and mud (Ip $>$ 8500, in blue). Red arrows point to low Ip
values related to sand channel facies, highlighting the improvement introduced with the
proposed method
Figure 41 - Distance in MDS space between the true facies model and the retrieved facies
models from last iteration. The models closer to the true facies model are the ones from the
proposed method69
Figure $42 - a$ Wavelet; b Histogram of Ip from well-log data and from Ip mean model from 6^{th}
iteration71
Figure 43 – Evolution of Global Similarity during seismic inversion procedures71
Figure $44 - \mathbf{a}$ Vertical section of the true seismic data with well position (black dashed line); \mathbf{b}
Synthetics seismic calculated from Ip mean models of the 6th iteration GSI-LA-Self-Update; c
GSI; d GSI-LA. Black arrows point to areas where it is possible to verify the similarity
between the real seismic and the synthetics from all tested methods72
Figure 45 – Vertical sections of Ip mean model computed from the 6 th iteration from: a GSI-
LA-Self-Update; b GSI; c GSI-LA73
Figure 46 - Vertical section extracted from the: a residuals between synthetic and real
seismic; b best-fit lp; c best-fit similarity models from 6 th iteration, with the proposed method.
Red arrows point to low Ip values related to turbidite channels or faults74
Figure 47 – Vertical section of local spatial patterns - Dip azimuth (°) for the 2 nd iteration; b
Vertical section of local spatial patterns - Dip azimuth (°) for the 5th iteration, with the
proposed method
Figure 48 - Schematic representation of the iterative geostatistical seismic inversion
integrating seismic attributes into the objective function81
Figure 49 - (left) Vertical section of the reference seismic reflection data; (center) Vertical
section of the reference acoustic impedance model; (right) Vertical section of the reference
facies model. The vertical black lines represent the location of the wells used as conditioning
data in the geostatistical seismic inversion83
Figure 50 – [top] Evolution of global similarity (S) over iterations for GSI with attributes and
classic GSI. [bottom] Detail of the evolution of global similarity (S) during 6th iteration, for
different tests of GSI with attributes compared to classic GSI84
Figure 51 – Vertical section of synthetic seismic computed from the Ip mean model of 6th
iteration from classic GSI and GSI with attributes85
Figure 52 – Vertical sections of seismic attributes integrated into the objective function and
computed from reference seismic and synthetic seismic in the last iteration of the seismic
inversion procedure

Figure 53 – Vertical section of Ip mean model of 6th iteration from classic GSI and GSI with
attributes87
Figure 54 - Vertical sections of facies reference model and most likely facies model of 6th
iteration from classic GSI and GSI with attributes. Sand (Ip \leq 8500, in yellow) and mud (Ip $>$
8500, in blue)89
Figure 55 - Projection in the MDS space (2D top view) of the Ip and facies models, from last
iteration, for the different seismic attributes and comparison with the reference models. It is
possible to observe the distance to the reference models and the dispersion within the
ensembles. The reference models are represented by a black dot90
Figure 56 - Distance in MDS space for Ip and facies models, between the true model and
the realization models from last iteration, for GSI with attributes and classic GSI90
Figure 57 – Evolution of global similarity (S) over iterations in GSI-LA classic and GSI-LA
with attributes. The global similarity (S) for: (blue) GSI-LA classic = 0.89; (orange) GSI-LA
variance = 0.91; (yellow) GSI-LA RMS with 1 st derivative = 0.9291
Figure 58 - Distance in MDS space for Ip and facies, between the true model and the
retrieved models from last iteration for GSI-LA classic and GSI-LA with attributes92
Figure 59 – Vertical section of Ip mean model of 6th iteration from GSI-LA classic and GSI-LA
attributes92
Figure 60 – Vertical section of synthetic seismic computed from the Ip mean model of 6^{th}
iteration from GSI-LA classic and GSI-LA attributes93
Figure 61 – Evolution of Global Similarity during the iterative seismic inversion94
Figure 62 - (From left to right) Vertical section of the observed seismic reflection data,
synthetic seismic, residuals and Ip mean model from the last iteration (6th iteration)94
Figure 63 – [left] Vertical section of first derivative seismic attribute computed from observed
seismic and synthetic seismic. [right] Vertical section of variance seismic attribute computed
from observed seismic and synthetic seismic from last iteration (6 th iteration)95

List of Tables

Table 1 – Confusion matrix with the percentage of true positive and true negative class	sified
pixel values (correctly classified) and the percentage of false positive and false nega	ative
classified pixel values (misclassified) for the three tested methods: (a) GSI, (b) GSI-LA	۱, (c)
GSI-LA-Self-Update	70
Table 2 – Global Similarity for different tests with GSI	84

1. Introduction

1.1. Scope and Motivation

The demand for natural georesources increased in the last decades, making this a key issue for modern societies. Geoscientists have worked towards finding solutions to address this challenge. In subsurface data acquisition and in subsurface modelling, several advances have been made, aiming to better characterize the subsurface geology. The prediction of subsurface rocks properties models are important steps for the exploration of georesources, particularly for hydrocarbons exploration. Nevertheless, new hydrocarbon discoveries tend to be associated with complex geological environments, often located in underexplored areas, such as deep marine environments, where given the absence or scarcity of data, geological conceptual models tend to be simplistic and underestimate the heterogeneities of the subsurface geology (Dubrule 2003), increasing risks and uncertainty of the projects (Doyen 2007; Caers 2011). For hydrocarbon reservoir characterization, subsurface numerical models are essential tools for decision making and risk assessment. They allow the quantitative prediction of subsurface geology, by estimating petro-elastic rock properties (e.g. porosity, density, acoustic impedance or facies) and their spatial distribution. In complex geological environments, the spatial distribution of subsurface rock properties may be highly heterogeneous, as a result of local lithofacies variations or related to the geometry of geological structures, as curvilinear or deltaic channels, faults or folds.

At early exploration stages, direct measurements of the subsurface, such well-log data are normally scarce due to the high costs associated to their acquisition, implying complex and risky logistic procedures. During exploration, hydrocarbon reservoir characterization depends mainly on seismic reflection data, an indirect measurement of the subsurface obtained from geophysical studies, who has a large spatial coverage. This leads to inaccurate quantification of rock properties. A better characterization of potential hydrocarbon reservoirs, at initial exploration stages is key to establish subsurface numerical geological models, putting a challenge on how to quantify rock properties in absence of direct measures, such as well-log data. Here, geological analogues supported by background knowledge about the area, can contribute to predict subsurface geological models (Deutsch 2002; Demyanov and Arnold 2018).

Seismic inversion methods are modelling techniques currently used to derive subsurface rock properties into numerical models, allowing in some approaches, the integration in the same framework of different data type, with different coverage and resolution. Depending on available data and purpose, different seismic inversion methods can be used, considering

their assumptions and limitations. There are two main approaches, a Deterministic and a Probabilistic or Stochastic (Francis 2006; Bosch et al. 2010; Filippova et al. 2011). The Deterministic approach produces smoothed representations of the subsurface geology, dependent on an initial guess model built using available well-log data and geological background knowledge. This can be unsuitable to describe a complex geological environment (Doyen 2007) making impossible to quantify uncertainty, given the uniqueness of the solution. Uncertainty assessment is a crucial, particularly at early exploration stages, for decision making and to reduce risks (Caers 2011).

Contrary to Deterministic, Probabilistic or Stochastic approaches allow estimating the uncertainty, from multiple equally likely realizations of the model solution. Stochastic methods are more complex to implement, but produce high resolution subsurface numerical models, due to the integration of seismic data with well-log data in the same framework (Azevedo and Soares 2017). Although these methods are conditioned by a spatial correlation pattern (e.g. variogram model), when applied to complex geological scenarios, they cannot ensure accurate predictions about the subsurface, that account for local heterogeneities of rock properties. Hence, the integration of local spatial correlation patterns in these situations can be a solution for subsurface models improvement. The estimation of these local spatial correlation patterns can be achieved by computing local variogram models, what are computational demanding, or through proxies obtained from seismic attributes analysis or image processing tools, for instance.

Most of the seismic inversion methods use a model-based approach successfully, but with the caveat of being less flexible or adaptable to data. This can lead to the propagation of errors, resulting in less reliable models. Stochastic seismic inversion methods are normally constrained by fixed and pre-defined global or local spatial correlational patterns, which remained unchanged through the entire inversion procedure. Recently, data-driven approaches allowing self-learn procedures have been emerged for reservoir characterization, aiming to improve subsurface geological models (Demyanov and Arnold 2018).

In this thesis are proposed methods based on the global geostatistical seismic inversion for hydrocarbon reservoir characterization, which aim to improve the reproduction of the local spatial continuity patterns of subsurface rock properties models, resulting from the inversion procedure. Particularly, the proposed methods aim to be applied in complex geological environments, characterized by non-stationary local spatial continuity patterns and at early exploration stages, to overcome the scarcity or absence of well log data.

1.2. Objectives

The main objective of this thesis is the development of methodologies for the integration of subsurface geological information into geostatistical seismic inversion, for seismic reservoir characterization in complex geological environments and at early exploration stages. This objective can be divided in the following steps:

- Develop and implement a procedure to integrate information about the subsurface geology into the geostatistical seismic inversion, to overcome the scarcity or absence of well-log data in frontier areas and early exploration stages;
- Develop and implement a data-driven approach to infer and update local anisotropies from seismic reflection data, aiming characterize the local spatial continuity patterns of subsurface geology, for integration into geostatistical seismic inversion;
- Develop and implement the integration of seismic attributes in geostatistical seismic inversion, to improve the reproduction of the stratigraphic and structural geological patterns of the subsurface geological models.

1.3. Thesis Structure

This thesis is organized in seven chapters as follows:

Chapter 1 introduces the problem addressed and presents the motivation and objectives of the thesis, ending with an overview of the thesis structure.

Chapter 2 introduces the importance of subsurface geological modelling and presents an overview of the main geostatistical modelling techniques, related to the work developed in this thesis, detailing the stochastic sequential simulation methods used.

Chapter 3 addresses the topic of seismic reservoir characterization and continues the overview of geostatistical modelling techniques by presenting the main seismic inversion methods. The geostatistical methods used in this thesis is described in this chapter.

In Chapter 4 is presented a geostatistical seismic inversion procedure that uses geological analogues to overcome the lack of well-log data, aiming to improve the prediction of the subsurface geological models and assess uncertainty in unexplored areas and early exploration stages.

A manuscript describing the work presented in this chapter, that I am first author of, was published in the peer reviewed *Interpretation* journal and presented at a scientific conference as oral presentation. The manuscript was adapted to be presented in this thesis.

In Chapter 5 describes a geostatistical seismic inversion procedure that integrates local anisotropies directly inferred from seismic data and self-updated during the iterative process. The proposed geostatistical seismic inversion procedure aims to improve the geological subsurface models in complex geological scenarios, dealing with non-stationary patterns.

This chapter corresponds to a peer reviewed manuscript in *Mathematical Geosciences* journal that I am the first author. This work was also presented in a scientific conference as oral presentation. This chapter is presented as it was published in Open Access, licensed under a <u>Creative Commons Attribution 4.0 International License</u> and no changes were made.

Chapter 6 presents the work developed in the integration of seismic attributes into the objective function of geostatistical seismic inversion procedure, to improve the stratigraphic and structural patterns of the subsurface models. The initial stage of this work was presented in a scientific conference as a poster presentation and extended abstract.

In Chapter 7 the thesis is concluded with the discussion of the main contributions and possible future work.

2. Geostatistical Modelling for Subsurface Geology

In Earth sciences, geostatistical modelling techniques are often used to describe natural phenomena. Geostatistics provides a range of statistical tools to estimate the spatial or temporal distribution of a given property at unknown locations, from sparse sample data (e.g. well-log data) (Goovaerts 1997). In subsurface geological modelling, geostatistical tools are used to build numerical models to describe the spatial distribution of rock properties and facies, making them essential tools in hydrocarbon reservoir characterization (Dubrule 2003, Doyen 2007).

Within geostatistical modelling techniques there are two main approaches, a deterministic and a probabilistic, from which kriging methods and sequential simulation methods stand out, both aiming the characterization and quantification of continuous (e.g. porosity) or discrete properties (e.g. facies) (Goovaerts 1997). Another important group of modelling techniques are seismic inversion methods that have gained increasing relevance in the last years in subsurface geological modelling (Dubrule 2003). As the present thesis is based on seismic inversion procedures, these methods will be discussed in detail on Chapter 3.

To infer the spatial distribution of a property of interest, from a sparsely sampled data (e.g. well-log data), geostatistical methods can integrate a spatial continuity pattern to constrain the inference of the property, improving the reliability of the estimated models (Goovaerts 1997). Bi-point statistics methods (e.g. Kriging, sequential simulation) use variogram models $\gamma(h)$ (Equation 1) to describe the spatial continuity. However, other geostatistical methods use different techniques, for instance object-based modelling uses pre-defined objects and Multi-point Statistics (MPS) uses training images (Azevedo and Soares 2017).

The variogram (or semi-variogram) (Equation 1) measures the degree of spatial dispersion (spatial variability) between pairs of points N(h) (i.e. experimental data (e.g. well-log data)) and can be explained as the expected squared difference between two data values Z(x) and Z(x+h) separated by a distance vector h, where the N(h) is the number of pairs of points for each distance value h (Deutsch and Journel 1992).

Equation 1
$$\gamma(h) = \frac{1}{2N(h)} \sum_{\alpha=1}^{N(h)} [Z(x_{\alpha}) - Z(x_{\alpha} + h)]^2$$

Another possible way to measure spatial continuity is by computing the covariance as expressed by Equation 2, where $m(x_{\alpha})$ and $m(x_{\alpha} + h)$ refers to the points average at

location x_{α} and $x_{\alpha} + h$ respectively. The covariance measures the spatial correlation (spatial similarity) between sample values.

Equation 2
$$C(h) = \frac{1}{N(h)} \sum_{\alpha=1}^{N(h)} [Z(x_{\alpha}).Z(x_{\alpha}+h)] - m(x_{\alpha}).m(x_{\alpha}+h),$$

Both measures can be related through Equation 3, this relation is showed in Figure 1, where h is the distance vector.

Equation 3
$$\gamma(h) = C(0) - C(h)$$

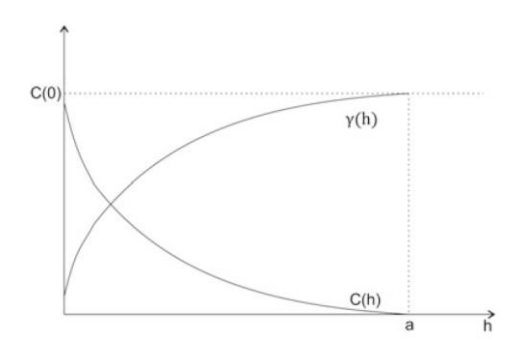


Figure 1 – Representation of the relation between the variogram $\gamma(h)$ and the covariance C(h) (adapted from Azevedo and Soares 2017).

Kriging is an estimation procedure introduced by Georges Matheron in 1960. Initially applied to mining industry its use ended up spreading across other earth sciences domains (Chilès and Desassis 2018). Kriging is a linear and exact interpolator used to estimate the spatial distribution of a variable by linear interpolating the values of the experimental data (e.g. well-log data), which are reproduced in the estimated model. The procedure is constrained by a spatial continuity pattern represented by a variogram $\gamma(h)$ (Equation 1). The interpolated model is considered a smooth representation of the property of interest; the method tends to reproduce the average value in areas far from the experimental data (Deutsch and Journel 1992, Goovaerts 1997). Although it may be valid, on its own, this smoothed representation has limited power to describe the subsurface geology, particularly in complex geological scenarios, leading to unreliable subsurface models. Furthermore, as the interpolated model is unique solution, it is not possible to quantify the uncertainty associated to the estimated model (Caers 2011, Azevedo and Soares 2017).

Stochastic sequential simulation methods are other group of geostatistical methods, which have advantages over kriging (Deutsch and Journel 1992). They are probabilistic methods and are widely used in subsurface geological modelling for reservoir characterization, having

for instance a central role within seismic inversion procedures (Drubule 2003). Stochastic methods have multiple equally likely solutions, allowing the uncertainty assessment of the simulated models (Caers 2011). Within Stochastic simulation methods some of the most popular are Sequential Gaussian Simulation (e.g. SGS; Deutsch & Journel 1992), Direct Sequential Simulation (e.g. DSS; Soares 2001) and Conditional Simulation using Multi-point Statistics (e.g. Caers 2001, Strebelle 2002, Strebelle and Zhang 2005), regardless of have different approaches, all these methods follow a sequential simulation procedure and are based on the application of Bayes' rule in a successive sequence of steps (Azevedo and Soares 2017).

As stochastic sequential simulation is used in the seismic inversion methods proposed in this thesis, these methods will be discussed in detail in the next section.

2.1. Stochastic Sequential Simulation Methods

Conventional stochastic sequential simulation methods have the underlying assumptions of the stationarity of the natural phenomenon to be modelled, which implies the stationarity (i.e. the invariance) of the mean and variance of the probability distribution function (pdf), as well as the stationarity of the variogram model $\gamma(h)$. This is translated in the adoption of a global probability distribution function (pdf) (i.e. global histogram) and a global spatial continuity pattern (i.e. global variogram model) and as inferred from the available experimental data, for the entire study area. Furthermore, these methods follow the classical sequential simulation approach, which can be briefly summarized by (Deutsch and Journel 1992, Goovaerts 1997):

- 1. Randomly select inside the simulation grid a node x_u to be simulated;
- 2. Estimate the local cumulative distribution function (cdf), considering the experimental data $z(x_{\alpha})$ and previously simulated values $z^{s}(x_{i})$ in the neighbourhood of x_{u} ;
- 3. Draw a simulated value $z^s(x_u)$ from the local cdf, using Monte Carlo simulation (i.e. Monte Carlo inverse transform algorithm);
- 4. Repeat the steps until the all the nodes in the grid have been simulated.

Any stochastic sequential simulation procedure implies conditions to the retrieved simulated models, such as (Deutsch and Journel 1992):

- 1. Reproduce the experimental data values at its own location;
- 2. Reproduce the first and second order statistical moments (i.e. mean and variance) as estimated from the experimental data;

- 3. Reproduce the probability distribution function and joint distributions (i.e. histograms and bi-histograms) as inferred from the experimental data;
- 4. Reproduce the spatial covariance represented by the variogram model for bi-point statistics methods and as inferred from the experimental data. In Multiple-point statistics (MPS) methods the spatial continuity represented by the training image must be reproduced.

Within Stochastic Sequential Simulation methods, Sequential Gaussian Simulation (SGS; Deutsch and Journel 1992) along with Sequential Indicator Simulation (SIS; Deutsch and Journel 1992) are probably the best knowns stochastic simulation methods, used for continuous (e.g. porosity) and categorical variables (e.g. facies) respectively. Regardless of its widespread use, SGS and SIS have some limitations as they require a prior transformation of the original variable, which for SGS implies the transformation into the Gaussian domain (Goovaerts 1997, Soares 2001). When the variable to infer is represented by a skewed, a multi-modal or a joint distribution, the SGS may struggle to reproduce the original variogram model, due to prior Gaussian transformation (Soares 2001, Azevedo and Soares 2017).

To overcome these limitations, in 1994 Journel introduced the principle of direct sequential simulation, seeking to infer directly from the original data, the spatial distribution of a continuous variable without needing prior transformation. Journel (1994) showed that, if the simulated values were drawn from the local conditional distribution function centered at the simple kriging estimates (Equation 4), with conditional variance equal to simple kriging variance (Equation 5), the original spatial co-variances was reproduced. However, it was realized that while this allows the reproduction of the variogram model of the original variable, it does not guarantee in all situations the reproduction of the histogram of the original variable, since the local mean and variance are not sufficient to fully describe the local cumulative distribution function (Soares 2001). Based on the principle stated by Journel (1994), a new proposal for direct sequential simulation (DSS) algorithm was presented by Soares (2001), which solved these variogram model and histogram reproduction problems, essential condition in any simulation algorithm (Soares 2001, Azevedo and Soares 2017). The great advantage of DSS algorithm compared to SGS is the ability of directly simulate the spatial distribution of a variable at unknown locations, with no need of prior transformation and at the same time ensuring the reproduction of the marginal and joint distributions of the original variables (Soares 2001, Azevedo and Soares 2017).

In next section Direct Sequential Simulation (DSS; Soares 2001) and some DSS based algorithms are presented in detail, since these methods are the stochastic simulation procedures used to explore the model parameters and to infer the spatial distribution of the subsurface rock properties, in the geostatistical inverse methods proposed herein.

2.1.1. Direct Sequential Simulation

Direct Sequential Simulation algorithm (DSS; Soares 2001) is a stochastic sequential simulation procedure used to predict the spatial distribution of a continuous variable z(x) represented by a global cumulative distribution function (cdf) $F_z(z) = prob\{z(x) < z\}$. As other stochastic sequential simulation methods (e.g. SGS; Deutsch and Journel 1992), Direct Sequential Simulation (Soares 2001; Nunes et al. 2010) follows the classical sequential simulation approach and is based on the Bayes' rule in successive sequence of steps (Azevedo and Soares 2017).

In DSS algorithm the spatial continuity of the property of interest is represented by a single and global variogram model $\gamma(h)$, which is assumed to be stationary for the entire study area and is inferred from the experimental data, like the global probability distribution function, represented by a single histogram. Along with the global cdf $F_z(z)$, the variogram model is reproduced in the simulated models (Soares et al. 2001).

In SGS the definition of the local cdf is obtained with the simple Kriging estimate $z(x_u)^*$ (Equation 4) and with simple Kriging estimation variance $\sigma_{sk}^2(x_u)$ (Equation 5), implying the Gaussian transformation (Equation 6) of the original variable to define the local cdf, from which the simulated value is obtained by inverse transform φ^{-1} (Soares 2001, Azevedo and Soares 2017).

Equation 4
$$z_{SK}(x_u)^* = m + \sum_{\alpha=1}^n \lambda_{\alpha}[z(x_{\alpha} - m)]$$

Equation 5
$$\sigma_{sk}^2(x_u) = C_0 - \sum_{\alpha=1}^n \lambda_\alpha C(x_{\alpha}, x_u)$$

The difference between DSS and SGS lies here, since the local cdf in DSS is defined by sampling directly the original global cdf $F_z(z)$, using the local mean and variance of the conditioning data (Figure 2). In DSS the Gaussian transformation (Equation 6) is only used to sample the intervals $F_z'(z)$ of the original global cdf $F_z(z)$ as illustrated in Figure 2. Soares (2007) proposed that the auxiliary interval $F_z'(z)$ to be sampled can be defined by the local

Gaussian cdf $G(y(x_u)^*, \sigma_{sk}^2(x_u))$, obtained by the multi-Gaussian transform (Equation 6, Equation 7) of the $F_z(z)$ interval, centered at simple Kriging estimate $z(x_u)^*$ with the amplitude range equivalent to the simple Kriging variance $\sigma_{sk}^2(x_u)$. Then Monte Carlo simulation is used to draw a value of y^s (Equation 8) from the local interval of G(y). Afterwards the simulated value $z^s(x_u)$ (Equation 9) is obtained by the inverse transform φ^{-1} (Figure 2) (Soares 2001). All DSS based algorithms follow this approach to obtain the simulated values (Azevedo and Soares 2017).

Equation 6
$$y(x_u) = \varphi(z(x)), with \ G(y(x)) = F_z(z(x))$$
 Equation 7
$$G(y(x_u)^*, \sigma_{sk}^2(x_u)), \ where \ y(x_u)^* = \varphi(z(x_u)^*)$$
 Equation 8
$$G(y(x_u)^*, \sigma_{sk}^2(x_u)): \ y^s = G^{-1}(y(x_u)^*, \sigma_{sk}^2(x_u), p)$$
 Equation 9
$$z^s(x_u) = \varphi^{-1}(y^s)$$

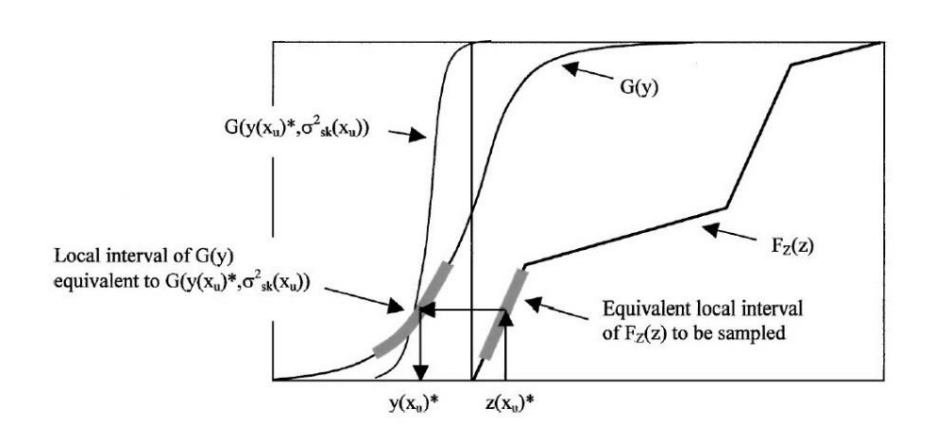


Figure 2 – Sampling process in DSS. The global cdf of $F_z(z)$ is sampled by intervals defined by the local mean and variance of $z(x_u)$: The value $y(x_u)^*$ corresponds to the local estimate $z(x_u)^*$. The $G(y(x_u)^*, \sigma_{sk}^2(x_u))$ define the interval of $F_z(z)$ from where the simulated value $z(x_u)^*$ is drawn (adapted from Soares 2001).

The DSS algorithm can be detailed by the following steps (Soares 2001):

- 1. Using a random seed generate a random path through all the nodes x_u , u = 1, ..., N of the simulation grid, where x_u is the node to be simulated and N is the total number of nodes:
- 2. Following the random path estimate the local mean and variance with simple kriging estimate $z(x_u)^*$ and corresponding simple kriging variance $\sigma_{sk}^2(x_u)$, conditioned to

- the original experimental data $z(x_i)$ and previously simulated values $z^s(x_i)$ and considering the neighborhood of the node x_u to be simulated;
- 3. Define the auxiliary interval F'(z) of the global cdf F(z) to be sampled based on the equivalent Gausssian transform (Equation 6, Equation 7). The interval F'(z) is centered at the local mean and with the range of the local variance estimated in the previous step and as previously explained;
- 4. Draw a value of $z^s(x_n)$ from the cdf F(z), by:
 - a. Randomly generate a value *p* from the uniform distribution between [0, 1];
 - b. Generate a value y^s from $G(y(x_u)^*, \sigma_{sk}^2(x_u))$ (Equation 8);
 - c. Return the simulated value $z^s(x_u)$ from the inverse transform of the Gaussian cdf (Equation 9);
- 5. Add the simulated value $z^s(x_u)$ to the conditioning data;
- 6. Loop until all the *N* nodes of the simulation grid have been simulated.

Changing the seed used to define the initial random path, allows the realization of others equally likely simulated models, from which the associated uncertainty can be assessed, for instance by computing the variance between the different simulated models.

The great advantage of DSS algorithm compared to SGS or SIS is the ability to directly simulate the spatial distribution of a continuous variable, by sampling directly the distribution functions from the experimental data, without assuming the Gaussian hypothesis of the original variable and ensuring the reproduction of the marginal and joint distributions, the variogram model and the experimental data values at its own locations (Soares 2001, Azevedo and Soares 2017).

DSS algorithm have been adapted to include joint probability distributions functions (co-DSS; Horta and Soares 2010) allowing the co-simulation of two dependent variables, where a primary variable is predicted condictioned to a secondary variable (e.g. permeability co-simulated with porosity). Furthermore, Nunes et al. (2017) proposed a DSS based algorithm wich includes multi-local probability distribution functions, by dividing the simulation grid into sub-regions, allowing the simulation and co-simulation procedure be conditioned by probability distributions functions and variogram models from each sub-region. Another DSS based algorithm includes non-stationary spatial patterns, allowing to better describe heterogeneous geological scenarios, like curvilinear channels, by conditioning the simulation procedure to local spatial patterns (local anisotropy) represented by local variogram models (DSS-LA; Horta et al. 2010).

2.1.2. Direct Sequential Co-Simulation with Joint Probability Distributions

In reservoir characterization it is often necessary to jointly predict the spatial distribution of two or more dependent variables, for instance, predict permeability conditioned to porosity (Soares 2001, Azevedo and Soares 2017). Considering this, DSS algorithm has been adapted to allow co-simulation with joint probability distributions functions (co-DSS; Horta and Soares 2010). Given a conditional joint distribution $F(Z_2(x)|Z_1(x))$ and following the sequential simulation procedure, a primary variable $z_1(x_u)$ is simulated first with DSS algorithm, then the secondary variable $z_2(x_u)$ is co-simulation conditioned to the previous one. The primary variable $z_1(x_u)$ should be the most relevant or with the most continuous spatial pattern (Soares 2001, Horta and Soares 2010).

Co-simulation with joint probability distributions can be summarized by the following steps (co-DSS; Horta and Soares 2010):

- 1. Define the primary variable $Z_1(x)$ to be simulated first and define the secondary variable $Z_2(x)$;
- 2. Estimate the global bi-distribution $F(Z_2(x), Z_1(x))$ of the depent variables from the experimental data;
- 3. Simulate the primary variable $Z_1(x)$ with DSS algorithm for the entire simulation grid;
- 4. Generate a random path covering all nodes x_u , $u = 1, ..., N_s$ of the simulation grid;
- 5. Considering the neighborhood of the secondary variable $Z_2(x_u)$, estimate the local mean and variance with co-located simple co-kriging estimate $[Z_2(x_u)^*]_{CSK}$ and corresponding variance $\sigma^2_{CSK}(x_u)$, conditioned to the original experimental data $Z_2(x_\alpha)$, previously simulated values $Z_2^s(x_u)$ and co-located data of the first simulated variable $Z_1^s(x_u)$;
- 6. Define the auxiliary interval $F'_{z2}(z)$ of the global cdf $F_{z2}(z)$ to be sampled as previously referred for DSS (Figure 2);
- 7. Draw a value of $Z_2^s(x_u)$ from the cdf $F_{z2}(z)$, by:
 - a. Randomly generate a value *p* from the uniform distribution between [0, 1];
 - b. Generate a value y^s from $G(y(x_u)^*, \sigma_{CSK}^2(x_u))$ (Equation 8);
 - c. Return the simulated value $Z_2^s(x_u)$ from the inverse transform of the Gausssian cdf (Equation 9);
- 8. Add the simulated value $z^s(x_u)$ to the conditioning data;
- 9. Loop until all the *N* nodes of the simulation grid have been simulated.

In the co-simulation models is guaranteed the reprodution of the marginal and joint probability distributions functions (bi-histograms), between the primary and secondary variables, along with the reproduction of the mean and variance, of the variogram model and the experimental data values at its own locations (Soares 2001, Horta and Soares 2010).

2.1.3. Spatial Characterization of Non-Stationary Patterns

Subsurface geology can be highly heterogeneous (i.e. non-stationary), characterized by the local spatial variation of the geological continuity patterns (Figure 3). This may occur at different scales, associated with sedimentary depositional events or tectonic process (e.g. channels, faults or folds), or at a smaller scale associated to local variations in rock properties (e.g. porosity or permeability) (Demyanov and Arnold 2018). In complex geological environments, like in deep marine depositional environments, these spatial heterogeneities may have an impact in the spatial distribution of rock properties. Therefore, characterize the spatial continuity patterns of the subsurface geology, is extremely important in reservoir modelling, to build more accurate and consistent subsurface models. In complex geological environments, this can be a challenging task. One example, are reservoirs associated to turbidite channels, with its typically curvilinear or deltaic profiles characterized by non-stationary spatial continuity patterns (Figure 3) (Caers 2005, Demyanov and Arnold 2018).

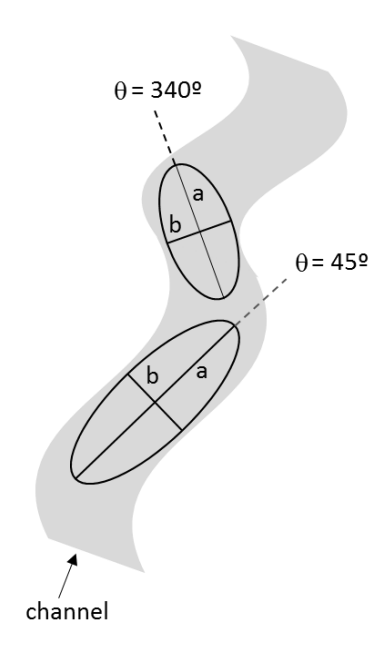


Figure 3 – Representation of a geological non-stacionary pattern from a meandriform channel. The local anisotropy variation is represented by the ellipses with different orientations (Θ) and axis ratio (a|b). The spatial distribution of the rock properties will be affected by the curvilinear shape of the channel.

In geostatistical modelling, non-stationarity natural phenomena have been modelled using object-based or pixel-based (or cell-based) modelling techniques. Object-based or Boolean methods (e.g. Deutsch and Wang 1996, Holden et al. 1998, Skorstad et al. 1999) are suitable to reproduce non-stationary patterns of categorical variables (e.g. facies), by using pre-defined geometrical objects, with its own shape and relative spatial distribution, representative of the different facies geometries (i.e. geological elements). These objects are placed in a simulation grid and the match with the data (e.g. well-log and seismic) evaluated using an optimization technique (e.g. simulated annealing). This step adds significant computational costs to the procedure. Although these objects are able to reproduce curvilinear profiles, it is difficult to constrain them to local data (Caers 2005, Demyanov and Arnold 2018).

Multi-point statistics (MPS) (e.g. Strebelle 2002, Arpat and Caers 2007, Mariethoz et al. 2010), is a pixel-based tool, widely used to reproduce curvilinear profiles (e.g. turbidite channels) using conceptual representations of the subsurface geology, referred to as training images (TI). Training images rely only on the knowledge about the area, and are not constrained to data or to any location, but they should represent the geometry of the geological structures that are intended to be modelled and all the geometrical relations (Strebelle and Zhang 2005).

Among the pixel-based methods are two-point statistics methods (e.g. Kriging), that are based on the use of a variogram and spatial covariance model. The first attempt to model non-stationary patterns using two-point statistics, was made by Soares 1990, who introduced the Morphological Kriging, followed by Xu 1996 and Luis and Almeida 1997, who took this idea and applied to stochastic sequential simulation of fluvial sand channels, considering morphological information and local continuity directions (Horta et al. 2010). Although twopoint statistics have several advantages, like being easily constrained by the available data (e.g. well-log, seismic); it used to have some limitations on reproducing non-stationary geometries and capturing connectivity, such as in fluvial-deltaic reservoirs (Caers 2005, Demyanov and Arnold 2018). To overcome these limitations, Horta et al. (2010) proposed the introduction of local anisotropy information (direction of maximum continuity and anisotropy ratio) in the direct stochastic sequential simulation algorithm, for the characterization of continuous variables represented by non-stationary spatial continuity patterns (e.g. curvilinear channels). This idea was later applied to history matching of a fluvial deltaic reservoir by Caeiro et al (2015). More recently, Nunes et al. (2017) proposed the use of regional variogram models in the stochastic sequential simulation step, were each region was represented by different continuity patterns.

2.1.3.1 Direct Sequential Simulation and Co-simulation with Local Anisotropy

Stationarity is one of the assumptions of DSS algorithm and other classic stochastic sequential methods however; subsurface geology is often characterized by heterogeneous medium, particularly in complex geological environments, where these heterogeneous spatial patterns may be related to differences in rock properties or facies. This is easily verified in deep marine sedimentary environments such as turbidite systems, characterized by its channels with curvilinear or deltaic geometries. For hydrocarbon reservoir characterization is of outmost importance that the simulated models reproduce these anisotropic spatial patterns, to better characterize the spatial distribution of the rock properties of interest. Therefore, the simulated models will hardly be geologically consistent and reliable, considering the real subsurface geology (Horta et al. 2010, Horta 2010). To solve the limitation imposed by the stationarity assumption, Horta et al. (2010) proposed the direct sequential simulation with local anisotropy (DSS-LA), an extension to the DSS algorithm to handle with spatial heterogeneities, allowing modelling curvilinear or deltaic geometries (e.g. turbidite channels), by conditioning the simulation procedure to local variogram models (local anisotropies) (Figure 3, Figure 4).

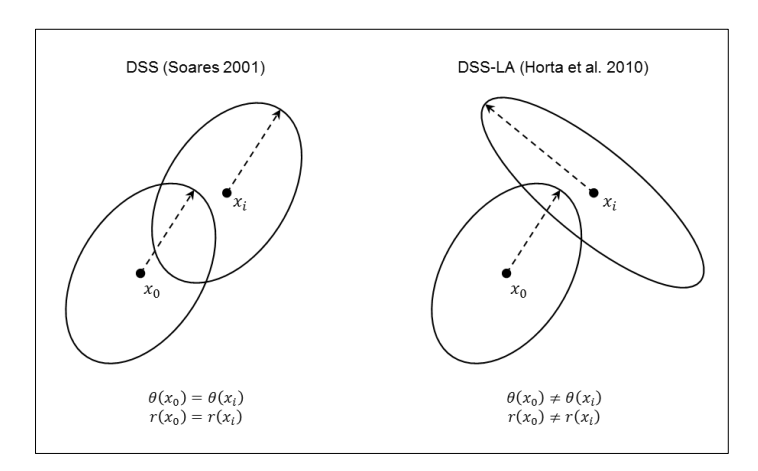


Figure 4 – Representation of the search radius for standard DSS and DSS-LA (adapted from Horta et al. 2010).

In DSS algorithm the selection of the conditioning experimental data used for the estimation of the local mean and variance, is made within the elliptical search radius defined by the global variogram parameters, that is the direction of maximum continuity given by the azimuth $\theta(x)$, and the anisotropy ratio between the range of maximum continuity r(x) (major axis of the search ellipsoid) and the range of minimum continuity (minor axis of the search ellipsoid) (Figure 4). The DSS-LA uses the local anisotropy parameters (local variogram) to conditioning the stochastic simulation procedure to the main continuity direction $\theta(x)$ and

anisotropy ratio r(x) of the search ellipsoid, which may change at each grid node (Figure 4). The data-to-data covariance matrix and the data-to-unknown covariance vector are computed with local covariance by the local anisotropy parameters $\theta(x)$ and r(x) (Horta et. al. 2010).

The direct sequential simulation with local anisotropy algorithm (DSS-LA) is summarized by the following steps (Horta et. al. 2010):

- 1. Define a auxiliary model with the local anisotropy parameters (i.e. azimuth, main and minor range of the search radius) (Figure 4), obtained by computing the local variogram model, or inderectly with other procedure (e.g. seismic attributes);
- 2. Generate a random path over the simulated grid nodes x_u , u = 1, ..., N, where x_u is the node to be simulated and N is the total number of nodes;
- 3. Estimate the local mean and variance with simple kriging estimate $z(x_u)^*$ and corresponding simple kriging variance $\sigma_{sk}^2(x_u)$, conditioned to the original experimental data $z(x_i)$, previously simulated values $z^s(x_i)$ and considering the neighborhood of the node x_u to be simulated. The estimation of the local mean and variance is also conditioned to the local anisotropy parameters azimuth $\theta(x)$ and ranges r(x) as explained above;
- 4. Define the auxiliary interval F'(z) of the global cdf F(z) to be sampled, based on local mean and variance as in classic DSS (Figure 2);
- 5. Draw a value of $z^s(x_u)$ from the cdf F(z), using Monte Carlo simulation as previously described for classic DSS (Section 2.1.1);
- 6. Add the simulated value $z^s(x_u)$ to the conditioning data;
- 7. Loop until all the *N* nodes of the simulation grid have been simulated.

The DSS-LA algorithm allows co-simulation (co-DSS; Horta and Soares 2010) as previously described in Section 2.1.2. Furthermore, the simulated models reproduce the probability distribution function (histogram), the experimental data and the spatial continuity patterns (global and local variogram models).

In Chapter 5 is presented a geostatistical seismic inversion method applied to a complex geological environment, characterized by heterogeneous geometries (non-stacionary spatial patterns), where DSS-LA is the stochastic sequential simulation procedure used to estimate the spatial distribution of subsurface rock properties.

2.1.4. Direct Sequential Simulation and Co-simulation with Multi-local Distribution Functions

Direct Sequential Simulation and Co-simulation with multi-local distribution functions (Nunes et al. 2017) intends to handle with non-stationary spatial continuity patterns (anisotropic spatial patterns), through the regionalization of the study area. The simulation grid is divided into sub-regions representative of the subsurface geology (e.g. facies), to each is assigned a spatial continuity pattern (regional variogram model) and a probability distribution function, instead of using a single histogram and single variogram model for the entire study area, as in classic DSS algorithm. The use and definition of the sub-regions aims the improvement of the simulated models and its geological consistency (Nunes et al. 2017).

Direct Sequential Simulation and Co-simulation with multi-local distribution functions can be summarize by the following steps (Nunes et al. 2017):

- 1. Define a regionalization model, dividing the simulated grid into sub-regions based on the best suitable criteria (e.g. facies) considering the main objective;
- 2. With a random seed generate a random path over the simulation grid nodes x_u , u = 1, ..., N, where x_u is the node to be simulated and N is the total number of nodes;
- 3. Estimate the local mean and variance with simple kriging estimate $z(x_u)^*$ and corresponding simple kriging variance $\sigma_{sk}^2(x_u)$, conditioned to the original experimental data $z(x_i)$ and previously simulated values $z^s(x_i)$. To avoid artefacts simple kriging considers all conditional data from different sub-regions within the neighborhood of the node x_u to be simulated;
- 4. Define the auxiliary interval $F'_{sr}(z)$ of the sub-region cdf $F_{sr}(z)$ to be sampled based on the equivalent Gausssian transform (Equation 6, Equation 7). The interval $F'_{sr}(z)$ is centered at the local mean and with the range of the local variance estimated in the previous step;
- 5. Draw a value of $z^s(x_u)$ from the cdf $F_{sr}(z)$ by:
 - a. Randomly generate a value p from the uniform distribution between [0, 1];
 - b. Generate a value y^s from $G(y(x_u)^*, \sigma_{sk}^2(x_u))$ (Equation 8);
 - c. Return the simulated value $z^s(x_u)$ from the inverse transform of the Gaussian cdf (Equation 9);
- 6. Add the simulated value $z^s(x_u)$ to the conditioning data;
- 7. Loop until all the *N* nodes of the simulation grid have been simulated.

For the resulting simulated models is ensure the reproduction of the global and sub-regions probability distribution functions. The reproduction of the original global probability

distribution function (pdf_g) is ensured by calculating the simple kriging estimate and corresponding variance, considering the conditional experimental data and previously simulated values from different sub-regions. Since the interval of the cumulative distribution function to be sampled is defined for each sub-region $F_{sr}(z)$, instead of considering the global cdf F(z), it is ensured the reproduction of the sub-region probability distribution function (pdf_{sr}) . To handle with co-simulation (co-DSS; Horta and Soares 2010), this procedure follows the steps described in section 2.1.2.

After presenting the DSS algorithms, it is important to highlight that these methods have some important aspects in common, some of them with advantages over the other simulation methods. One of these advantages is the ability of DSS algorithms using directly the original experimental data, without implying the prior transformation assuming the Gaussian hypothesis of the data values, as in SGS. Furthermore, in DSS algorithms the reproduction of the original probability distribution function (histogram) and joint probability distribution function (bi-histogram), as inferred from the experimental data is guaranteed, what does not always happens in other methods, such as SGS. Moreover, DSS algorithms ensure the reproduction of the experimental data at their own locations; the reproduction of the spatial continuity pattern (i.e. global and local variogram models) and the reproduction of the mean and variance, as inferred from the experimental data. This brings an important advantage to the geostatistical inverse methods suported by DSS algortihms, particularly when applied to complex geological environments or at early exploration stages, allowing to estimate more accurate and reliable geological subsuface models and quantify the associated uncertainty (Soares 2001, Azevedo and Soares 2017), which is the case of the inversion methods presented herein.

3. Geostatistical Seismic Reservoir Modelling

3.1. Seismic Inversion for Reservoir Characterization

In deep marine environments subsurface geology is normally unknown because it's expensive and difficult to collect direct measurements of the subsurface. Therefore, indirect measurements like seismic reflection data, which are easier to obtain are more frequently used in reservoir characterization. Predicting subsurface geology is a complex and essential part of hydrocarbon reservoir characterization. Understand and predict the spatial distribution of subsurface rock properties (e.g. porosity, facies and acoustic impedance) is important for decision making, to delineate strategies and to minimize risks.

Geostatistical modelling techniques have been used to build three-dimensional numerical models of the subsurface. Initially these models were built based on well-log data and geological conceptual models, corresponding to smooth representations of the subsurface geology and making it impossible estimating uncertainty (Drubule 2003; Caers 2011).

Due to its large spatial coverage and representativeness of the subsurface geology, seismic reflection data become an essential tool for reservoir characterization, translating the response of subsurface medium to the seismic waves. Unlike seismic data, well-log data is usually sparse, but its value lies on being a direct measurement of the subsurface and have high vertical resolution. Based on these observed data, we intend to infer the unknown subsurface geology, by characterizing rock properties and their spatial distribution. This can be solved by posing the prediction of the subsurface geology as an inverse problem (Figure 5), since seismic inversion allows derive petro-elastic rock properties from seismic reflection data (Doyen 2007; Bosch et al. 2010). In reservoir characterization, the seismic inverse problem (Figure 5) can be summarized by the following equation (Equation 10):

Equation 10
$$m = F^{-1}(d_{obs}) + e,$$

where m are the model parameters we aim to infer (e.g. acoustic impedance), d_{obs} the observed data (seismic reflection data and well-log data) and e represents the measurement errors and the errors about the model (Tarantola 2005; Tompkins et al. 2011). The mapping between the observed seismic data and the subsurface rock properties (preto-elastic rock properties) is provided by the forward model F (Figure 5). As F^{-1} is unknown, predicting the subsurface rock properties from recorded seismic data is a challenging nonlinear problem, ill-posed, with multiple solutions (Tarantola 2005).

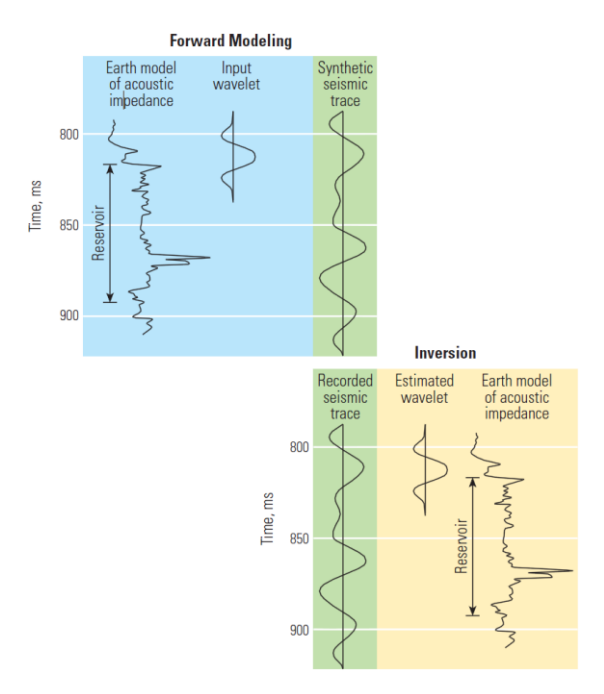


Figure 5 – Relation between the forward modeling and seismic inversion (adapted from Barclay et al. 2008).

The forward model F (Figure 5) in the full stack seismic inversion, for the normal incidence angle, can be expressed by Equation 11.

Equation 11
$$A = RC * w$$

Where A represents the amplitudes of the synthetic seismic, derived from the convolution of the reflection coefficients RC (interface reflectivity) with a wavelet w. The reflection coefficients (normal incidence) are related to the interface between two adjacent geological layers in the subsurface with different rock properties (Figure 6) and can be calculated with the following equations (Equation 12, Equation 13):

Equation 12
$$RC = \frac{Ip_2 - Ip_1}{Ip_2 + Ip_1},$$

Equation 13
$$Ip = \rho * Vp$$

where Ip is the acoustic impedance (Equation 13) and can be computed by the product of rock density with the velocity of the seismic wave Vp (velocity of the compressional seismic

wave). The geological layers above and below the interface considered are designed by 1 and 2 respectively (Azevedo and Soares 2017).

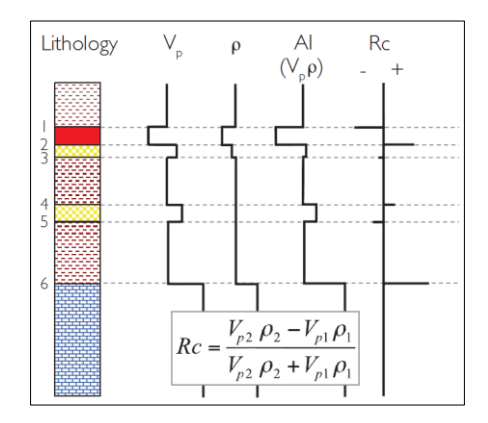


Figure 6 – Schematic representation of reflection coefficient and its relation with acoustic impedance and lithological interfaces (adapted from Simm and Bacon 2014).

Acoustic impedance (Ip) models resulting from seismic inversion, are considered representations of the subsurface geology (Doyen 2007). It is an important elastic rock property very useful for reservoirs characterization, from which other petro-elastic rock properties can be derived (Figure 7). As an example, low acoustic impedance values are typically related to high porosity values therefore, knowing the correlation between both properties it is possible to estimate porosity models from acoustic impedance, using geostatistical modelling techniques (e.g. DSS and co-DSS, Soares 2001) (Azevedo and Soares 2017).

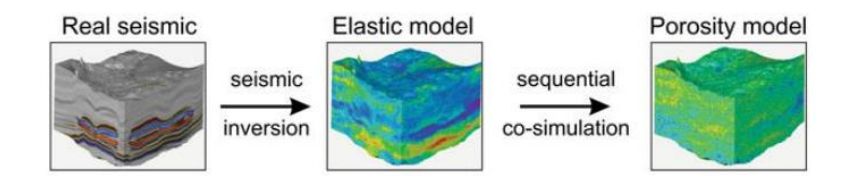


Figure 7 - Schematic representation of geostatistical modelling workflow to derive petrophysical rock properties from acoustic impedance (elastic model) resulting from seismic inversion (adapted from Azevedo and Soares 2017).

3.2. Overview of Seismic Inversion Methods

Seismic inversion methods are powerful modelling techniques used for reservoir characterization and uncertainty assessment, as they are able to integrate seismic reflection data and well-log data in the same framework, enabling the prediction of three-dimensional numerical models of the subsurface geology (Doyen 2007; Caers 2011; Azevedo and Soares 2017). There are several seismic inversion methods, each one with its own assumptions, advantages and limitations hence, choosing the most suitable method depends on the main

objective, available data and time. Seismic inversion methods can be divided in two main groups – Deterministic and Probabilistic or Statistical-based methods (Francis 2006; Bosch et al. 2010; Filippova et al. 2011).

Deterministic seismic inversion methods (e.g. Russell and Hampson 1991) are trace-by-trace approaches that are wildly used and can be considered optimization procedures. The model parameters are perturbed throughout the inversion procedure, in order to obtain a unique best-fit solution of the problem, which minimizes the difference between the observed seismic and the generated synthetic seismogram. These methods use an initial low-frequency model, related to the prior knowledge about the subsurface geology, to constrain the seismic inversion procedure. In the deterministic approach, the solution of the inverse problem is considered a smooth representation of the subsurface geology, what may be insufficient to describe the complexity of some geological scenarios. Furthermore, the model solution is unique, making it impossible to quantify the associated uncertainty (Bosch et al. 2010; Azevedo and Soares 2017).

Within Determinist methods, sparse spike inversion (e.g. Olden-burg et al. 1983; Hampson and Russell 1985) and model-base generalized linear inversion (e.g. Russell and Hampson 1991), are the most used deterministic methods in the industry (Russell 1988; Bosch et al. 2010). Sparse-spike inversion is a deconvolution procedure, where reflection coefficients are obtained from the deconvolution of the seismic trace under sparseness assumptions of the reflectivity series, followed by the computation of the sparse acoustic impedance, which is combined with a low-frequency model to constrain the observed data and improve spatial consistency of the models. Usually low-frequency models are obtained from well-log data or velocity analysis (Bosch et al. 2010; Azevedo and Soares 2017). The model-based inversion uses an initial subsurface model (i.e. low frequency model) which is perturb iteratively until a minimization criteria defined by the objective function is satisfied. In model-based inversion the objective function is defined by, the difference between the synthetic and the real seismic data along with a possible regularization term, to restrict possible solutions and to ensure lateral continuity and models consistency (Bosch et al. 2010; Azevedo and Soares 2017). Contrary to other methods, deterministic seismic inversion methods are not constrained by well-log data, which will not have a direct impact on the inversion results, still that, they are normally used to help building the low frequency model. The initial low frequency model should be carefully defined, since it will constrain the inversion procedure, having a big impact on the results. Nevertheless, deterministic methods are valid and can be useful, but its main advantage is related to easy implementation (Azevedo and Tylor 2022).

Probabilistic or Stochastic seismic inversion methods are other group of seismic inversion procedures that gained importance in the last years. Contrary to Deterministic methods, they

retrieve high-resolution subsurface earth models, allowing the prediction of the associated uncertainty since they have multiple solutions (Bosch et al. 2010; Filippova et al. 2011; Azevedo and Soares 2017).

Seismic reflection data is band-limited, due to the absence of lower and high frequencies (Figure 8). The presence of lower frequencies in the inverted models, came from the integration in the inversion procedure, of a prior model also known as low frequency model. In Stochastic seismic inversion methods, the high frequencies content of the retrieved models (Figure 8), are a result of the integration of well-log data, which has a high vertical resolution comparing to seismic data, and the integration of a spatial continuity pattern given by a variogram model, necessary for stochastic simulation (Drubule 2003; Azevedo and Soares 2017).

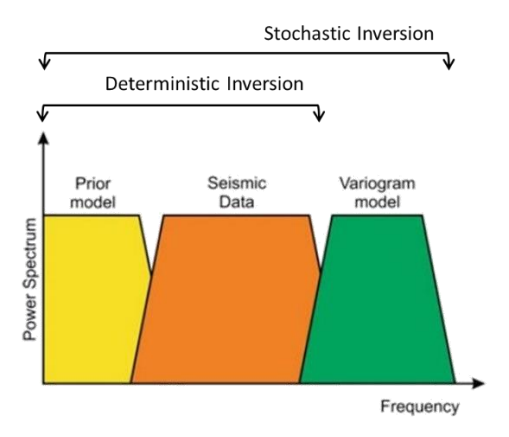


Figure 8 – Schematic representation with the differences in bandwidth extension of inverted models from deterministic and stochastic inversion (adapted from Azevedo and Soares 2017).

Due to the stochastic simulation stage, these group of methods become more computational expensive. One of the advantages of these methods is the integration of well-log data to condition the seismic inversion, implying its reproduction at their location (Deutsch and Journel 1992; Soares 2001). As these methods follow a probabilistic approach, the solution of the inverse problem is an ensemble of multiple equally likely realizations, through which is possible to predict the associated uncertainty (Deutsch and Journel 1992). Both approaches can handle with post-stack or pre-stack seismic data (Azevedo and Soares 2017).

Within this group of methods, there are two main approaches that should be mentioned. One, are Bayesian linearized seismic inversion methods (e.g., Buland and Omre 2003; Grana and Della Rossa 2010; Grana 2016; Grana et al. 2017), other are Geostatistical seismic inversion methods (e.g. Soares et al. 2007).

The Bayesian linearized seismic inversion was introduced by Buland and Omre (2003). In the Bayesian linearized seismic inversion the solution of the inverse problem (Equation 14) is given by the posterior distribution function $P(m|d_{obs})$ of the model parameters m given the observed data d_{obs} .

Equation 14
$$P(m|d_{obs}) = \frac{P(d_{obs}|m)P(m)}{P(d_{obs})},$$

Where $P(d_{obs}|)$ is the likelihood function, which represents the probabilistic relation between the observed data d_{obs} and the model parameters m. P(m) is the prior distribution function of the model parameters m and is related to the prior knowledge about the model m to be estimated. The prior distribution P(m) must be carefully defined, as it will condition the inversion procedure, having a great impact on the results (Buland and Omre 2003; Grana et al. 2017). $P(d_{obs})$ is a normalization constant. The solution of the inverse problem is represented by the posterior distribution $P(m|d_{obs})$, which corresponds to the best solution of the model m considering the available information (Buland and Omre 2003).

The method implies two main assumptions:

- The distribution of model parameters (prior distribution function) and errors are Gaussian (log-Gaussian);
- 2. The linearization of the forward model that is, the relationship between the predicted model and the real data.

Although the inverse problem is non-linear, the Bayesian approach considers that the physical model is linear or could be linearized, requiring a pre-processing to ensure the linearity of the problem. Since the model parameters are represented by a Gaussian distribution, the solution of the inverse problem (posterior distribution) will be also Gaussian, which is not always the case, as some rock properties (e.g. porosity, permeability) has a non-Gaussian behavior, resulting from differences in lithology or fluid content. Some recent works (e.g. Grana et al. 2017), try to solve this limitation by assuming a multi-Gaussian distribution of the model parameters. In these cases, the Gaussian mixture models (multi-Gaussian distribution) are linear combinations of Gaussian components that are used to describe the multimodal behavior of the model parameters (Grana et al. 2017).

One of the advantages of the Bayesian approach against Geostatistical seismic inversion methods are the lower computational costs, however Bayesian linearized seismic inversion methods have a limited exploration of the uncertainty space in lieu of exact information (Tarantola 2005).

Geostatistical seismic inversion methods are other group of Statistical-based inverse methods that use iterative procedures and stochastic optimizers to explore and perturb the model parameters. They were first introduced by Bortoli et al. (1992) followed by Haas and Dubrule (1994) who presented the trace-by-trace inversion. Later on, Soares et al. (2007) presented a new approach, by proposing the global stochastic seismic inversion (GSI). One of the advantages of geostatistical methods, is they do not require the linearization of the forward model. Additionally, they use well-log data and a spatial continuity pattern to constrain the seismic inversion procedure, retrieving multiple equally likely realizations of high resolution subsurface models, from which it is possible to quantify the associated uncertainty.

In seismic inversion the non-stationary phenomena, have also been addressed, particularly in complex geological environments, aiming to improve the prediction of the elastic models. In deterministic seismic inversion methods, the spatial continuity is addressed in the prior model, which will have its limitation since it is a smooth representation of the subsurface geology. Conversely, geostatistical methods allow the integration of spatial continuity patterns to conditioning the inversion procedure, what it is an advantage over deterministic methods. However, this is not a straightforward procedure within Bayesian inversion framework, where the spatial continuity patterns have been addressed by including varying spatial covariance matrices to conditioning the seismic inversion (e.g.; Aune et al. 2013; Bongajum et al. 2013; Madsen et al. 2020). Geostatistical seismic inversion methods (e.g. GSI; Sores 2017) have here an advantage over the other methods, since the simulation step of the inversion procedure is conditioned by a spatial continuity pattern, given by a variogram model. Nevertheless, when applied to non-stationary geological environments, such as curvilinear or deltaic channels, or tectonic structures (e.g. faults, folds), stochastic methods have some limitations in correctly capturing the spatial continuity (i.e. local anisotropy), leading to less accurate and reliable subsurface models, increasing uncertainty. This is due to the use of a single and global variogram model to represent the spatial continuity pattern of the subsurface geology. Recently, Pereira et al. 2020 proposed the use of local anisotropies (i.e. local variogram models), in the geostatistical seismic inversion procedure, were the local anisotropies were obtained from seismic attributes. However, like in classic geostatistical seismic inversion, the variogram models are fixed during inversion procedure. Hence, if the spatial continuity model is not accurate, the propagation of errors through the iterative process may occur. In the scope of this thesis is proposed a data-driven approach within the geostatistical seismic inversion framework to overcome this limitation.

The next section is focused on this group of seismic inversion methods, since the work presented in this thesis uses geostatistical seismic inversion methods.

3.3. Geostatistical Seismic Inversion Methods

Geostatistical or stochastic seismic inversion methods are iterative procedures, which use stochastic optimization techniques for the perturbation of the model parameters (Doyen 2007), what makes these methods more computationally expensive. A variety of stochastic optimizers has being used, such as simulated annealing (Sen and Stoffa 1991; Ma 2002), genetic algorithms (Mallick 1995, 1999; Boschetti et al. 1996; Soares et al. 2007), neighbor algorithm (Sambridge 1999) and stochastic sequential simulation and co-simulation (Bortoli 1993; Haas and Dubrule 1994; Grijalba-Cuenca and Torres-Verdin 2000; Soares et al. 2007; Nunes et al. 2012; Azevedo et al. 2015; Azevedo and Soares 2017; Azevedo et al. 2018; Pereira et al. 2019, 2020).

Geostatistical inverse methods usually use a spatial continuity pattern of the rock properties of interest, given by a variogram model, to constrain the inversion procedure and help reproducing local heterogeneities, related to local variations in rock properties. The use of stochastic optimizers (e.g. stochastic sequential simulation and co-simulation (Soares 2001)) imply the reproduction of the mean and standard deviation of the observed data (i.e., well-log data), as well as the reproduction of the variogram model (Doyen 2007; Filippova et al. 2011).

Within geostatistical seismic inversion methods one can stand out two main approaches, initially Bortoli et al. (1992) followed by Haas and Dubrule (1994), introduced Geostatistical methods, following a sequential trace-by-trace approach, to invert seismic data into acoustic impedance models. Subsequently, a global approach was proposed by Soares et al. (2007), who presented the global stochastic seismic inversion method (GSI) (Azevedo and Soares 2017).

3.3.1. Trace-by-trace geostatistical seismic inversion

In the trace-by-trace geostatistical seismic inversion (e.g. Bortoli et al. 1992; Haas and Dubrule 1994), the inversion procedure is performed individually for each seismic trace (Figure 9). The method is based on a stochastic sequential simulation procedure wherein, initially is defined a random path, whereby each seismic trace is visited individually through the entire volume. At each trace location and following the pre-defined random path, a set of N_s acoustic impedance traces are simulated from the well-log data and the previously simulated traces, using sequential Gaussian simulation algorithm (SGS, Deutsch and Journel 1992). For each simulated acoustic impedance traces, are derived the corresponding reflection coefficients, which are then convolved with a wavelet, to compute the

corresponding N_s synthetic seismic traces. For each of these N_s synthetic traces, is evaluated the mismatch with the corresponding real seismic trace, given an objective function, for instance the Pearson's correlation coefficient (Equation 15) or other.

Equation 15
$$\rho_{X,Y} = \frac{cov(X,Y)}{\sigma_X.\sigma_Y}$$

Following the pre-defined random path, at each trace location, for the synthetic seismic trace that best match the real seismic, the corresponding acoustic impedance trace is kept and considered conditioning data along with the well-log data, in the simulation of the following acoustic impedance traces (Figure 9). The procedure ends when all trace locations inside the volume are visited (Doyen 2007; Azevedo and Soares 2017).

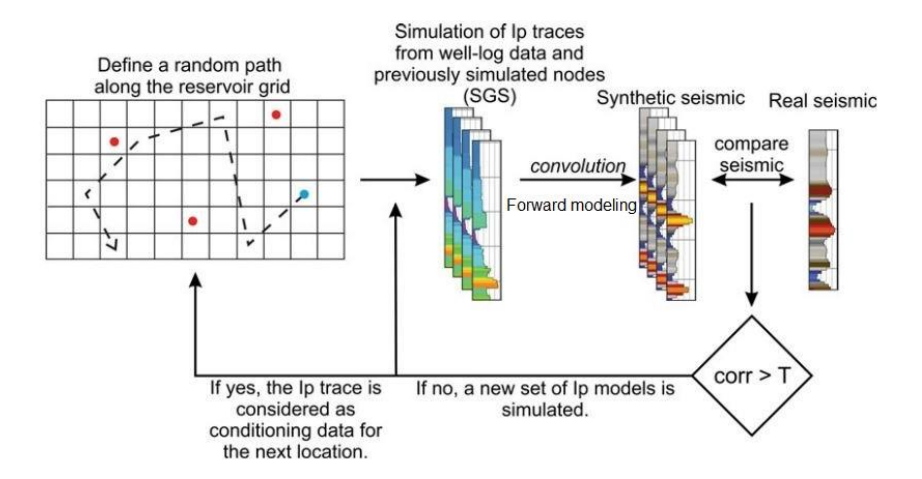


Figure 9 – Schematic representation of the trace-by-trace geostatistical seismic inversion workflow (Bortoli et al. 1992, Haas and Dubrule 1994). In the first step the red dots represent the well-log data and the blue dot the first location of the random path (dashed line) where a set of Ns acoustic impedance traces will be simulated (adapted from Azevedo and Soares 2017).

The uncertainty assessment can be done through an ensemble of invert models from different runs. The pre-defined random path is only kept during an individual run, if other inversion runs are considered, the pre-defined random path and consequently the conditioning data at each trace location will change, allowing the realization of an ensemble of equally likely inverted models (Doyen 2007; Azevedo and Soares 2017).

It is important to mention that, the trace-by-trace geostatistical seismic inversion method has a disadvantage that should not be ignored. In areas with low signal-to-noise ratio, the traceby-trace approach imposes inverted models fitting the noisy real seismic data, instead of remaining high uncertainty areas. As inverted traces are considered conditioning data in the following location defined by the random path, this can lead to the propagation of noise values through the entire volume (Azevedo and Soares 2017; Azevedo and Tylor 2022). To surpass the limitations of the trace-by-trace approach, Soares et al. (2007) presented the global stochastic seismic inversion method (GSI), proposing a global approach for the inversion procedure.

3.3.2. Global Stochastic Seismic Inversion

Global stochastic inversion (GSI) was introduced by Soares et al. (2007) proposing, an iterative geostatistical seismic inversion procedure with a global optimization technique, based on a cross-over genetic algorithm principle (Figure 10) wherein, the perturbation of model parameters during the stochastic simulation stage has a global approach, rather than a trace by trace approach. One of the main consequences of global approach is to avoid the artificial matching between the best-fit models and the observed seismic data in noisy areas, where the signal-to-noise ratio is low, remaining these areas with higher uncertainty (Soares et al. 2007).

The inversion method was proposed for the acoustic domain, to invert full stack seismic data into acoustic impedance (Ip) models. Further was extended for the elastic domain to invert prestack or partial angle stack seismic data (e.g. GEI (Nunes et al. 2012); geostatistical AVA direct facies inversion (Azevedo et al. 2015); geostatistical seismic AVA inversion (Azevedo et al. 2018) and geostatistical rock physics AVA inversion (Azevedo et al. 2019)).

Briefly, the method is based in two keys ideas:

- 1. The direct stochastic sequential simulation (DSS, Soares 2001) and co-simulation (co-DSS, Horta and Soares 2010) are the stochastic procedures used to perform the perturbation of the model parameters in the iterative process;
- To follow the sequential procedure of the genetic algorithm optimization for the convergence of the iterative process towards an objective function (Soares et al. 2007; Caetano 2009; Azevedo and Soares 2017).

At the end of each iteration the objective function evaluates the misfit between the synthetics and the real seismic data, based on the global and local correlation coefficients in a trace-by-trace basis, driving the convergence of the procedure (Figure 10). These correlation coefficients and corresponding acoustic impedance

traces are used as the affinity criterion to create the next generation of models (Soares et al. 2007; Caetano 2009; Azevedo and Soares 2017).

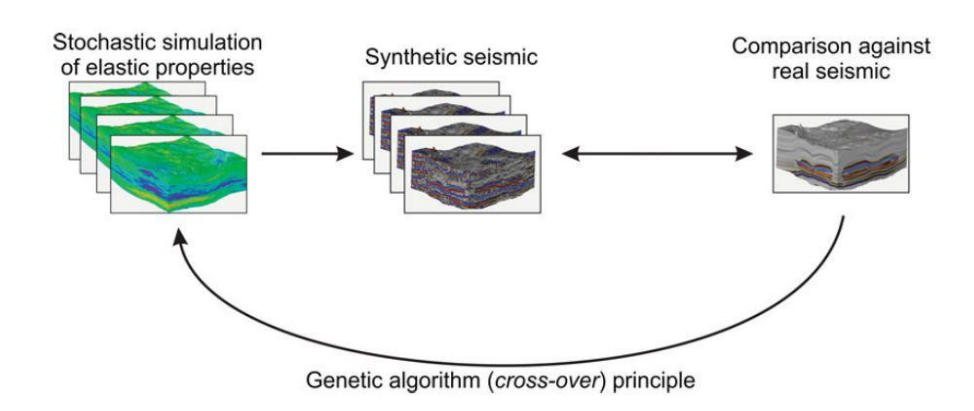


Figure 10 – General workflow of iterative global stochastic seismic inversion methods (adapted from Azevedo and Soares 2017).

The objective function in GSI is represented by Equation 16, where S evaluates the similarity between the real (x) and the synthetic seismic (y) traces in terms of waveform and amplitude content. The values of S vary between -1 and 1 whereby, the closer to one more similar synthetic and real seismic traces are.

Equation 16
$$S = \frac{2*\sum_{s=1}^{N} (x_s*y_s)}{\sum_{s=1}^{N} (x_s)^2 + \sum_{s=1}^{N} (y_s)^2},$$

During the inversion procedure the stochastic sequential simulation and co-simulation stage is constrained by the well-log data and a spatial continuity pattern represented by a global variogram model of the rock property of interest. As a result of the stochastic sequential simulation and co-simulation process, at the end of the inversion procedure, the Ip models have some characteristic in common meaning, they will reproduce the well-log data at their locations, the variogram model representative of the spatial continuity pattern, the marginal probability function represented by a histogram inferred from the well-log data and the joint probability distribution, if a secondary variable is predicted at the same time (Doyen 2007; Soares et al. 2007; Filippova et al. 2011; Azevedo and Soares 2017).

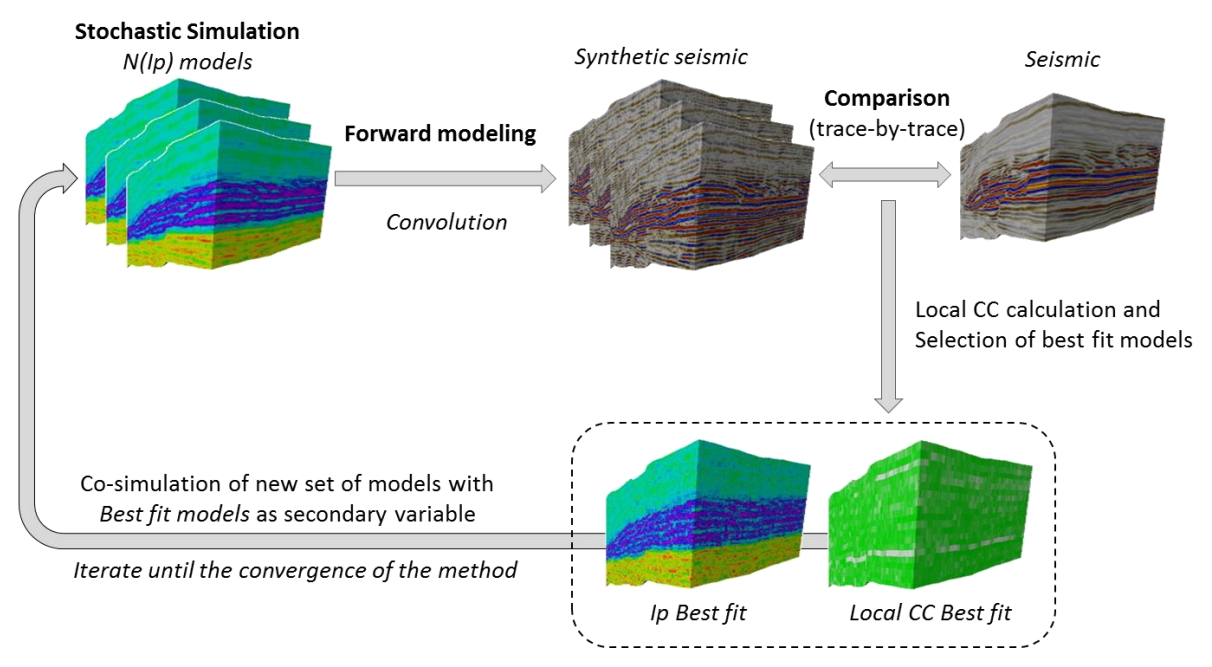


Figure 11 – Global stochastic seismic inversion (GSI) workflow (adapted from Azevedo and Soares 2017).

The global stochastic inversion can be summarized in the following steps (Figure 11):

- 1. First iteration starts with the simulation of a set of N_s realizations of Ip, conditioned to well-log data and to a global variogram model, using DSS algorithm (Soares 2001);
- 2. For each realization of Ip model the corresponding reflection coefficients are compute;
- 3. N_s synthetic seismograms volumes are computed by convolving the reflection coefficients with an estimated wavelet:
- 4. The synthetic and real seismic data are compared in terms of local correlation (S) (Equation 16) in a the trace-by-trace basis (Figure 12);
- 5. The traces with highest local correlation (S) and corresponding Ip values (Figure 13) are stored in two auxiliary volumes (best fit models), used as secondary variable for the cosimulation of a new set of N_S Ip models in the next iteration;
- 6. Return to step 2 and iterate until the global correlation between the synthetic and the real seismic data is below a given threshold.

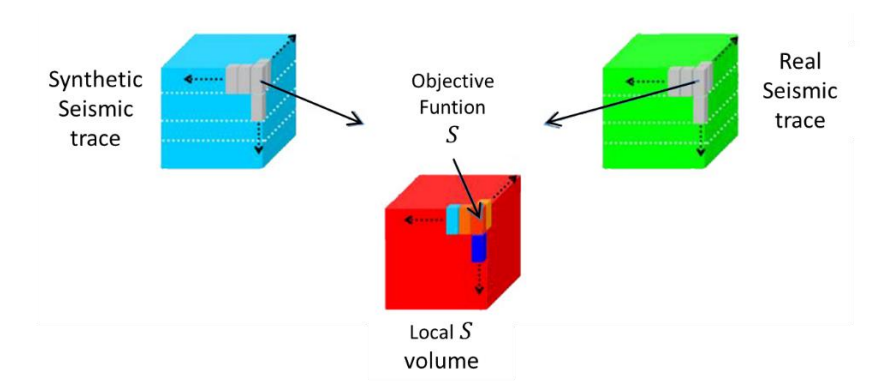


Figure 12 – Calculus of the mismatch between synthetic and real seismic data in a trace-by-trace basis. The objective function can be defined as the Pearson's correlation coefficient, but other equations may be applied (adapted from Caetano 2009).

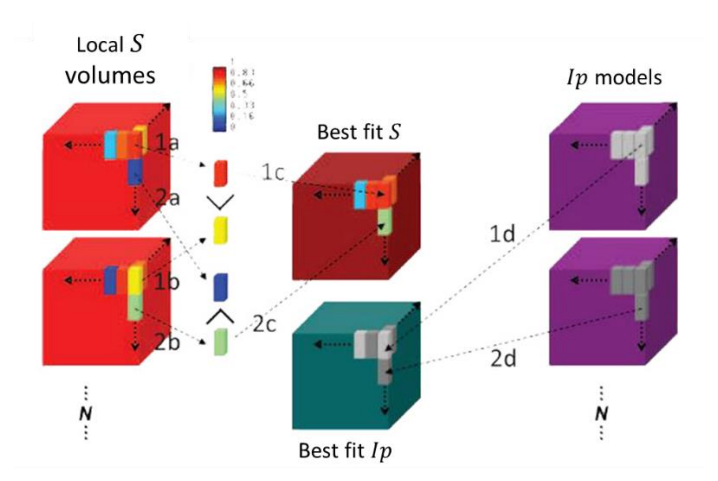


Figure 13 – Creation of the auxiliary volumes creation (Best CC and Best AI), from the traces with highest correlation coefficient and corresponding Ip traces (adapted from Caetano 2009).

The work developed in the scope of this thesis and presented in Chapter 4, 5 and 6 builds upon the Global Stochastic Seismic Inversion algorithm (GSI), to invert full stack seismic data into acoustic impedance models.

4. Geostatistical seismic inversion for frontier exploration

Paper published in Interpretation and presented at AAPG/SEG ICE 2016, Barcelona.

<u>Pereira A.</u>, Nunes R., Azevedo L., Guerreiro L. & Soares A. 2017. Geostatistical Seismic Inversion for Frontier Exploration. Interpretation 5(4), T477-T485.

4.1. Introduction

Subsurface three-dimensional numerical models are important tools in reservoir characterization, they are used as representations of the subsurface geology, allowing quantify subsurface rock properties, helping predict reservoir quality and architecture. Subsurface geological modelling normally relies on sparse direct measurements of subsurface rock properties (e.g. density, porosity) and seismic reflection data from which, the intention is to predict a quantitative spatial representation of the petro-elastic rock properties, describing the spatial continuity pattern and property variability for an entire area of interest (Doyen 2007).

Subsurface geology can be very complex and heterogeneous, determining the spatial distribution pattern of rock properties, often conditioned by the presence of different rock types or facies (Pringle et al. 2006, Howell 2014). In reservoir characterization, understanding these spatial patterns and quantify uncertainty is crucial for risk assessment (Caers 2011).

At early exploration stages or in unexplored areas (i.e. frontier areas), reservoir characterization can be challenging, due to the lack or scarcity of direct measurements of the subsurface rock properties, such as well-log data, what makes the prediction of reservoir properties derived from traditional modelling techniques, a difficult task (Deutsch 2002, Howell 2014). In these particular cases, it is important to integrate geological information about the area, along with seismic reflection data and well-log data if available, to produce more accurate representations of the subsurface and reduce uncertainties and risks. This can be done using geological analogues, like outcrops analogues (e.g. Caers and Zhang 2004, Grammer et al. 2004, Pringle 2006) or other type of geological analogues, as long as they share some similarity with the system we intend to describe (Howell 2014, Martinius et al. 2014). Geological analogues can provide information related to geobodies geometry, connectivity or dimensions and can help infer spatial statistics useful for reservoir modelling.

Nevertheless, it is critical to evaluate the analogues choice and purpose, to avoid mistakes in models predictions (Deutsch 2002, Howell 2014).

Seismic inversion methods are modelling techniques widely used in reservoir characterization, to predict subsurface rock properties. Acoustic impedance (Ip) is an elastic rock property derived from seismic inversion procedures, which may be related to porosity, helping predict reservoir potential and behavior. Seismic inversion is based on the physical relation between seismic reflection data (i.e. seismic amplitude) and the subsurface elastic response, which is linked to subsurface rock properties (Drubule 2003). Seismic inverse problems are nonlinear and ill-posed and have multiple solutions (Tarantola 2005). There are two main ways to solve a seismic inversion problem, a deterministic and a probabilistic approach. Deterministic seismic inversion methods are based on optimization techniques. They use the available well-log data only to build a priori elastic model, from where the resulting model is consider a smooth representation of the subsurface geology, not allowing quantify the associated uncertainty. Contrary to deterministic methods, probabilistic procedure, particularly geostatistical seismic inversion methods, use the available well-log data to conditioning the invention procedure, to build high-resolution subsurface rock property models, allowing uncertainty assessment of equally likely inverted elastic models, what is important for reservoir characterization (Caers 2011, Bosh et al. 2010). As conventional geostatistical seismic inversion methods are constrained locally by existing well-log data, applying them to frontier areas or early exploration stages can be challenging. To overcome the lack of well-log data, the seismic inversion method presented herein, aims to integrate data from geological analogues to conditioning the seismic inverse procedure. The method is an extension of global geostatistical seismic inversion (GSI; Soares et al. 2007), driven by the direct sequential simulation (DSS; Soares 2001) with multi-local distribution functions algorithm (Soares 2001, Nunes et al. 2017), as model perturbation technique. The seismic inversion procedure, use a global optimizer based on a genetic cross-over algorithm, driven by the match between the real seismic reflection data and the synthetic seismic, derived from the elastic models during the inversion procedure. The proposed geostatistical seismic inversion method integrates prior geological knowledge about the area and data related to subsurface rock properties (i.e. lp), obtained from geological analogues. The geological analogues data is from nearby appraisal wells located outside the target area, but geologically related, since they are inside the same sedimentary basin, sharing similar characteristics. The method was applied to a real case study located in the Algarve Basin in the southwestern Iberian margin.

4.2. Methodology

The proposed seismic inversion method aim to extend the application of geostatistical inversion methods to unexplored areas (i.e. frontier areas), overcoming the limitation of lack of direct measurements (i.e. well-log data) through the use of geological analogues, used to infer the rock properties probability distribution function and spatial continuity patterns, improving the subsurface geological models and allowing quantify uncertainty. Furthermore, the proposed method aims to address the problem of geological spatial heterogeneities (nonstationarity), associated to the spatial distribution of different facies, by dividing the inversion grid into regions with geological meaning and imposing regional variogram models to those regions, for better describe the subsurface rock properties with non-stationary spatial patterns. Thus, the seismic inversion procedure follows the Global Stochastic Inversion (GSI; Soares et al. 2007), where the stochastic sequential simulation method used to predict the spatial distribution of subsurface rocks properties for non-stationary environments in frontier areas, is the direct sequential simulation (DSS; Soares 2001) with multi-local distribution functions (Soares 2001, Nunes et al. 2017), instead of using classical direct sequential simulation (DSS; Soares 2001, Nunes and Almeida 2010). With this, the method is able to incorporate within the inversion procedure, geological regions defined from seismic interpretation of the available seismic reflection data and simultaneously using a priori knowledge about the subsurface geology obtained from geological analogues (e.g. nearby wells) and traslated into probability distribution functions of the rock property of interest (e.g. acoustic impedance). In Nunes et al. (2017) it is possible to find a detailed mathematical description of this stochastic sequential simulation algorithm, but due to its importance in the proposed iterative geostatistical seismic inversion procedure, its main steps are introduced herein.

The definition of a regionalization model is the first required step for this stochastic sequential simulation procedure, as presented by Nunes et al. (2017). The regionalization model divides the simulation grid into regions or zones with different shapes or sizes, aiming to make the assumption of stationarity of rock properties (i.e. main statistical moments) more valid. Therefore, the regionalization model should be geological consistent and each region should translate geological heterogeneities, which must be related for instance with different spatial distribution patterns (non-stationary patterns) associated to different rock properties or facies (e.g. sandy channels interbedded with clays). Instead of just using a global probability distribution function of the rock property of interest and a unique spatial continuity pattern expressed by a global variogram model, the simulation procedure allows to assign a pdf and a variogram model to each region, giving more geological representativeness to the retrieved models. The algorithm starts with the definition of a random path through all the grid nodes,

where at each node location, the local mean and variance is estimated with simple kriging estimate and corresponding simple kriging variance, conditioned to the available experimental data and previously simulated values, from different adjacent regions, to avoid artefacts in the transitions between regions and ensures the reproduction of the global pdf. During the simulation procedure is imposed a spatial continuity pattern for each region and expressed by a regional variogram model. For each region where the estimation is being performed, the simulated value is generated from the cumulative distribution function of that region, defined by the local mean and variance computed from the simple kriging estimate and corresponding kriging variance. This ensures the reproduction of the probability distribution function of each region. The simulated value is added to the conditioning data, to be used in the simulation of the next node of the simulation grid. Changing the seed of the random path for different runs of the simulation procedure, will change the conditioning data therefore, will generate different equally likely realizations of the model. However, all the models will reproduce the global and regional distribution functions of the property of interest, the imposed variogram model of each region and the experimental data at its own location.

4.2.1. Geostatistical seismic inversion using geological analogues

The geostatistical seismic inversion method for frontier areas can be briefly introduced as follows (Figure 14). The method make use of a regionalized geological model, built from seismic interpretation and a spatial continuity pattern imposed by a variogram model, assigned to each interpreted region, to handle with non-stationary patterns. Simultaneously, to handle with the lack of experimental data, common in frontier areas or at early exploration stages, the probability distribution function of the subsurface rock property to be estimated, is built from geological analogues (i.e. analogues well-log data), and used as a priori conditioning data.

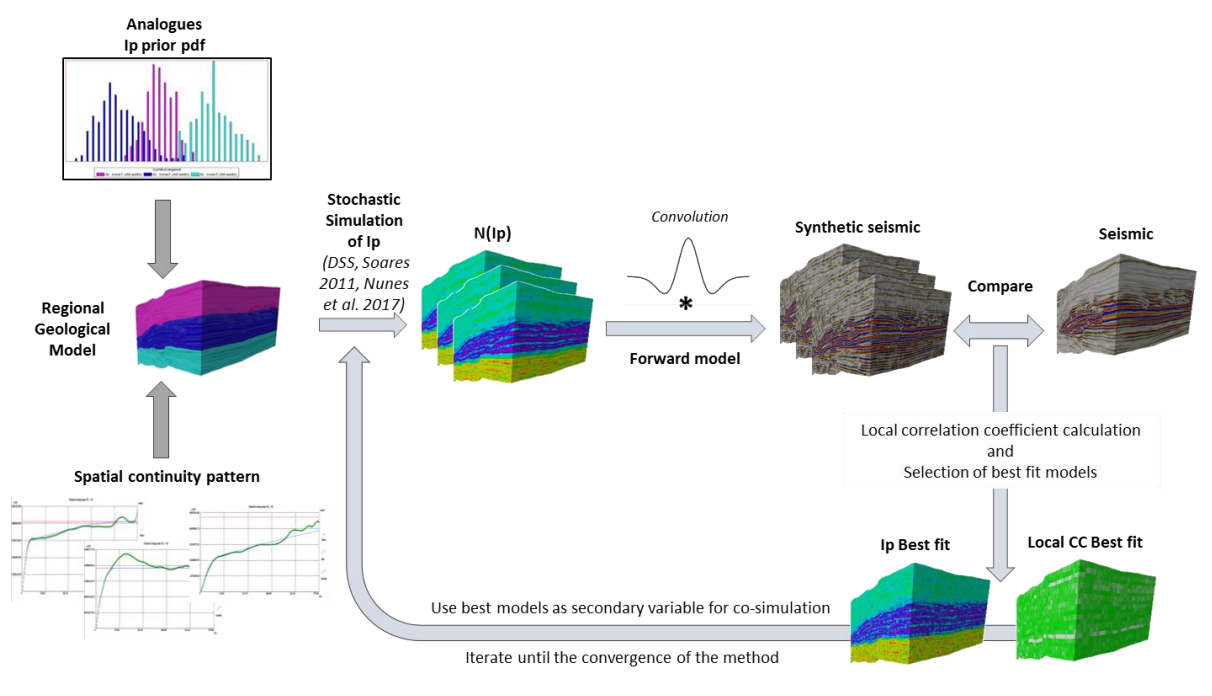


Figure 14 – General workflow of geostatistical seismic inversion for frontier exploration using geological analogues.

One of the first mandatory steps of this procedure is the definition of a regionalized geological model, where the target area, represented by the inversion grid is divided into regions or zones. Subsurface geology can be very complex and characterized by heterogeneous patterns associated to different facies distribution, particularly in deep marine environments, where this can be a relevant issue for reservoir characterization. Dividing the grid volume into regions, has several advantages, one of them is the possibility to better handle the prediction of the spatial distribution of subsurface rock properties, related to geological structures with non-homogeneous geometries (non-stationary spatial patterns) (e.g. turbidite channels). If the regions have a geological meaning, for instance related to geobodies or facies, for each region it is possible to assign a spatial continuity pattern, represented by a regional variogram model, which will be imposed in the simulation step of the inversion procedure, improving the reproduction the subsurface geology. Using only a global variogram model will hardly be representative of a complex geological environment and not suitable to describe geological structures with heterogeneous geometries, such as deep water depositional sedimentary structures. The definition of the regions can be based on the interpretation of the seismic reflection data (Figure 21) or any other procedure or criteria with geological meaning, thus the interpretation of seismic reflection data should include the main geological units visible in the seismic data and be consistent with the stratigraphy of the region. Furthermore, the definition of the regional geological model should also consider the information from outcrop analogues or geological knowledge about the area (i.e. sedimentary basin).

After defining the regional geological model, it is necessary to establish the expected elastic response of the subsurface rocks for each region, assigning a probability function of the rock property to be modelled to each one. As in frontier areas or at early exploration stages the direct measurements (i.e. well-log data) of the subsurface rock properties are often not available, or the available wells are scarce and sparse, these probability distributions function (i.e. histograms) may be inferred from geological analogues, such as analogues well-logs (e.g. from nearby wells). It is important to establish the relation between regions therefore, the probability distribution functions should be representative of the elastic rock properties of a given region and reflect the relation with adjacent geological regions, considering for instance, possible progressive transitions between them (i.e. progressive facies transitions), represented by partially overlapping histograms (Figure 14). The definition of the probability distribution functions is a critical step, which will I have a high impact in the seismic inversion results hence, the integration of additional information from expertizes of different fields (e.g. rock physics, petrophysics, sedimentology) must be considered.

Within seismic inversion procedure, the stochastic sequential simulation step, besides using conditioning data, is imposed a spatial continuity pattern represented by a variogram model for each region. Variograms are normally inferred from the available well-log data, however in the absence of real data, the variogram model can be computed directly from the seismic reflection data, if is ensured the coherence between the horizontal and vertical variogram models and the expected subsurface geology (e.g. dimensions of sedimentary structures). It is expected that the variogram model inferred from seismic reflection data, will overestimate the variogram parameters (i.e. main and minor ranges), due to the seismic resolution. Therefore, the vertical range of the variogram model must represent a commitment between the expected variability of the geological units (e.g. sedimentary sequences) and the sampling interval of the seismic reflection data. Additionally, in the inversion procedure, due to the flexibility of the stochastic sequential simulation step, it is possible to impose a different variogram model to each region and thus estimate more consistent and reliable subsurface geological models.

The geostatistical seismic inversion for unexplored frontier areas using geological analogues can be summarized with the following steps (Figure 14):

1. Define a regional geological model, by dividing the inversion grid into regions, related to the main geological units or facies, using seismic interpretation or other approach;

- Assign to each region a probability distribution function (i.e. histogram) based on geological analogues (e.g. nearby well-log data), which should be representative and in line with the prior geological knowledge about the area. The pdf for each region may be overlapped, reflecting uncertainty regarding the property of interest;
- 3. In the first iteration, stochastic simulation of N realizations of Ip, from the pdf obtained from geological analogues and assign to each region in the previous step, using direct sequential simulation with multi-local distribution functions (Soares 2001, Nunes et al. 2017). During the procedure a spatial continuity pattern represented by a variogram model per region is imposed. If real well-log data inside the area is available, may be used simultaneously;
- 4. Compute *N* synthetic seismograms by convolving the reflection coefficients obtained from the simulated Ip models (in step 3) with a wavelet;
- 5. Compute on a trace-by-trace basis the correlation coefficient (e.g. Pearson coefficient) between synthetic seismic and real seismic data;
- 6. From the *N* realizations of Ip, selection of the traces that produce the highest correlation coefficient between synthetic and real seismic. These traces are stored along with the corresponding correlation coefficients in two auxiliary volumes;
- 7. In the next iteration the auxiliary volumes from the previous step are used in the stochastic sequential co-simulation with multi-local distribution functions (Soares 2001, Nunes et al. 2017) of a new set of *N* Ip models;
- 8. Return to step 3 and continue until the global mismatch between the synthetic and the real seismic data is below a given threshold.

At the end of the iterative seismic inversion process, the resulting rock property models reproduce the probability distribution functions and the spatial continuity pattern imposed by the variogram model assigned to each region. If well-log data is available, the procedure will also reproduce the well-log data at its own location.

4.3. Case Study

The method was applied to a real case study located in the offshore Algarve Basin in the southwestern Iberian margin (Figure 15). Due to the interest in the basin for hydrocarbon exploration, in the last decades two-dimensional and three-dimensional seismic reflection data was acquired. A reduced number of appraisal wells were also drilled (i.e. Algarve-1, Algarve-2, Corvina, Ruivo and Imperador), which are outside the seismic volume used in this study, but are in a nearby surrounding area of the basin. In some wells is reported the

possibility of hydrocarbon generation, mainly gas (Matias 2007, Matias et al. 2011. Furthermore, some intervals of the well-logs show potential reservoir rocks associated to siliciclastic facies, which can be correlated to the seismic data, enabling these wells to be used as geological analogues.

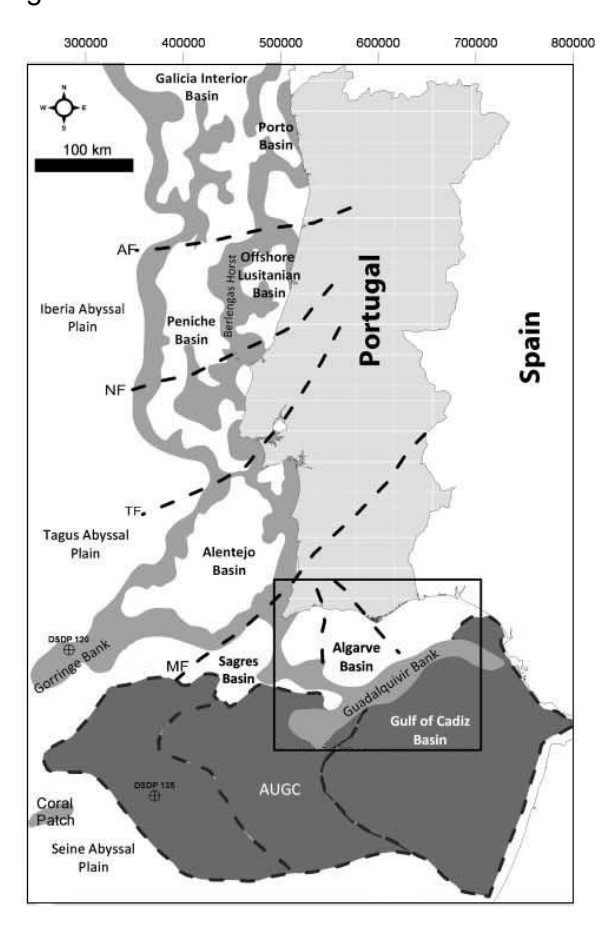


Figure 15 – Map with the location of the Algarve basin in the southwestern Iberian margin (adapted from Matias et al. 2011).

In the seismic reflection data it is possible to identify potential hydrocarbon migration pathways (e.g. gas chimneys, pockmarks) and possible hydrocarbon accumulations, related to bright spots and high seismic amplitudes values, mainly associated to turbidites systems. Nevertheless, it still remain unproved the hydrocarbon generation and accumulations in the Algarve Basin (Matias 2007, Matias et al. 2011).

4.3.1. Geological Setting - Stratigraphy

The Algarve Basin is a Meso-Cenozoic sedimentary basin whose formation is related with two major tectonic events, one in the Mesozoic Era and the other mainly during the Cenozoic Era (Figure 16). The Mesozoic was dominated by four rift phases associated to the opening of the Central-North Atlantic and Tethys oceans, with some episodes of tectonic inversion in

between. In Late Cretaceous period and throughout the Cenozoic the tectonic regime changes to a compressional phase due to the northwest Africa and southwest Euroasia collision (Ramos et al. 2016, Terrinha et al. 2002, 2006).

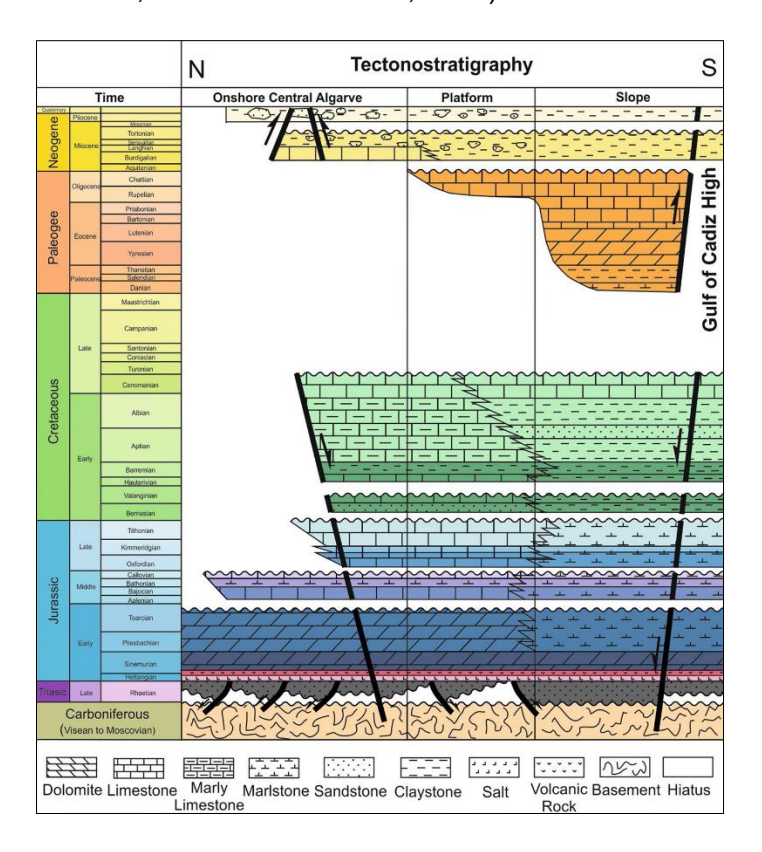


Figure 16 – Simplified Tectostratigraphy of the Algarve basin (adapted from Ramos et al. 2016).

In the Algarve Basin, the sedimentary record goes from early Triassic period to the Holocene, with several hiatus being identified during this period and represented by large erosional unconformities. In the early Cretaceous the sedimentation starts with the deposition of red fluvial siliciclastic sequences, above the basement of Paleozoic age, followed by lacustrine shales, carbonates, dolomites and the Hettangian pelite—evaporites, covered by a volcanic-sedimentary complex (Terrinha et al. 2006, Roque 2007). Only at the bottom of the offshore well Ruivo-1 (Figure 17) was identified the Hettangian evaporites, missing the rest of the Triassic record (Roque et al. 2007, Matias et al. 2011). The Jurassic sedimentation goes from dolomites, limestones to marls. After a hiatus, in the Cretaceous period occurs the deposition of limestones and marly limestones, interbedded with sandstones. In the Late Cretaceous-Paleogene, the tectonic inversion of the basin begins, probably with uplift and erosion occurring, given the lack of sedimentary records in this period (Terrinha et al. 2002, Ramos et al. 2006). The Paleogene period is only recognized in the some of the offshore wells (Figure 17), corresponding mainly to dolomites and limestones (Lopes et al. 2006, Matias et al. 2011).

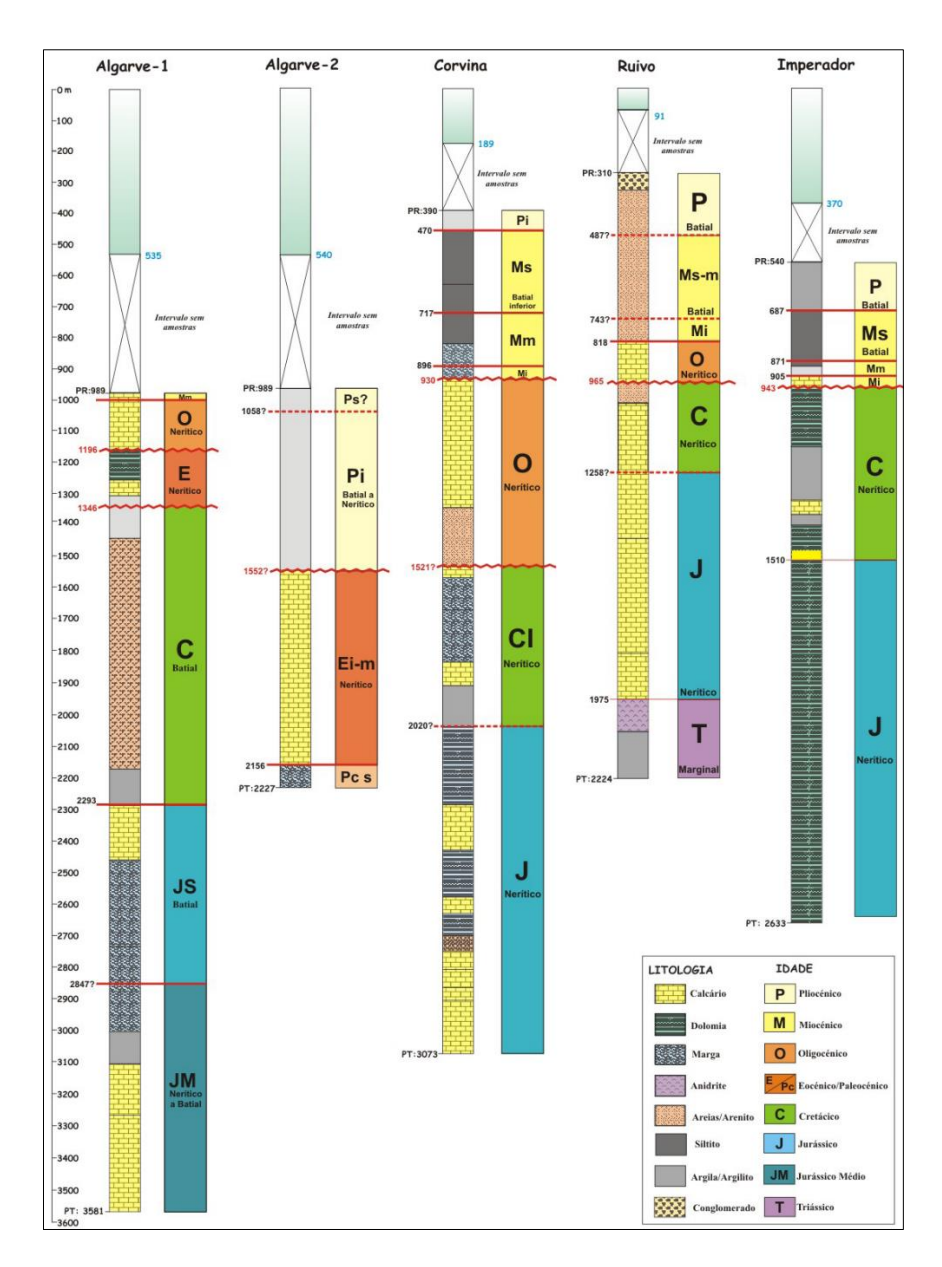


Figure 17 – Lithostratigraphy of the offshore wells from the Algarve Basin by Roque (2007) (adapted from Roque 2007).

The Neogene period comprises two major sequences, represented by limestones and siliciclastic limestones sequences and by a siliciclastic sequence with marine siltstones and fine sandstones. The base of the Miocene is represented by a regional unconformity related to the Neogene inversion, placing these sediments directly over the oldest geological units in some areas of the basin (Ramos et al. 2006, Terrinha et al. 2006). The Algarve Basin was also affected by salt tectonics, what may had influence a potential petroleum system present in the basin (Matias et al. 2011).

4.3.2. Dataset Description

The dataset used for this work was a three-dimensional post-stack seismic reflection data, from where was extracted a target area (Figure 18) and three nearby wells placed outside seismic volume (Figure 19) used as geological analogues. For confidentiality reasons, the wells used as geological analogues will be named W1, W2 and W3.

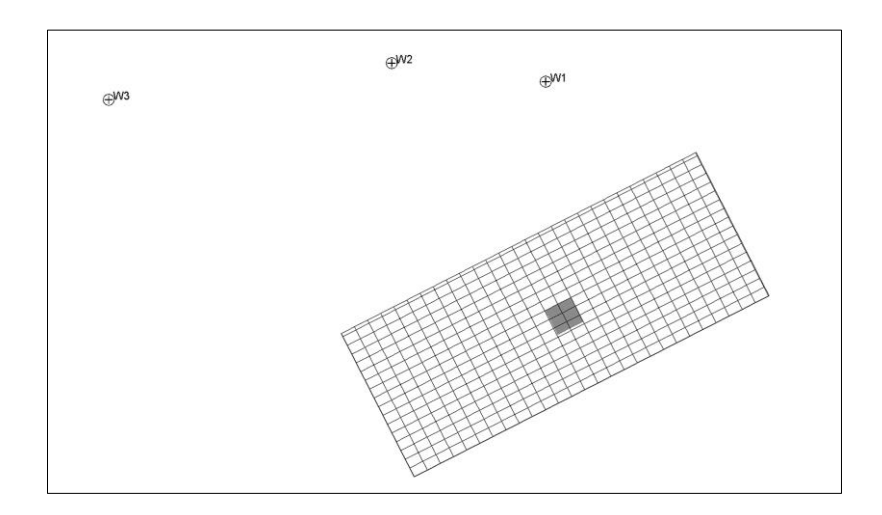


Figure 18 – Map view with the location of the available data. The grid represents the seismic data and the area of study is highlight in gray. The location of the wells used as analogs (W1, W2, W3), is outside the seismic grid area.

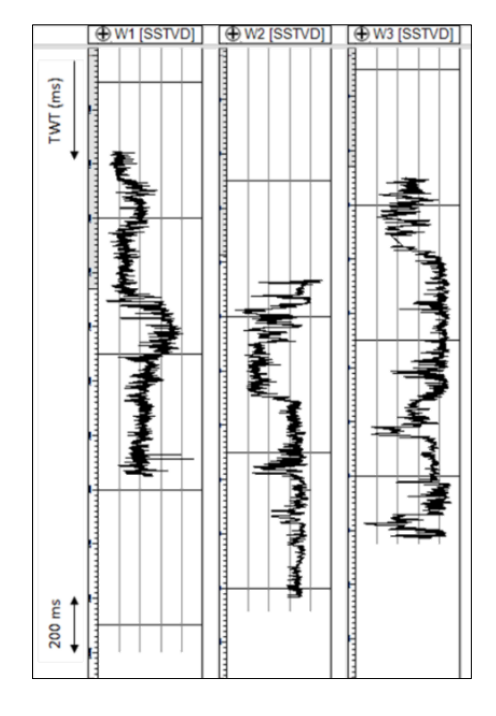


Figure 19 - Ip well-logs of the geological analogues wells, from where the initial a priori probability distributions function was extract, to be used as conditioning data in the seismic inversion procedure.

The sampling interval of the seismic reflection data is 2ms, with an inline and crossline spacing of 18.75m and 12.50m respectively (Figure 18, Figure 22). The geological target is a potential hydrocarbon reservoir, placed in sand channels of a turbidite system (Figure 20, Figure 22), at an average depth of -1600ms (TWT).

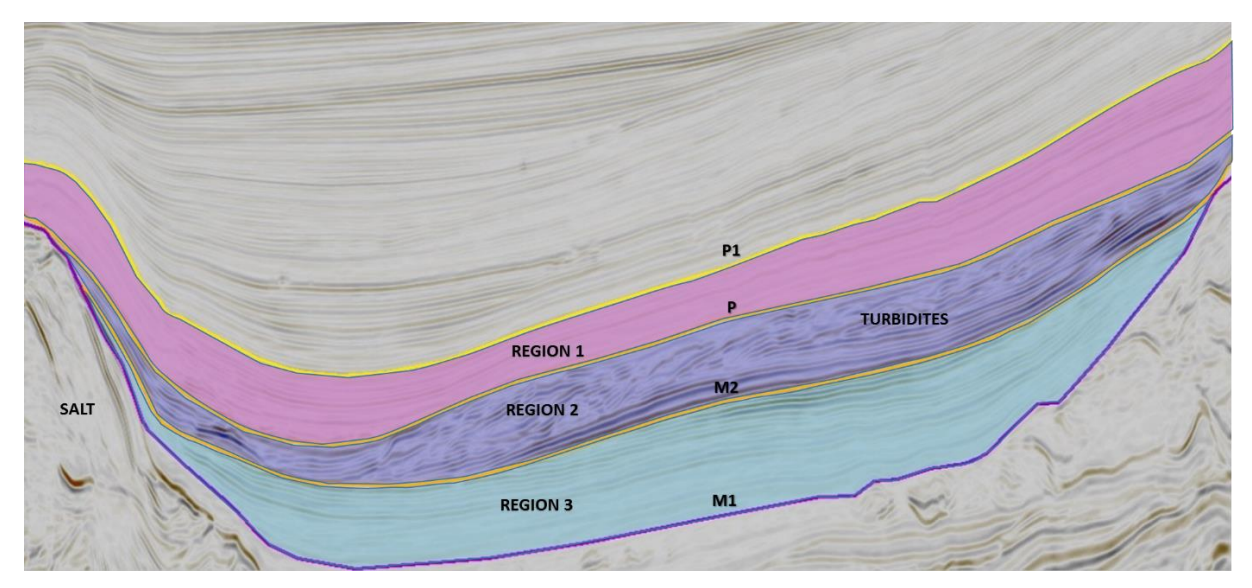


Figure 20 –Vertical section with the seismic interpretation of the three main seismo-stratigraphic units used to define the regional geological model. In region 2 it is possible to visualize the turbidite sequences (M – Miocene; P – Pliocene).

To define the volume corresponding to the target area (Figure 22), first was interpreted the seismic reflection data and defined three main seismo-stratigraphic units: the potential reservoir, the overburden and the underburden (Figure 20, Figure 21). The interpretation of the seismic reflection data and its correlation with the analogues well-log data, was based on the seismo-stratigraphic units defined by Roque (2007). The inversion grid corresponding to the target area was defined, with a grid dimension of 198 by 279 by 190 grid cells in *i-*, *j-* and *k-* directions respectively.

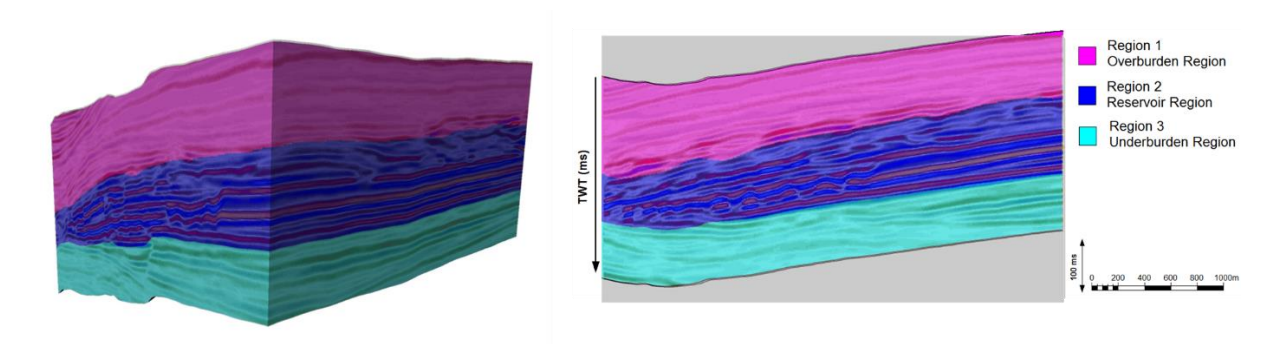


Figure 21 – [Left] 3D volume and [Right] Vertical section of the regional model with the three main seismic units: Region 1 – overburden region; Region 2 – reservoir region; Region 3 – underburden region.

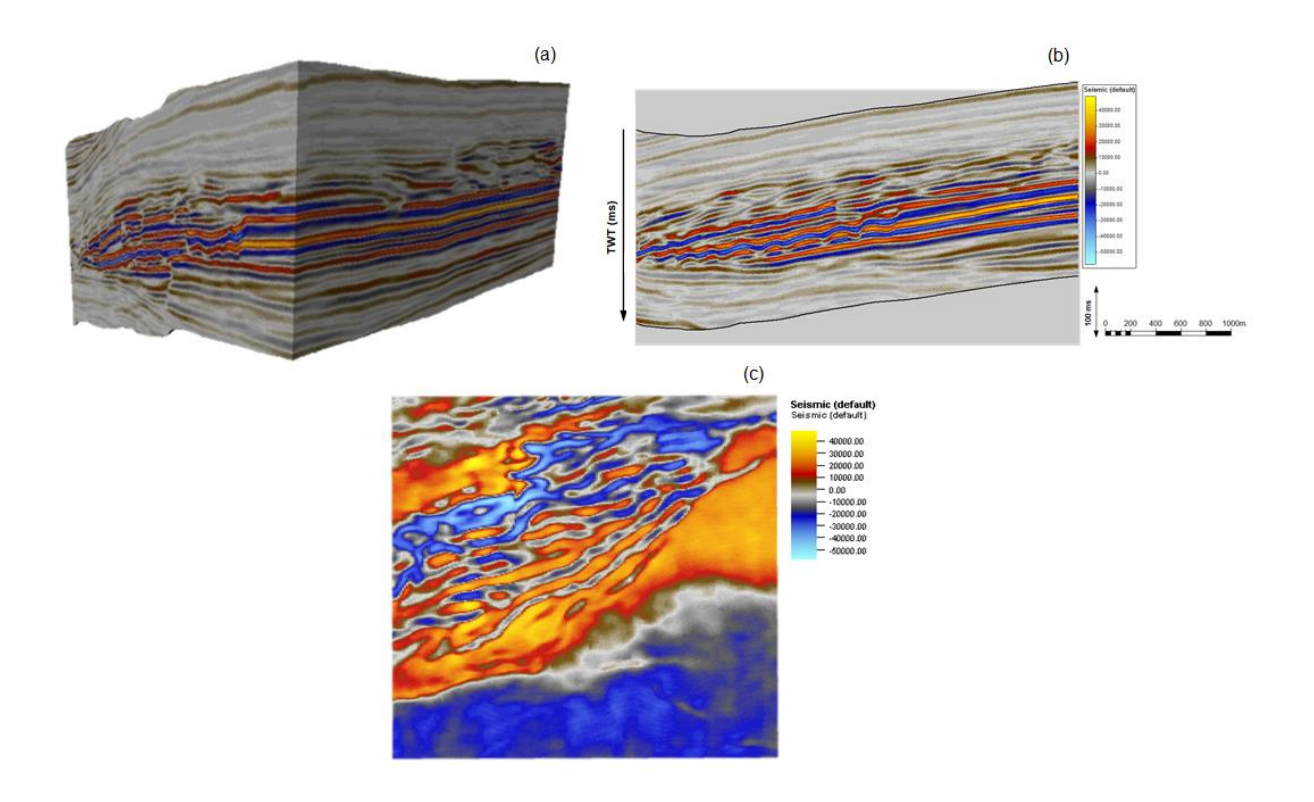


Figure 22 – Seismic reflection data for the area of interest: (a) seismic volume, (b) vertical section and (c) time slice from region 2 showing the turbidite channels.

As the proposed geostatistical seismic inversion method using geological analogues, is driven by stochastic sequential simulation and co-simulation with multi-local distribution functions (Ruben et al. 2017), it was assigned to each region of the grid a probability distribution function (*pdf*) (Figure 23) representative of the rock property of interest (i.e. acoustic impedance (Ip)). The Ip well-log data was firstly derived from the velocity and density well-logs using Equation 13. The definition of the initial acoustic impedance *pdf* from the Ip well-logs of the three analogues (Figure 19) was based on the correlation with the interpreted seismic data as previously explained and considering the reference literature (e.g. Mavko et al. 2009).

Taking advantage of the regionalization of the inversion grid, it was imposed a different variogram model to each region (Figure 24), aiming to better describe the spatial continuity pattern of Ip for each region, considering spatial heterogeneities. The horizontal variograms were computed from the seismic data, due to its high spatial coverage and given the lack of well-log data inside the grid volume. The vertical variograms were obtained from the analogues wells, due to its high vertical resolution and representativeness of the geological depositional sequences.

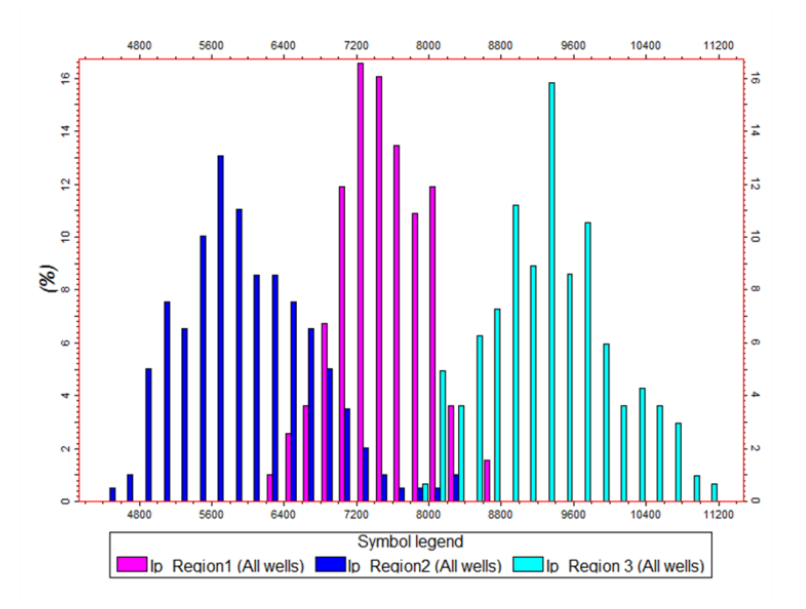


Figure 23 – Initial probability distributions functions of acoustic impedance for each region, obtained from well-logs analogues.

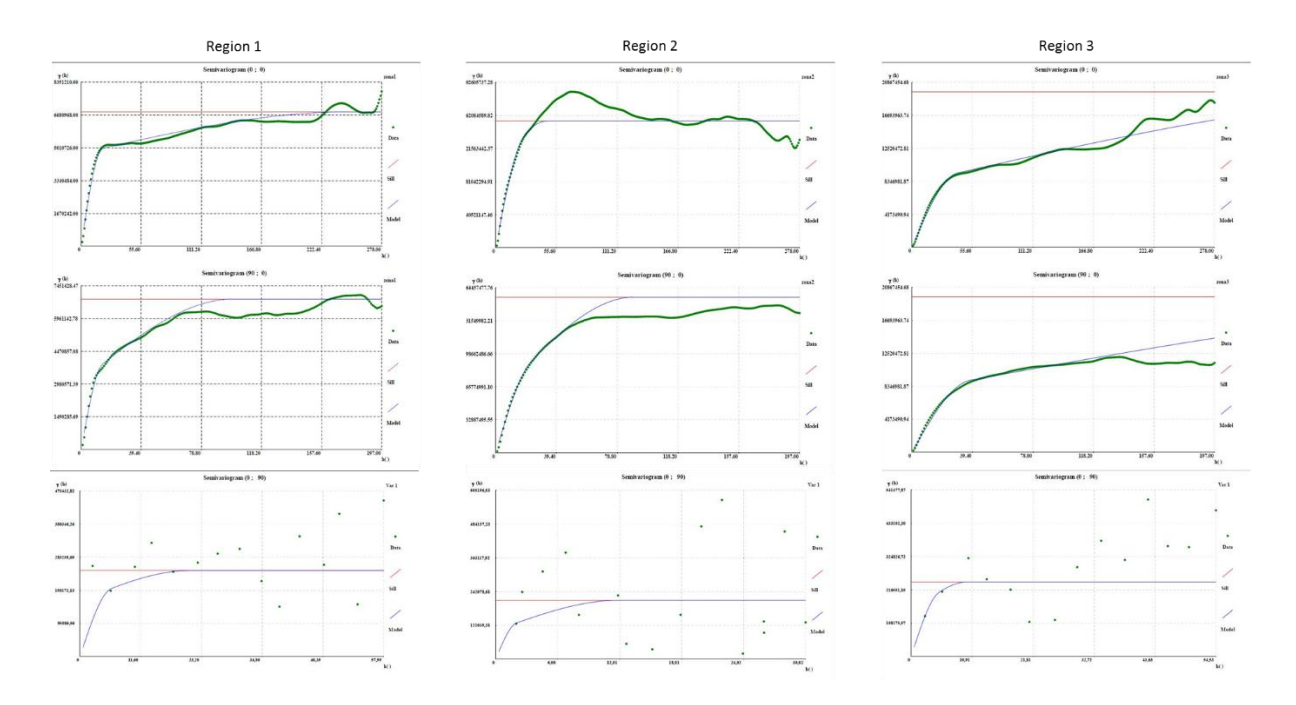


Figure 24 – Variogram models for each geological region: [Top] horizontal main direction, [Middle] horizontal minor direction, [Bottom] vertical direction.

In the inversion procedure, it was used a statistical wavelet representative of the seismic data from the time interval of interest. The wavelet was extracted from the seismic reflection data with a conventional wavelet extraction statistical technique (i.e. Weiner-Levinson filters) using a commercial software, where the statistical wavelet amplitude spectrum was computed from the square root of the autocorrelation amplitude spectrum of the seismic

traces within the interval of interest, with a time window of 1000ms. The statistical wavelet was not tied to the seismic reflection data, due to the lack of wells inside the prospect area and no uncertainty was assumed, simplifying the problem, although the quality of the extracted wavelet may has a high impact on the rock property inverse models.

The geostatistical seismic inversion using geological analogues was performed with six iterations, each one with thirty-two realizations models of Ip, conditioned simultaneously by a regionalization model with three sub-regions, each one with an Ip pdf inferred from the analogues well-logs.

4.4. Results

The proposed geostatistical seismic inverion method using gelogical analogues converged after six iterations, where the global correlation coefficient between real seismic data and the synthetic data was 0.85 (Figure 25). Nevertheless, the values vary for each defined region that is, in region 1 corresponding to the overburden, the correlation coefficient was 0.80, for the potential reservoir (region 2) and for the underburden (region 3) the correlation coefficient was 0.89 and 0.70 respectively (Figure 26).

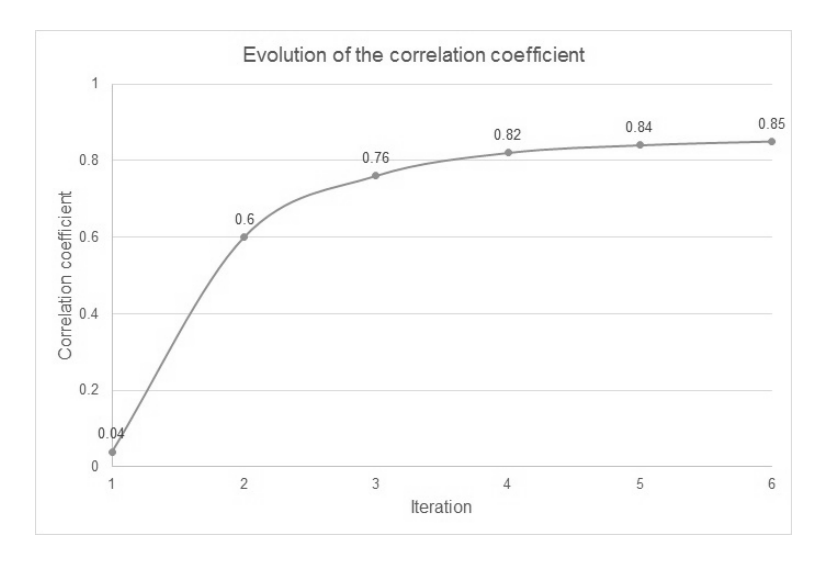


Figure 25 – Evolution of the correlation coefficient over the iterative process of seismic inversion. The convergence of the method occurs in iteration 6.

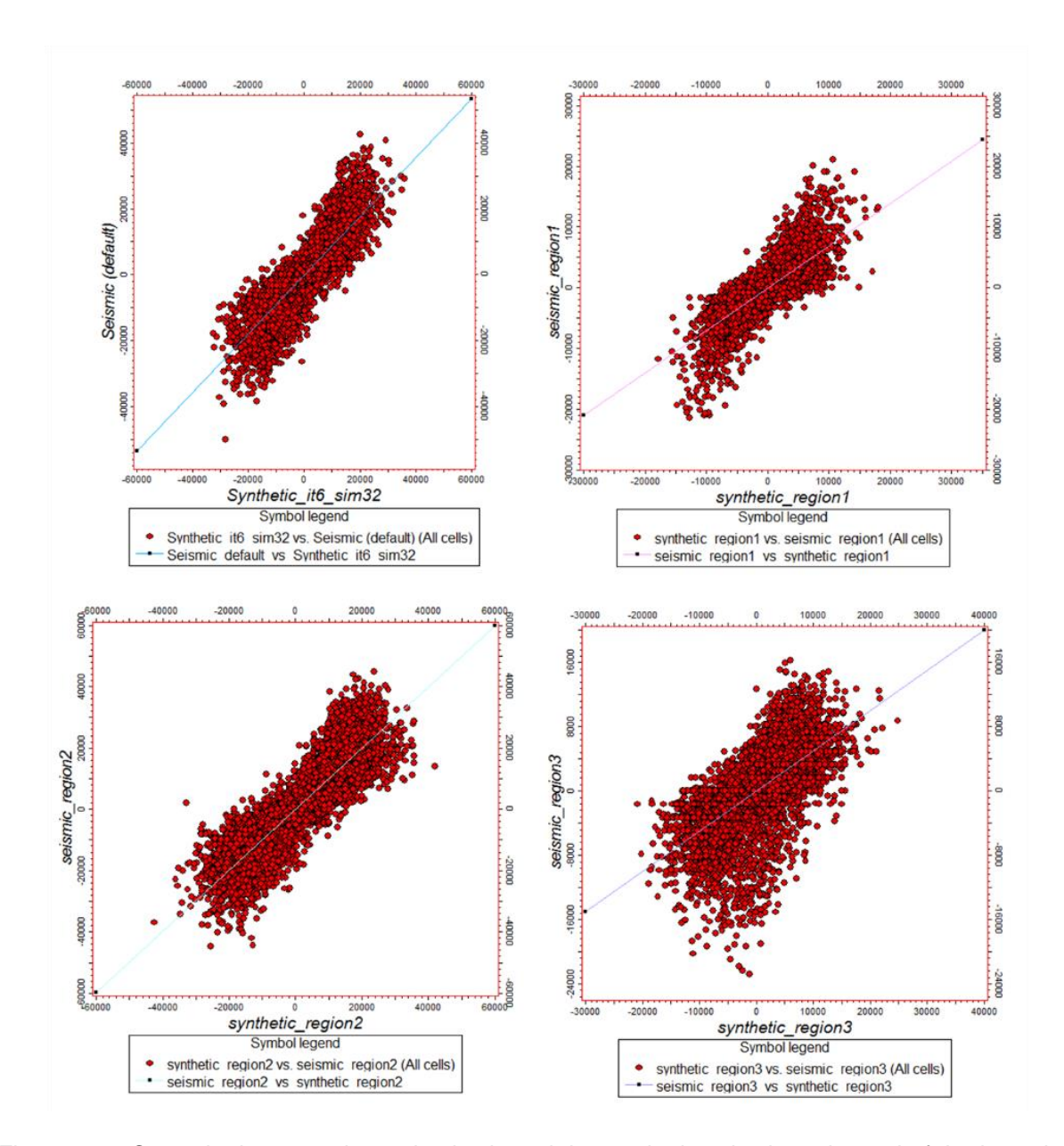


Figure 26 – Crossplot between the real seismic and the synthetic seismic at the end of the inversion procedure. The correlation coefficient for the: [Top left] entire volume is 0.85; [Top right] for Region 1 (overburden) is 0.80; [Bottom left] for Region 2 (reservoir) is 0.89; [Bottom right] Region 3 (underburden) is 0.70.

The main seismo-stratigraphic units in the seismic data (Figure 22) are reproduced in the synthetic seismic (Figure 27), regarding their location and spatial continuity patterns, particularly it is possible to clearly identify the sedimentary structures (i.e. turbidite systems) (Figure 27) in the reservoir interval (region 2 (Figure 21)). The original seismic amplitude content is also reproduced in the synthetic seismic (Figure 27). Still, the residuals between the real seismic data and the synthetic seismic data (Figure 28), highlights some differences between them, mostly related to the transitions between regions.

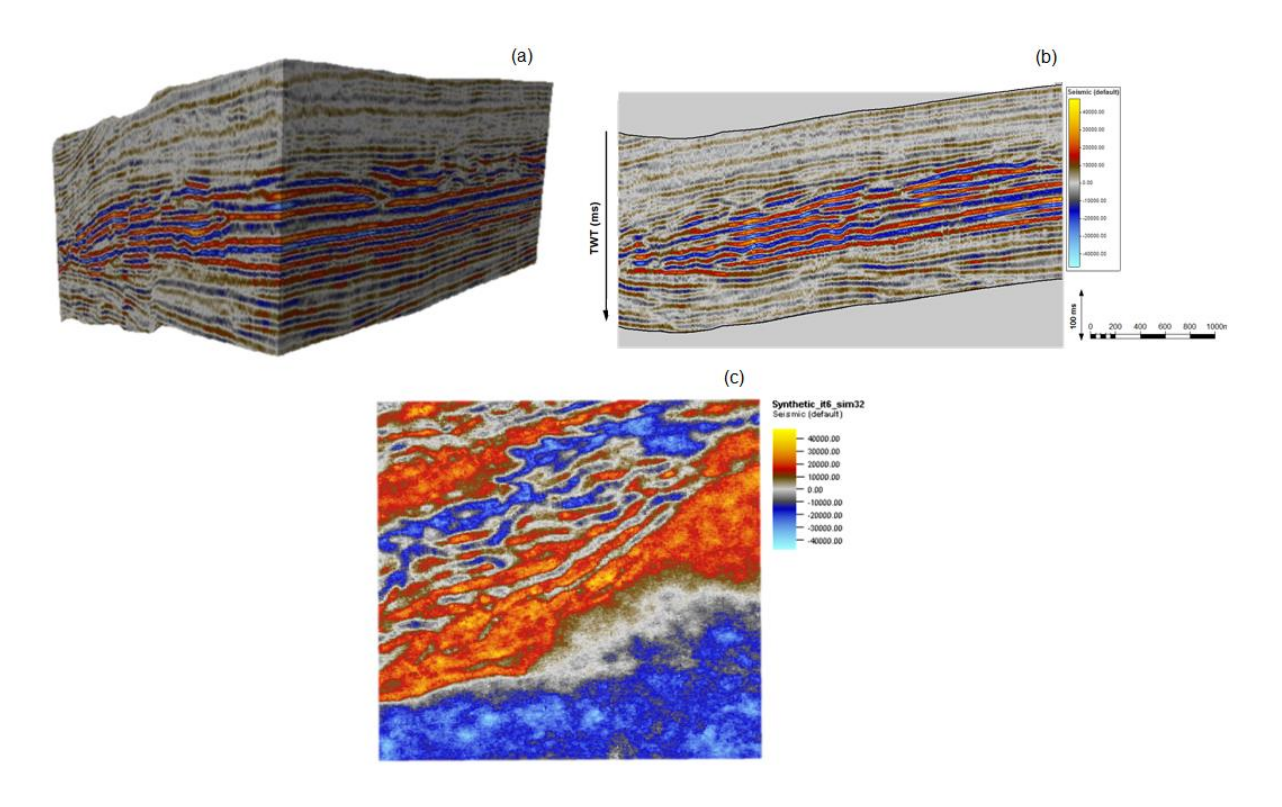


Figure 27 – Synthetic seismic computed from the acoustic impedance best-fit model in the last iteration: (a) synthetic seismic volume, (b) vertical section and (c) time slice from region 2 showing the turbidite channels.

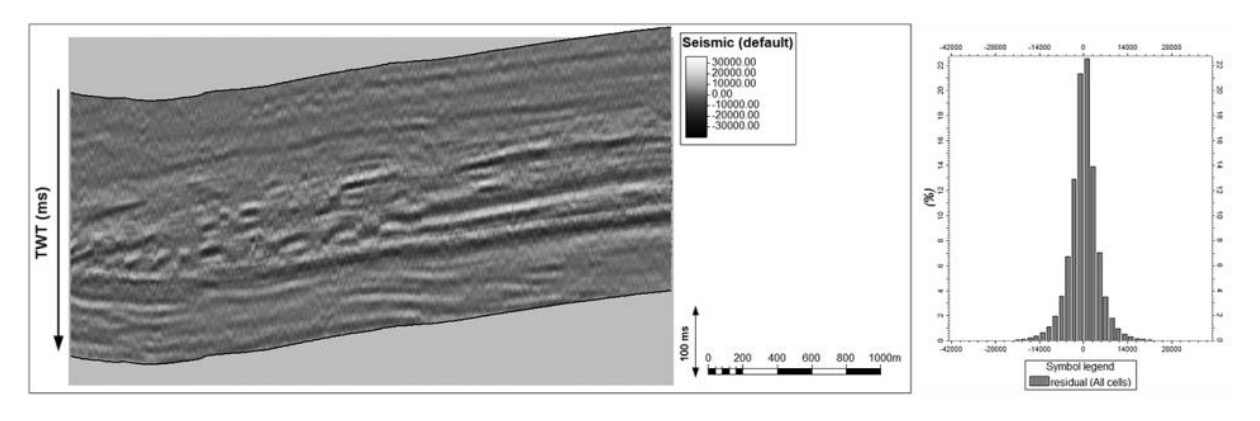


Figure 28 – [Left] Vertical section of the residuals between real seismic data and the synthetic seismic and; [Right] corresponding distribution function.

In Figure 29 is showed the Ip best-fit inverse model, where is possible to visualize in the vertical section, the channelized features associated to a turbidite systems, in the reservoir interval (region 2). It is important to highlight that the resulting subsurface models, are high-resolution models, able to capture the spatial continuity pattern of the main geological structures, along with some smaller details. Moreover, the retrieved elastic models of acoustic impedance, reproduces the probability distribution function of each region. In this

elastic model it is clear the differences between regions, associated to different facies, where the transitions between them, show variations in the depositional environment. In region 2 (middle region) are the lowest values of acoustic impedance, corresponding to the reservoir rocks, showing some potential targets related to turbidite channels.

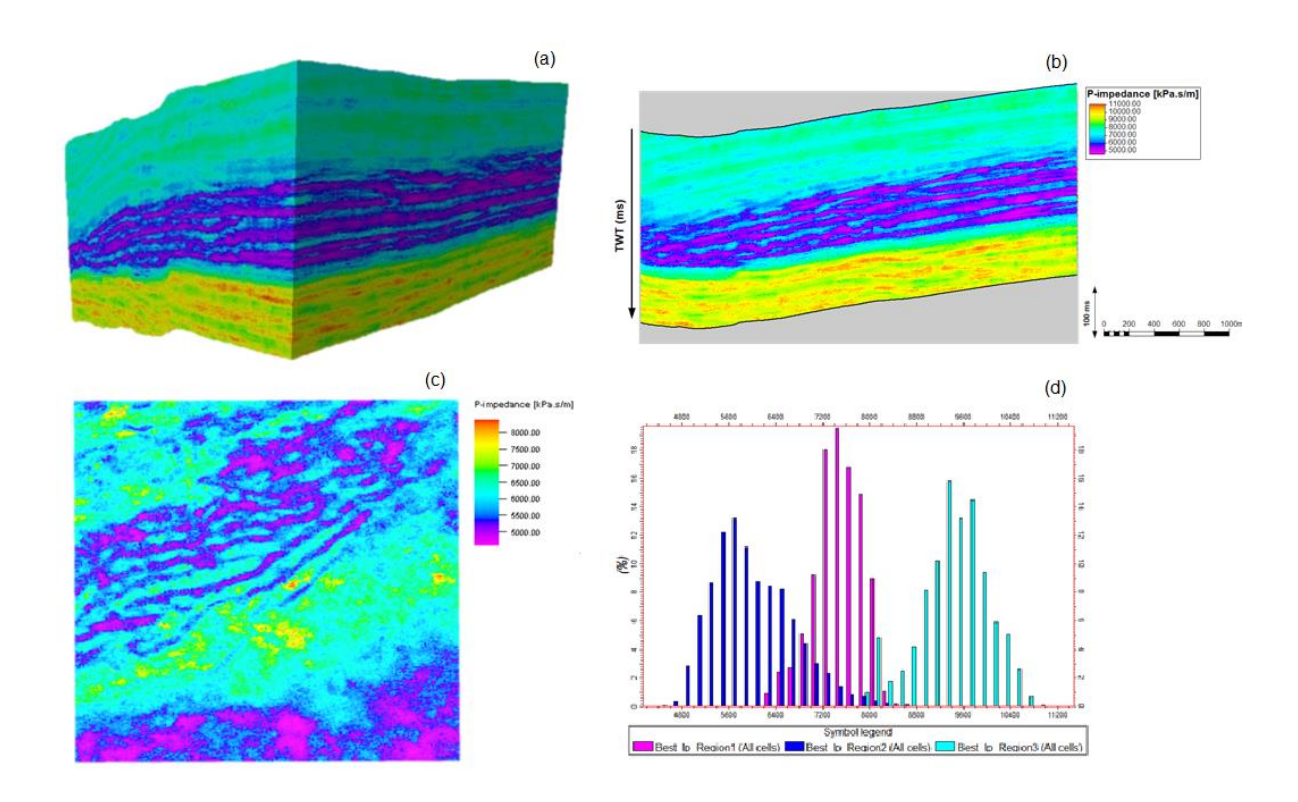


Figure 29 –Best-fit inverse model of acoustic impedance from 6th iteration: (a) Best Ip volume, (b) vertical section and (c) time slice from region 2 showing the turbidite channels. The lower Ip values (purple) are associated to turbidite channels. (d) Probability distribution function (pdf) of the Best-fit Ip model, reproducing the initial Ip pdf.

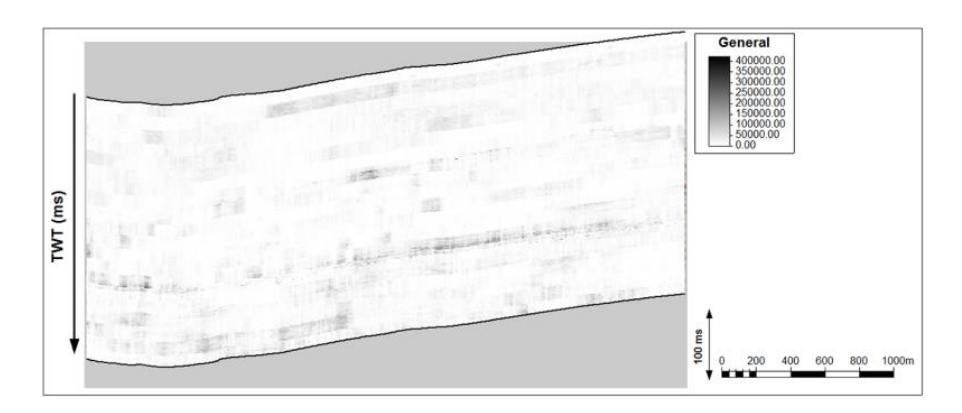


Figure 30 – Vertica section of variance computed from the 32 realizations of Ip models from the last iteration. Higher variance areas are associated with a higher uncertainty in the estimate Ip values.

The uncertainty assessment of the inverted Ip models was obtained by computing the variance of the Ip realization models from the last iteration (Figure 30). Although, the resulting synthetic seismic volumes are globally correlated with the real seismic, there are some areas where the inversion procedure struggled to converge, thus, these areas will remain with higher uncertainty, meaning high variance values. Nevertheless, the retrieved elastic models are reliable and geological consistent with the knowledge about the area.

4.5. Discussion

The geostatistical seismic inversion method introduce herein, applies to unexplored areas (i.e. frontier areas) or to early exploration stages, aiming to overcome the absence of well-log data inside of the area of interest, by allowing the direct integration of geological information from analogues into the inversion procedure. Simultaneously, aims to improve the prediction of the spatial continuity patterns of the subsurface rock properties in heterogeneous geological environments, by dividing the inversion grid into geological regions, assigning different rock properties distributions and different spatial continuity patterns to each region. This method was successfully applied to a real case study in an unexplored area, where geological analogues from nearby appraisal wells were used, allowing predict three-dimensional high-resolution models of acoustic impedance (Ip) and associated spatial uncertainty.

The regional geological model, used in the application example, to divide the inversion grid into regions (Figure 21), was built from seismic interpretation. Its use, shows improvements predicting the rock properties spatial continuity patterns, particularly useful for non-stationary environments. The predicted elastic models and the corresponding synthetic seismic data were able to reproduce the main sedimentary patterns (e.g. turbidite channels), where is also possible to identify subtle structures of potential interest. Moreover, the resulting best-fit elastic model (Figure 29) shows the benefit of integrating geological knowledge from analogues, where the a priori Ip distribution functions (i.e. histograms) were set after interpretation of appraisal wells from correlation with seismic data.

The global correlation coefficient between the observed seismic data and the synthetic data, computed from an elastic model of the last iteration was 0.85. In some regions (i.e. reservoir rocks) the correlation reaches 0.90. Nevertheless, in some areas mainly related to transitions between regions, the mismatch between the observed seismic reflection data and the synthetic seismic is high, remaining these areas with high uncertainty.

It is important to mention that in the present work, the impact on the inversion results of the uncertainty associated with the extracted wavelet was not evaluated. However, it is known

that the representativeness of the estimated wavelet will greatly affect the quality and reliability of the inverse elastic models. Nevertheless, the rescaling to the original amplitude values of the extracted wavelet was considered in the definition of the a priori distribution functions of Ip, to ensure the plausibleness and match of the synthetic seismic amplitude values with the observed seismic data. Hence, in the proposed seismic inversion method, due to the lack of direct measurements, the reproduction of the amplitude values will work as a proxy, to validate the resulting elastic models of the inversion procedure.

Like in deterministic seismic inversion methods, the resulting elastic models from the proposed method were inferred from seismic reflection data, without any direct measurement obtained from well-log data of the rock property of interest. Determinist methods rely on initial guess model to estimate a smooth representation of the subsurface geology.

In the proposed method the definition of the a priori geological model, with its region definition and rock properties probability distribution functions has its own associated uncertainty, which is add to the uncertainty of the generated models. Contrary to deterministic seismic inversion methods, the proposed geostatistical seismic inversion method presented herein, produce high-resolution subsurface models from which is possible to quantify the associated uncertainty, what is of outmost importance for reservoir characterization, particularly in unexplored areas and at early exploration stages. By using a regionalized model based on seismic interpretation and geological analogues as conditioning data for the seismic inversion procedure the resulting subsurface elastic models are more geological consistent and reliable.

4.6. Conclusion

At the end of the seismic inversion procedure, the global and regional probability distribution functions are reproduced, as well as the variogram model for each region. The relation between acoustic impedance regional probability distribution functions is also preserved, respecting the transitions between the geological regions. The retrieved models are geological accurate and reliable, given the available data and the knowledge about the area, where in some regions of the target area, the match between the inverted models and recorded seismic data ranges from 0.85 to 0.90.

The proposed geostatistical seismic inversion method was successfully applied for reservoir characterization of an unexplored frontier area. The method proves to have advantages over deterministic methods, commonly used in these cases, and which are only able to predict smooth representations of the subsurface geology, not allowing the uncertainty quantification. The method showed that dividing the inversion grid into a regional geological

model, representative of the subsurface geology and imposing regional variogram models to the seismic inversion procedure, improves the prediction of the spatial continuity patterns of the subsurface rock properties. Furthermore, in the absence of direct measurements of the subsurface (i.e. well-log data), conditioning the seismic inversion procedure to a priori distribution functions of elastic properties from geological analogues, allows predicting accurate and reliable subsurface models, what can be very useful for reservoir characterization and uncertainty assessment, particularly in unexplored frontier areas or at early exploration stages.

5. Updating Local Anisotropies with Template Matching during Geostatistical Seismic Inversion

Paper published in Mathematical Geosciences and presented at XI CNG - Congresso Nacional de Geologia. Coimbra, Portugal 2023.

<u>Pereira A.</u>, Azevedo L. & Soares A. (2023). Updating Local Anisotropies with Template Matching during Geostatistical Seismic Inversion, Mathematical Geosciences 55:497–519. (*Published in Open Access, licensed under a <u>Creative Commons Attribution 4.0 International License</u>)*

5.1. Abstract

Iterative geostatistical seismic inversion methods are widely used to predict petro-elastic rock properties from seismic reflection data. When the model perturbation technique uses twopoint geostatistics, these methods struggle to reproduce complex and non-stationary geological environments such as faults, folds and highly variable depositional systems. These limitations are often due to the use of a global variogram model to express the expected spatial continuity pattern of the property of interest. In complex geological environments a global variogram model might be unable to detect local heterogeneities and rapid variations of lithology, and result in non-realistic geological models. Local heterogeneities might be predicted from the data using seismic attribute analysis, which can be imposed during geostatistical seismic inversion as local anisotropy models. In these approaches, the information about the local spatial continuity patterns is fixed and will guide and condition the entire inversion procedure, which can lead to errors and uncertainty in areas where this approach is not appropriate due to high local uncertainty of geological features, given the poor signal-to-noise ratio of the data or the presence of important geological features below the seismic resolution. This work proposes an iterative geostatistical seismic inversion method which iteratively updates the local spatial continuity models based on the trace-by-trace misfit between observed and predicted seismic data. The update of the local spatial continuity models aims at surpassing the limitations of the seismic inversion methods that use a fixed a priori variogram model. The method is successfully illustrated in a challenging two-dimensional synthetic dataset and in a real case application. The results demonstrate the benefit of updating iteratively the imposed local spatial continuity patterns based on the data misfit. The inverted models are capable of better predicting the location of faults and reproducing the continuity of sinuous channels.

Keywords: Local anisotropies, Self-update, Template-matching, Geostatistical seismic inversion.

5.2. Introduction

Seismic inversion methods are widely used to predict the spatial distribution of the subsurface geology. They allow transform seismic amplitudes into two- or three-dimensional numerical models of elastic rock properties and facies (e.g., Bosch et al. 2010; Grana et al. 2022). The relationship between seismic data and predicted models can be summarized by Equation 17,

Equation 17
$$d_{obs} = F(m) + e,$$

where d_{obs} is the seismic data, m is the subsurface properties of interest, and e represents the measurement errors and assumptions about the physical model under investigation during data processing (Tarantola 2005; Tompkins et al. 2011). F is the forward model that provides the mapping between the observed data and the subsurface properties (Tarantola 2005). As F^{-1} is unknown, predicting the petro-elastic rock properties from seismic data is a challenging nonlinear inverse problem, ill-posed and with multiple solutions (Tarantola 2005).

Seismic inversion methods can be divided in two main groups with different assumptions, advantages and limitations (Francis 2006; Bosch et al. 2010; Filippova et al. 2011; Tylor-Jones and Azevedo 2022). Deterministic seismic methods (e.g., Russell and Hampson 1991), can be summarized as optimization procedures that start with an a priori elastic model, which is perturbed to minimize the mismatch (or maximize the similarity) between real and synthetic seismic data. Deterministic methods provide a single best-fit solution, which is a smooth representation of true variable and heterogeneous subsurface geology. Hence, they do not provide any uncertainty assessment of the inverted models.

The second group of seismic inversion methods are statistical-based (Grana et al. 2022). Contrary to deterministic methods, they allow assessing the uncertainty of the inverse solution. Under this framework, Bayesian linearized seismic inversion methods (e.g., Buland and Omre 2003; Grana and Della Rossa 2010; Grana 2016; Grana et al. 2017) assume a multi-Gaussian distribution of the model parameters and the errors within the data, and the linearization of the forward model. With these assumptions, the analytical description of the posterior distribution is also a multi-Gaussian distribution.

On the other hand, stochastic seismic inverse methods are iterative approaches that use global stochastic optimizers such as simulated annealing (Sen and Stoffa 1991; Ma 2002), genetic algorithms (Mallick 1995, 1999; Boschetti et al. 1996; Soares et al. 2007), neighbor algorithm (Sambridge 1999) and stochastic sequential simulation and co-simulation (Bortoli

1993; Haas and Dubrule 1994; Grijalba-Cuenca and Torres-Verdin 2000; Soares et al. 2007; Nunes et al. 2012; Azevedo et al. 2015; Azevedo and Soares 2017; Azevedo et al. 2018; Pereira et al. 2019, 2020).

Bayesian linearized seismic inversion methods have lower computational costs when compared against iterative stochastic seismic inversion methods. However, Bayesian linearized inversion methods have a limited exploration of the uncertainty space in lieu of exact a priori information (Tarantola 2005).

In the case of iterative geostatistical seismic inversion methods, the computational burden is due to the use of stochastic sequential simulation and co-simulation methods as model perturbation techniques. This issue has been tackled with the parallelization of the simulation algorithms to GPU (Ferreirinha et al. 2015) or the use of proxies to reduce the dimensionality of the model parameter space (e.g., Nunes et al. 2019). One of the advantages of geostatistical seismic inversion methods is the reproduction of the first and second statistical moments as computed from the observed data (i.e., the well-log data) and the reproduction of a variogram model used to express the expected spatial continuity pattern of the subsurface property of interest. This capability is ensured by the stochastic sequential simulation and co-simulation methods (e.g., Soares 2001).

Nevertheless, these methods have some limitations when applied to complex sedimentary and/or structural geological environments as they may lead to inverted models that are geologically unrealistic. These limitations are mainly related to the use of a single and global variogram to describe the spatial continuity pattern of the subsurface property, which is unable to represent the spatial distribution of the true geology.

In a Bayesian inversion framework, the issue of non-stationary spatial continuity models has been addressed by including varying spatial covariance matrices (e.g., Rasmus et al. 2020; Erlend et al. 2013; Bongajun et al. 2013). In iterative geostatistical seismic inversion, this limitation can be overcome by imposing local variogram models, which represent the local spatial continuity pattern in the rock property prediction (e.g., Pereira et al. 2020). The local variogram anisotropy models can be computed a priori and obtained, for example, from seismic attribute analysis of the observed seismic data. But, imposing local variogram models, which are fixed during the entire iterative procedure, can lead to the propagation of errors through the iterations if the assumed spatial continuity model is unreliable. This might happen in areas of low signal-to-noise ratio, where the local anisotropy variogram models are highly uncertain due to discontinuous seismic reflections.

This work proposes a self-update approach of the local variogram models (i.e., local anisotropy models) by integrating, at each iteration, the mismatch between predicted and

observed seismic data through the iterative seismic inversion approach. In the application examples shown herein, the local variogram models are updated using the template matching technique, due to is relatively low computational cost. However, alternative methods could be applied. Iteratively updating this information avoids fixing a single local variogram model that might reflect noise areas of incoherent information. The updated variogram models constrain the stochastic sequential co-simulation of a new set of realizations in the subsequent iterations of the seismic inversion (Figure 31).

In the next section, the proposed iterative geostatistical seismic inversion method is described in detail, and the concept of self-updating of local anisotropies using template matching is explained.

To evaluate the performance of the proposed method, the following section shows its application to synthetic and real examples. The self-updating inversion method is benchmarked against an iterative geostatistical seismic inversion (GSI), with a global variogram model, and to geostatistical seismic inversion with local anisotropies (GSI-LA) with fixed local variogram models, estimated a priori from seismic attribute analysis (Pereira et al. 2020). The three methods were compared in terms of the reproduction of the true seismic amplitude, the spatial continuity of the synthetic seismic and acoustic impedance models and corresponding facies prediction. Facies were classified from the acoustic impedance models co-simulated during the last iteration of the geostatistical seismic inversion, using an acoustic impedance threshold. Channels with low acoustic impedance values (i.e., sand channels) were classified as sand, and high acoustic impedance values were classified as mud (i.e., background facies). In addition, the Ip models were plotted in a multidimensional scaling space (MDS) computed with a Modified Hausdorff distance (e.g., Cox and Cox 1994; Scheidt and Caers 2009; Azevedo et al. 2014).

This section is followed by the discussion of the results and ends with the presentation of the main conclusions.

5.3. Methodology

This section details the proposed iterative geostatistical seismic inversion method with self-update local anisotropy models. The proposed method can be divided into four main steps: (1) initial data and stochastic sequential simulation of Ip models; (2) forward modelling; (3) local anisotropy update; and (4) stochastic update of the model parameters with stochastic sequential co-simulation.

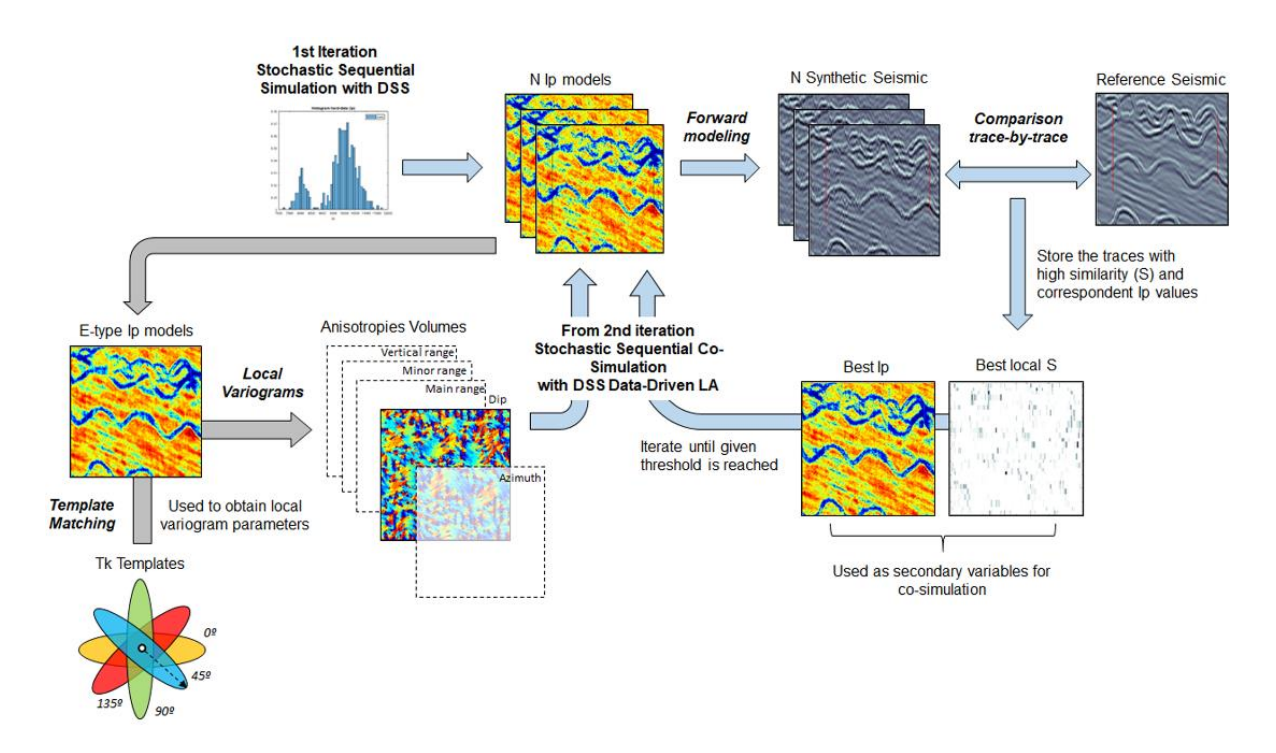


Figure 31 – Schematic representation of the iterative geostatistical seismic inversion with self-update local anisotropies (GSI-LA-Self-Update).

As the proposed method builds upon the global stochastic seismic inversion (GSI; Soares et al. 2007), its main steps are first described. This summary is followed by a detailed description of the steps introduced under the scope of this work.

5.3.1. Geostatistical Seismic Inversion

The global stochastic inversion (Soares et al. 2007) inverts fullstack seismic data for Ip. It can be summarized in the following sequence of steps:

- 1. In the first iteration, stochastic sequential simulation (e.g., direct sequential simulation (Soares 2001)) of *N* realizations of Ip from well-log data and using a global spatial continuity pattern expressed by a unique global variogram model.
- 2. Computation of *N* synthetic seismograms by convolving the reflection coefficients obtained from the simulated Ip models (in step 1) with a wavelet.
- 3. Analysis of the trace-by-trace similarity (S) between the synthetic and real seismic traces as summarized by Equation 18,

Equation 18
$$S = \frac{2*\sum_{s=1}^{N} (x_s*y_s)}{\sum_{s=1}^{N} (x_s)^2 + \sum_{s=1}^{N} (y_s)^2},$$

where x and y are the real and synthetic seismic traces, respectively, with Ns seismic samples. S is bounded between -1 and 1 and expresses how two seismic traces are similar in terms of amplitude content and waveform. If synthetic and real traces are similar, then S is close to one.

- 4. From the *N* realizations of Ip, the elastic traces that produce the highest similarity between synthetic and real seismic are stored in an auxiliary volume with the corresponding *S* value.
- 5. In the next iteration the auxiliary volumes from the previous step are used in the stochastic sequential co-simulation (e.g., Soares 2001) of a new set of *N* Ip models.
- 6. Return to step 2 and continue until the global mismatch between the synthetic and the real seismic data is below a given threshold.

All Ip models simulated and co-simulated during the iterative procedure reproduce the well-log data at their locations, and the histogram as retrieved from the Ip-log data. This iterative geostatistical seismic inversion method assumes a single variogram model of Ip, which is normally inferred from the existing well-log data and reproduced in all the realizations simulated and co-simulated during the iterative procedure.

The GSI assumes the stationarity of the spatial continuity pattern, which is hardly valid in complex geological environments. This limitation is explored in the present work by including local variogram models during the model perturbation step. The local variogram models are updated iteratively based on the data misfit computed from the previous iteration. The proposed iterative geostatistical seismic inversion methodology is detailed next.

5.3.2. Geostatistical Seismic Inversion with Self-Update Local Anisotropies

The main idea of the proposed geostatistical seismic inversion consists in updating the local spatial covariances (i.e., local variogram models), based on new secondary information (i.e., the mismatch between observed and synthetic seismic data). Information about local anisotropies is inferred directly from the data, and updated iteratively. The self-updating procedure aims at correcting unreliable estimates about the local spatial continuity patterns, as the iterative inversion converges. The proposed inversion approach uses the geostatistical seismic inversion framework (Section 5.3.1). The inversion starts with a global stationary covariance model $\mathcal{C}(h)$, assumed valid and representative of an entire area. The average impedance model of the ensemble of realizations generated at each iteration (i.e., the expect Ip value at each location x_0) is scanned by a pattern recognition classification technique to detect and quantify local non-stationary geological patterns, for example, local

anisotropic covariances $C_{\theta}(h)$, where θ represents the direction angles and anisotropy ratios of the local geological features (e.g., channels, fractures, shale barriers). The following section describes in detail the template matching technique, as an example for pattern recognition classification.

Once local covariance models $C_{\theta}(h)$ are modelled, they are allocated to the corresponding spatial location x_0 . At the subsequent iteration, the geostatistical co-simulation is performed with updated local models of covariances (Horta et al. 2010; Caeiro et al. 2015).

The geostatistical seismic inversion with self-update local anisotropies (GSI-LA-Self-Update) can be summarized in the following sequence of steps (Figure 31):

- In the first iteration, N Ip models are generated as described in step 1 for GSI (Section 5.3.1). During the stochastic sequential simulation, a global variogram model inferred from the available well-log data is used. Each of the geostatistical realizations is transformed into synthetic seismograms, and S (Equation 18) is computed.
- 2. At the end of the first iteration, the pointwise average (i.e., E-type) model of the generated Ip realizations is scanned by the pattern recognition classification algorithm. In template matching (Section 5.3.3), an ensemble of elliptical templates, T_k, with different combinations of anisotropy ratios and azimuths defined a priori, is used. Each template mimics different possible local variogram models with different parameters; the best template match (see Section 5.3.3 for details) is retained at each location and used as local anisotropy in the next iteration.
- 3. A new set of *N* lp models is then co-simulated with local anisotropies (Horta et al. 2010) revealed by the best template obtained in step 2.
- 4. The iterative procedure repeats steps 2 to 4 until a given number of iterations is reached or the global *S* between the real and synthetic seismic data is above a given threshold. In the application examples shown herein, the number of iterations was set to six.

The inversion method is introduced to invert fullstack seismic data for acoustic impedance (Ip), but its extension to the elastic domain (e.g., geostatistical seismic amplitude-versus-angle (AVA) inversion) (e.g., Azevedo et al. 2018) is straightforward. In these methods, the templates to estimate the local spatial continuity models would be deployed in the auxiliary models computed at the end of each iteration, for each elastic property (i.e., density, P-wave and S-wave velocities) individually.

5.3.3. Templates Matching and Local Anisotropy Estimation

Templates are commonly used in image processing for feature selection, matching, enhancement or detection (e.g., edge or object detection) (Brunelli 2009). In general templates correspond to kernels or vectors that can take any geometrical shape. They are used as a moving window that scans an image and tests a set of matching criteria between the image and the template. Template matching is used within the application examples shown herein due to its low computational cost and facility of implementation. Alternative methods for local anisotropy estimation could be used. This selection will impact the results obtained.

In the proposed method, the templates are used in the pointwise average model (E-type) of the N realizations of Ip models generated at a given iteration. At the first iteration, the E-type model is not informative regarding local anisotropies, as all the Ip realizations were generated without conditioning to the seismic data. However, as the iterative procedure assimilates the seismic data, it starts showing the expected spatial patterns observed in the seismic but with higher spatial resolution, originated by the stochastic sequential simulation. These patterns learn from the data and will appear stronger or weaker depending on the local trace-by-trace similarity S.

The set of templates (Figure 32) scans the E-type Ip model, calculated from the ensemble of Ip models generated at a given iteration, with pre-defined parameters such as direction and anisotropy ratio.

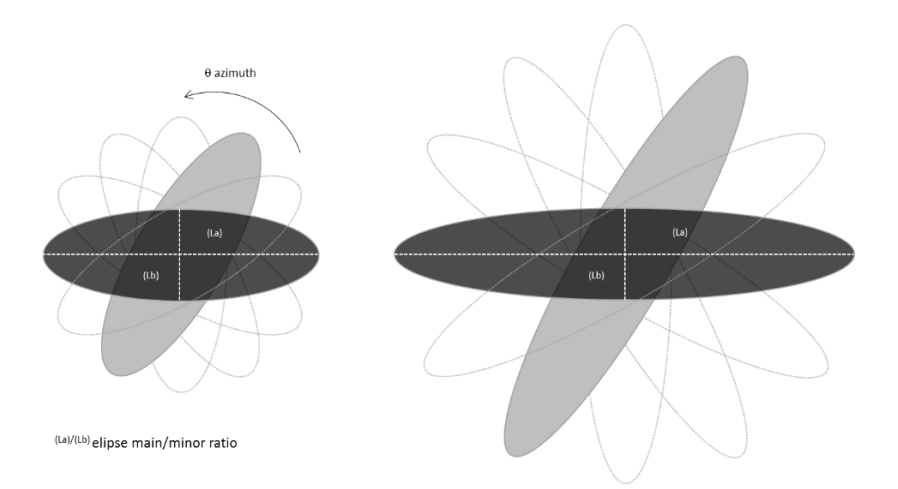


Figure 32 – Ensemble of pre-defined elliptical templates T_k , mimicking different local variogram models with different parameters (direction, main ^(La) and minor ratios ^(Lb)). The templates set corresponds to all possible combinations between these three parameters.

At each location, the variance between all the Ip values of a given template is computed. The template with the minimum variance is selected as representative of the local spatial

continuity model. This approach acts as a proxy of a local experimental variogram and modelling. The template matching criterion is the minimum variance inside the template T_k (Figure 33) and is summarized by Equation 19,

Equation 19
$$\text{matching criterion } _{T_k} = min \left(\left(\frac{1}{N_{T_k} - 1} \right) \times \sum (x_i - \mu)^2 \right),$$

where xi are the grid cell values inside the template T_k , μ is the mean of these values, and N_{Tk} is the total number of grid cells in template T_k . The local variogram models, as revealed by the selected templates, will be used in the next iteration to generate the new ensemble of lp models.

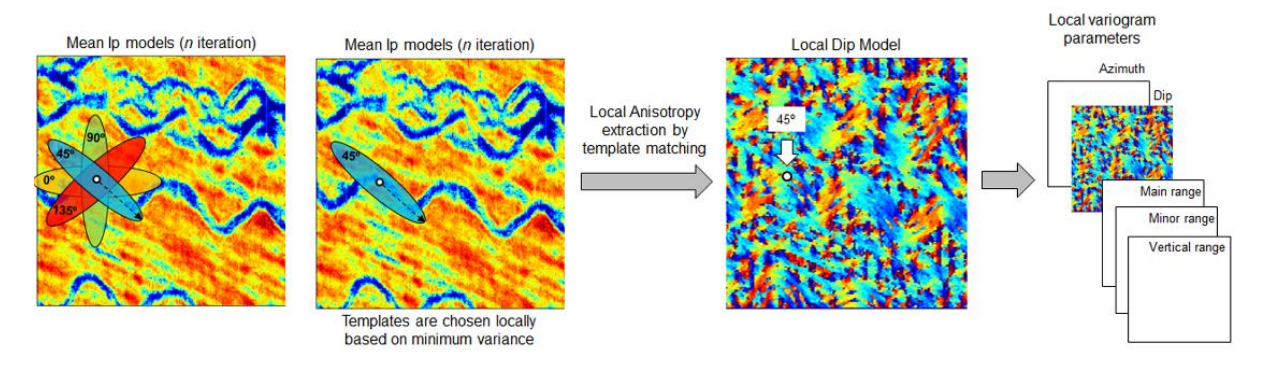


Figure 33 – Example of templates matching the true image and creation of the auxiliary anisotropy model expressed by the local variogram parameters obtained from the selected template.

5.4. Application Examples

The proposed method was tested in two different cases. The first one corresponds to a two-dimensional synthetic fullstack seismic section and the second to a real fullstack seismic. Both application examples represent complex geological environments related to deep water sedimentation and tectonics. The seismic data show patterns of non-parallel seismic reflectors related to the presence of turbidites channels, faults and folded horizons. This complex geology results in a highly anisotropic spatial continuity pattern of the subsurface petro-elastic properties, making the reproduction of these geological features a challenge in geostatistical seismic inversion, when using a global spatial continuity pattern expressed by one global variogram model.

5.4.1. Synthetic Case Application

This synthetic dataset mimics a deep-water sedimentary environment corresponding to a turbidite system with typical meandriform channels with low acoustic impedance values (Figure 34). The background facies is characterized by high Ip values with a strong anisotropy, contrasting with low Ip values modelled with an isotropic variogram model within the channel facies. The spatial distribution of Ip in the background facies was modelled with a spherical variogram model oriented with a constant dip of 27°. The range used for the major direction was set to 20 grid cells and the vertical variogram to 5 grid cells. The channels were modelled with an isotropic variogram model and a large horizontal variogram range of 200 grid cells and 2 grid cells in the vertical direction.

The data set includes a synthetic two-dimensional seismic profile (i.e., true seismic data) with a 200 by 200 cells grid dimension in i- and k- directions, respectively (Figure 34a). The observed seismic data do not include any noise, and the wavelet used to compute it was the same as applied in the inversion (i.e., no uncertainty about the wavelet was included in this study). Noise-free seismic data were considered because the non-stationary nature of the geological background is already a challenge for geostatistical methods based on two-point statistics (i.e., stochastic sequential simulation and co-simulation). Part of the conditioning data set are two wells at positions i = 25 and i = 185 with Ip logs from 50 to 180 ms and 60 to 170 ms, respectively.

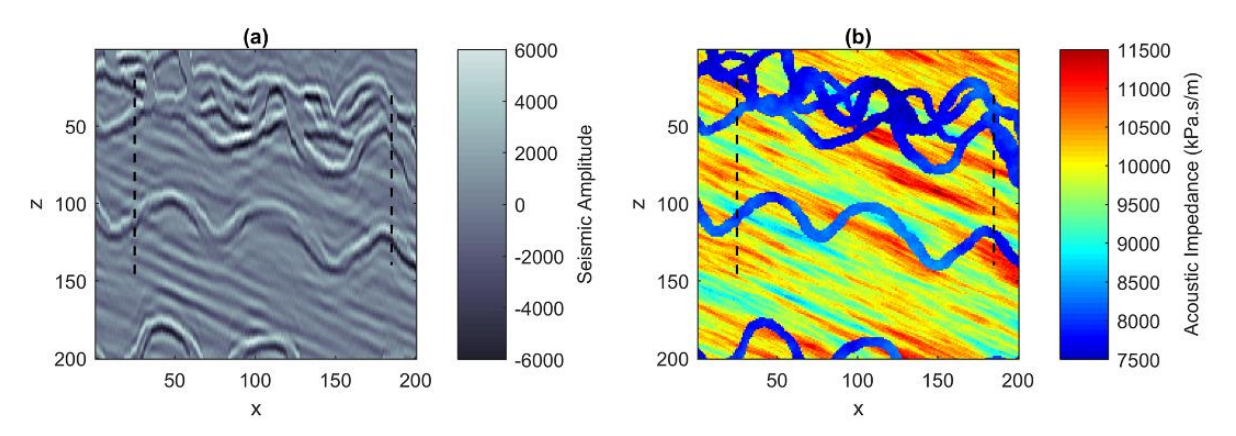


Figure $34 - \mathbf{a}$ True fullstack vertical seismic section; \mathbf{b} True acoustic impedance model. The vertical black lines represent the location of the wells used as conditioning data in the geostatistical seismic inversion.

The template matching used a set of ninety-six elliptical templates generated with different azimuths ranging from 0° to 360° with a step size of 15°. The set of templates also include different main and minor variogram ranges ratios reproducing different combinations of

possible local variogram model parameters (Figure 32). The main range varies with an interval from 12 to 24 grid cells, and the minor range varies between 4 and 8 grid cells, both with a sept size of 2. The local spatial continuity models estimated with template matching and used as input in the GSI-LA-Self-Update are shown in Figure 35. The proposed geostatistical seismic inversion was parameterized with six iterations generating thirty-two realizations of acoustic impedance models at each iteration. As described above, the simulation procedure was conditioned by a local variogram obtained from template matching and updated after each iteration. The results obtained were compared with those resulting from GSI and GSI-LA.

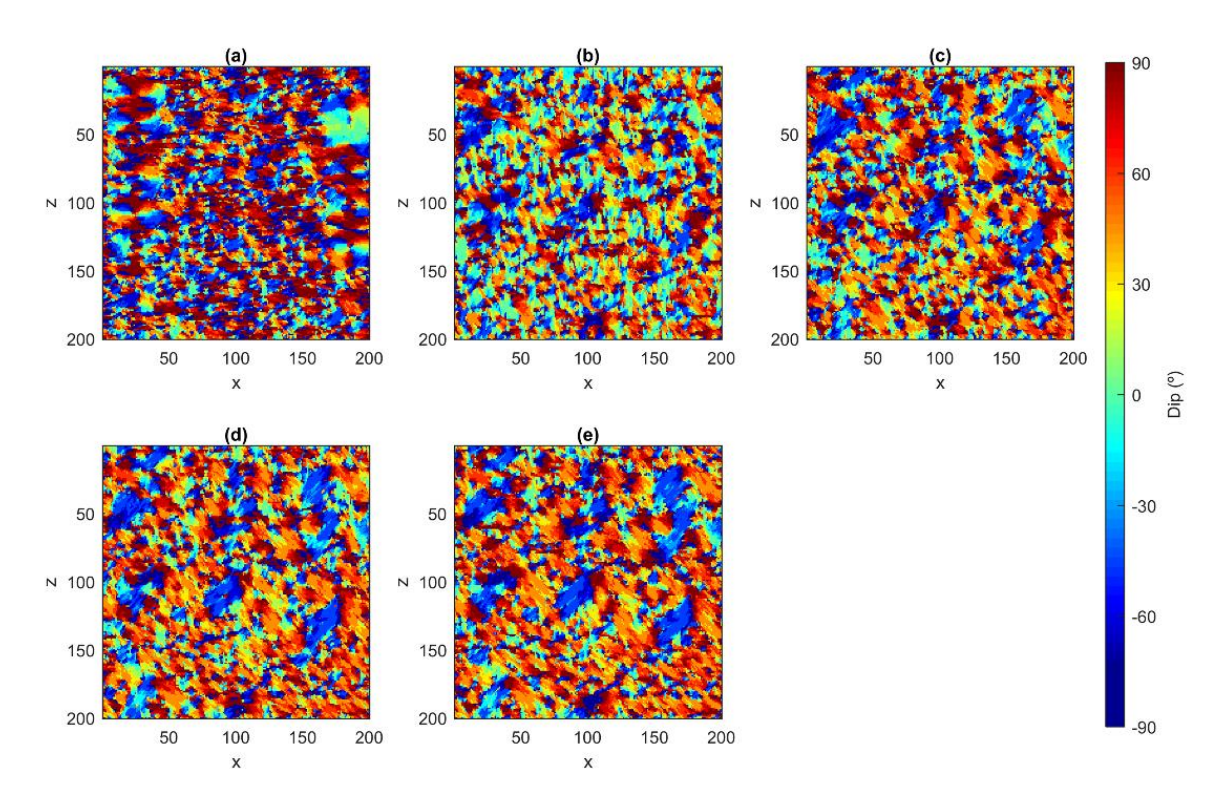


Figure 35 – Evolution of the local spatial continuity models estimated with template matching at the end of each iteration and used in GSI-LA-Self-Update for the next iteration: **a - e** 1st iteration to 5th iteration, respectively.

To ensure a fair comparison of the proposed method with GSI and GSI-LA, all inversions were parameterized equally in terms of data conditioning, number of iterations and simulations per iteration. The main difference between the runs lies in the variogram parameterization. GSI uses a global omnidirectional spherical variogram model with isotropic horizontal ranges of 20 grid cells and vertical range of 5 grid cells, and a pre-defined local variogram model in GSI-LA computed from seismic attributes (Figure 36).

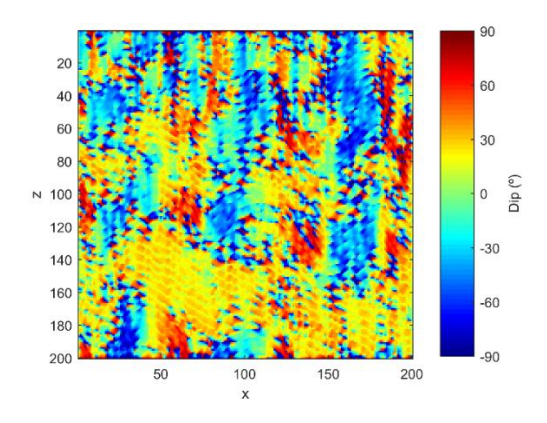


Figure 36 – Local spatial continuity model used in GSI-LA.

The proposed method converged after six iterations, achieving a global similarity S of 0.89 between the true and the predicted synthetic seismic (Figure 37). The performance of GSI-LA-Self-Update is similar to GSI-LA in terms of global similarity S (Equation 18). The global convergence of both geostatistical inversion methods with local anisotropy shows that using local information about the expected spatial continuity pattern leads to a significant improvement when comparing to the use of a global variogram model (Figure 37).

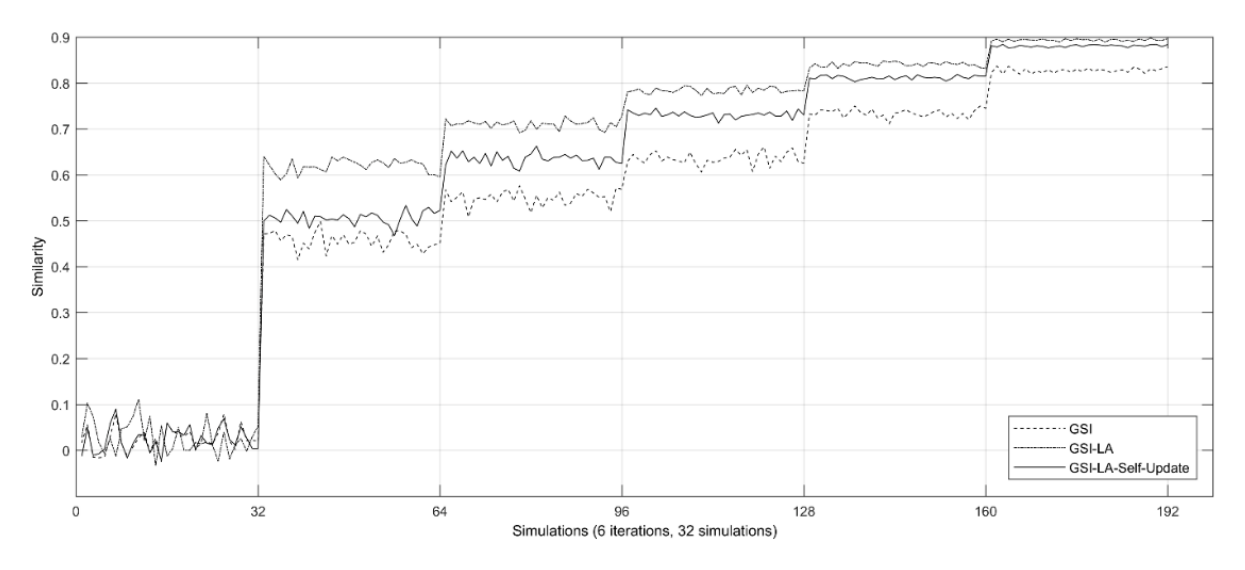


Figure 37 – Comparison of global similarity (S) evolution for the three geostatistical inversion methods considered.

Furthermore, the synthetic seismic predicted with the proposed method reproduce the location of the main seismic reflections and the amplitude content of the true seismic data (Figure 38). However, there are some areas where the proposed method struggled to converge, and hence are areas with higher uncertainty, corresponding to lower local *S* associated with abrupt changes in the spatial continuity of the true seismic reflections. These

regions are also associated with poorer estimations of the local continuity patterns. Figure 35 shows the evolution of the local variogram models through the six iterations. While the first iteration is non-informative, the model predicted at the end of the inversion does reproduce the main spatial features observed in the true one (Figure 36), with larger dip values.

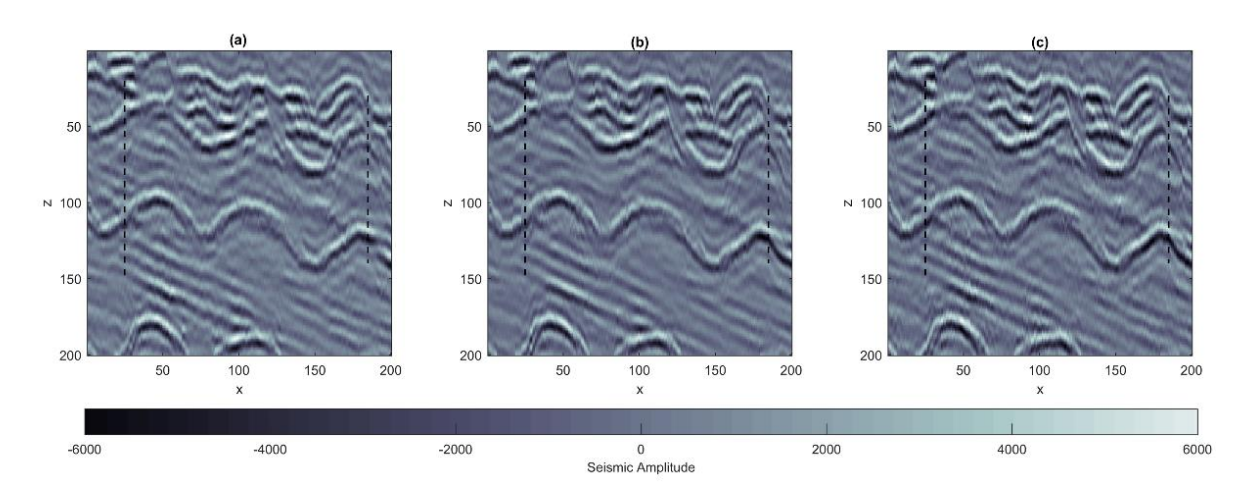


Figure 38 – Synthetic fullstack seismic vertical section calculated from the Ip mean model with: **a** GSI; **b** GSI-LA; **c** GSI-LA-Self-Update.

In seismic inversion, a good match between observed and synthetic seismic is not sufficient to ensure a good model of the subsurface properties. Due to the non-unique nature of the seismic inverse solution, considerably different elastic models might originate similar data. Figure 39 compares the average Ip model computed for the three geostatistical seismic inversion methods here studied. For illustration purposes, the pointwise average Ip model (i.e., E-type model) computed from the stochastic realizations, co-simulated during the last iteration of the inversion, is shown (Figure 39).

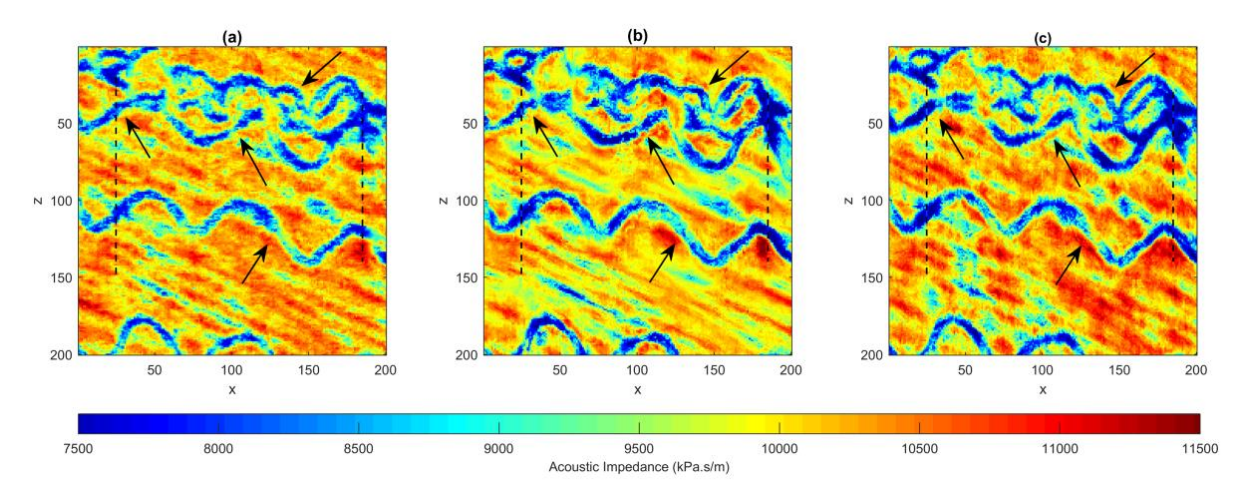


Figure 39 – Vertical sections of Ip mean models from last iteration for the three tested methods: **a** GSI; **b** GSI-LA; **c** GSI-LA-Self-Update. The lower Ip values correspond to meandriform sand-rich channels, and the high Ip values to mud-rich sedimentary sequences. Black arrows point to low Ip values, related to sand channel facies, highlighting the improvement introduced with the proposed method.

The mean Ip model shows a good match in terms of geological spatial continuity pattern, particularly of the meandriform channels, represented by low Ip values. At the large-scale, all the tested methods retrieve Ip models similar to the true one. However, the spatial continuity and connectivity within the channels is more evident with the proposed method of self-update. Also, sharp discontinuities are better predicted when using local information updated iteratively based on the data mismatch (Figure 39).

To evaluate the predicted models in terms of their spatial continuity, all realizations of Ip from the last iteration resulting from the three inversion methods were classified into two facies, using a single threshold in the Ip domain. Ip values below or equal to 8 500 kPa.s/m were classified as sand, corresponding to channel facies, and Ip values above 8 500 kPa.s/m were classified as mud, corresponding to muddy background facies. Predicting reliable facies is of outmost importance for volumes calculation and reserve estimation.

The comparison of the most likely facies models with the true facies model for the three methods is shown in Figure 40.

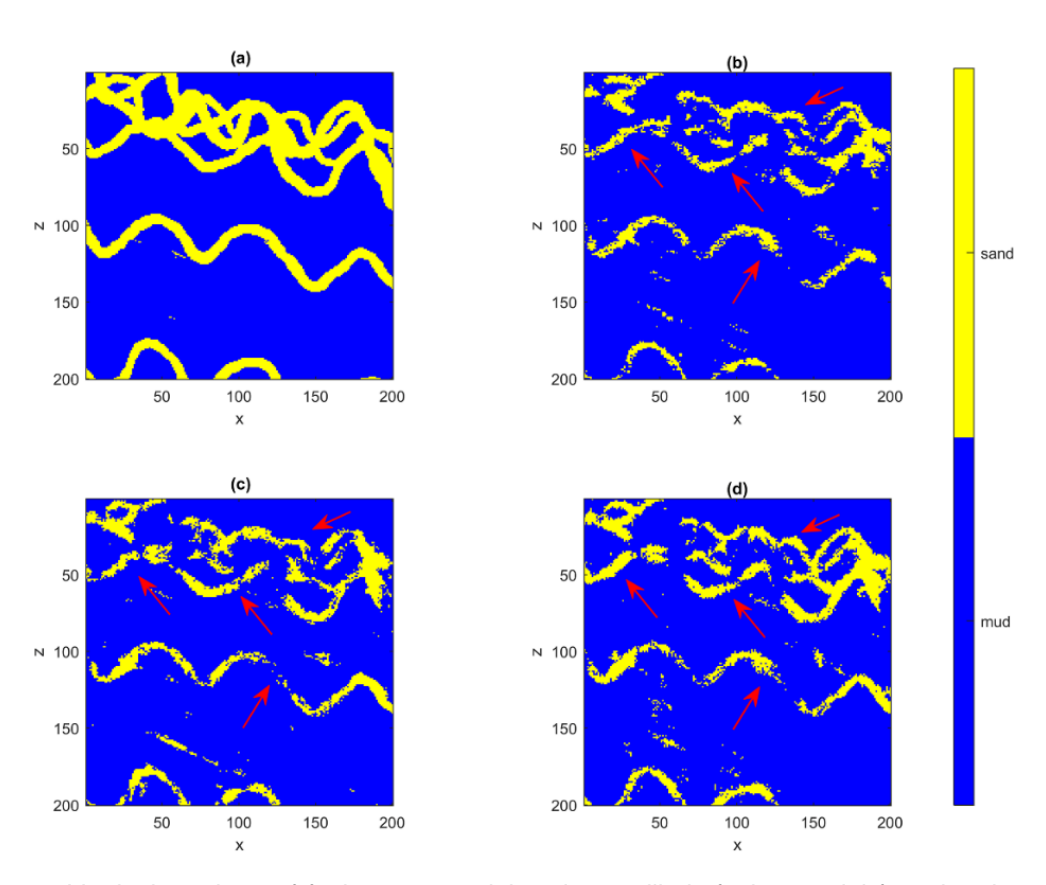


Figure 40 – Vertical sections of facies true model and most likely facies model from last iteration for the three tested methods: **a** Ip true model; **b** GSI; **c** GSI-LA; **d** GSI-LA-Self-Update. Sand (Ip \leq 8500, in yellow) and mud (Ip \leq 8500, in blue). Red arrows point to low Ip values related to sand channel facies, highlighting the improvement introduced with the proposed method.

This simple exercise enhances the interpretation of the pointwise Ip models (Figure 39). The proposed method shows a better local spatial continuity and connectivity of the geological sedimentary patterns, particularly for the low acoustic impedance values, related to sand. In this case, the proposed geostatistical seismic inversion model reproduces channels with increased continuity, a smaller number of artifacts and enhanced connectivity of the predicted channels when compared with the global and fixed local spatial continuity models. While the differences in the classified facies models are not large, they are highly relevant as channel connectivity is of outmost importance for fluid flow modelling and reserve calculation.

To quantify the differences between the predicted ensembles, the Ip volumes co-simulated in the last iteration were plotted in a two-dimensional MDS space using a dissimilarity matrix built with the Haussdorf distance. The Haussdorf distance was selected as it is sensitive to the shape of the features within the model (e.g., Scheidt and Caers 2009). To facilitate the interpretation of the results, the Euclidean distance was computed between each realization generated during the last iteration for the geostatistical seismic inversion methods considered and the true Ip (Cox and Cox 1994; Scheidt and Caers 2009; Azevedo et al. 2014) (Figure 41). The Ip models predicted by the proposed method show two distinct features: they are closer to the true Ip; and they have a similar range between the minimum and maximum distances. These results illustrate that iteratively updating the local variogram models with information from the data mismatch has a positive contribution (i.e., the models become more reliable), without compromising the exploratory capabilities of the original method (i.e., the variability within the ensemble of predicted models is preserved).

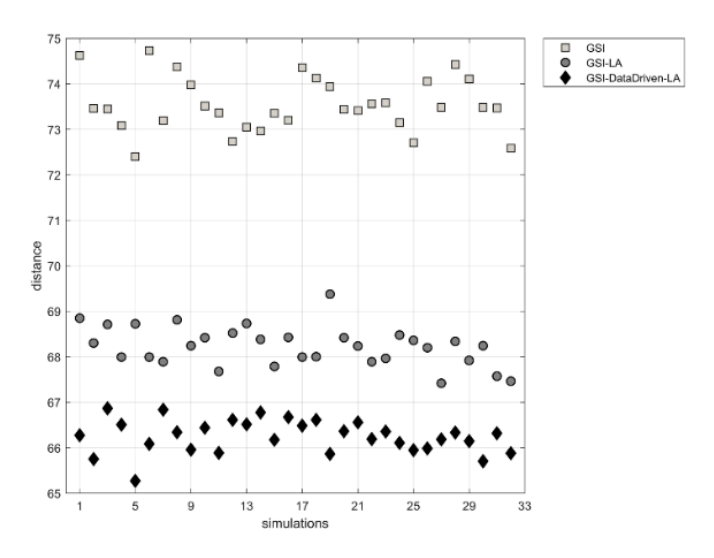


Figure 41 – Distance in MDS space between the true facies model and the retrieved facies models from last iteration. The models closer to the true facies model are the ones from the proposed method.

To evaluate the classified models and to explore their misclassification, Table 1 shows a confusion matrix. In this matrix, the diagonal values are the percentage of pixel values correctly classified (i.e., the predicted class is equal to the true class), while off-diagonal values are the percentage of misclassified pixel values. The confusion matrix shows that the GSI-LA-Self-Update performs better, estimating the highest total percentage of correctly classified pixel values (89.15%) and the smallest percentage (10.85%) of misclassified pixel values. Among these values, 76.16% of pixel values were correctly classified as mud and 12.99% of pixel values were correctly classified as sand. However, and as expected, the misclassification occurs mostly for sand, where 8.24% of pixel values were classified incorrectly as mud, since this class exhibits a more complex spatial distribution pattern. For the mud class, 2.61% of pixel values were misclassified as sand.

Table 1 – Confusion matrix with the percentage of true positive and true negative classified pixel values (correctly classified) and the percentage of false positive and false negative classified pixel values (misclassified) for the three tested methods: (a) GSI, (b) GSI-LA, (c) GSI-LA-Self-Update.

Confusion matrix		GSI Predicted Class		GSI-LA Predicted Class		GSI-LA-Self-Update Predicted Class	
		True Class	Sand	10.30%	10.93%	11.83%	9.40%
Mud	2.24%		76.53%	1.97%	76.80%	2.61%	76.16%
∑ True Class		86.83%		88.63%		89.15%	
∑ False Class		13.17%		11.37%		10.85%	

The bottom row displays the overall accuracy for each class

5.4.2. Real Case Application

The proposed method was applied to a real case study aiming at the prediction of the spatial distribution of acoustic impedance from a fullstack seismic data. The real seismic data was acquired over a complex geological sedimentary and tectonic setting. The study area is characterized by sedimentary layering sequences with a presence of turbidite systems, with typical meandering channels. Additionally, tectonic structures are also present in the seismic data and are related to faulting and folding, making it possible to observe several normal faults, tilt and deformation of the sedimentary sequences in the seismic data.

The dataset corresponds to a two-dimensional vertical seismic section, the inversion grid is composed of 100 by 1 by 206 cells in i-, j- and k- directions, respectively. Additionally, a well with Ip-log data (Figure 42b), is located in grid cell i = 74, with a length from grid cell k = 55 to 187, and a 101 ms wavelet (Figure 42a). For template matching, an ensemble of one

hundred and eight elliptical templates with azimuths varying between 0° and 55° dip with a step angle of 10° was created. The ellipse main and minor ratios were scanned within an interval of 12 to 32 grid cells and 4 to 12 grid cells with a two-cell step. The seismic inversion was performed with six iterations, with thirty-two realizations models of Ip in each iteration.

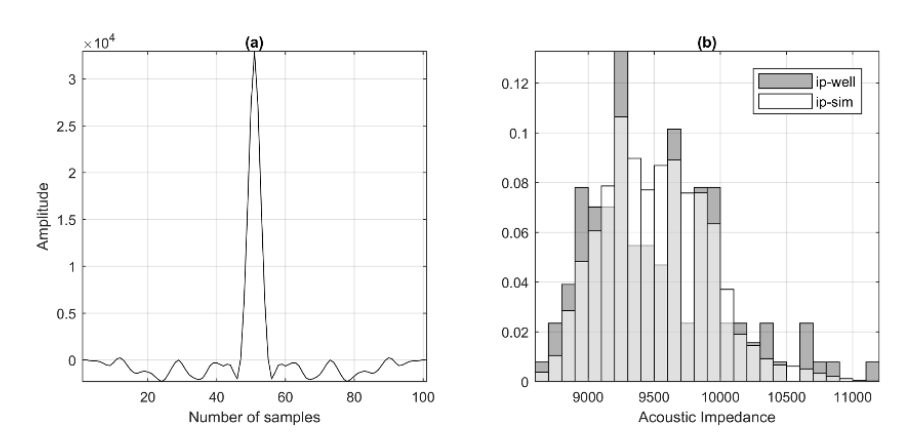


Figure 42 – **a** Wavelet; **b** Histogram of Ip from well-log data and from Ip mean model from 6th iteration.

To evaluate the performance of the proposed method, the results were compared with the results from GSI and GSI-LA, using the same initial data. At the end of the seismic inversion procedure, the proposed method converged, reaching a global similarity \boldsymbol{s} between the real seismic data and the synthetics of 0.82. GSI and GSI-LA also converged as expected, reaching a smaller global similarity of 0.76 and 0.80, respectively (Figure 43).

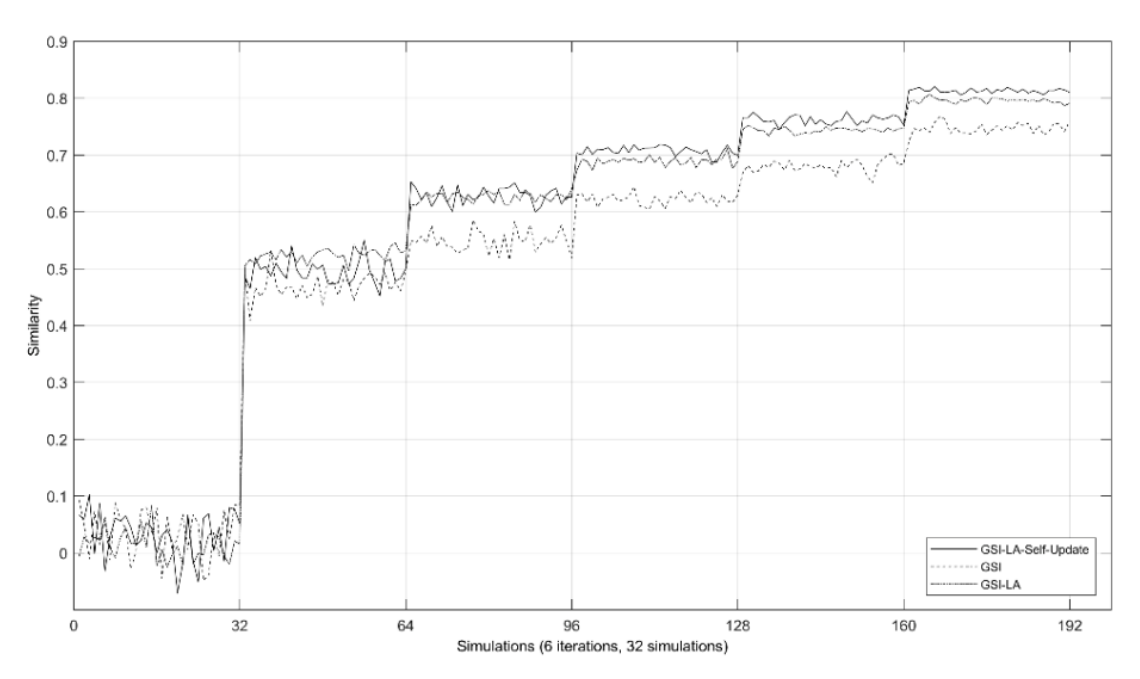


Figure 43 – Evolution of Global Similarity during seismic inversion procedures.

As expected, the synthetic seismic of the proposed method reproduces particularly well the real seismic data (Figure 44), not only in terms of seismic reflections position and continuity, seismic textures and corresponding anisotropies variations, but also in terms of the amplitude content. Regarding the sedimentary and tectonic geological structures, from the synthetic seismic data it is possible to interpret the sedimentary sequences including the seismic pattern related to stacked channels linked to a turbidite system. The dipping of the seismic reflectors with some tilting and fault patterns is also well reproduced in the synthetic seismic predicted by the proposed method.

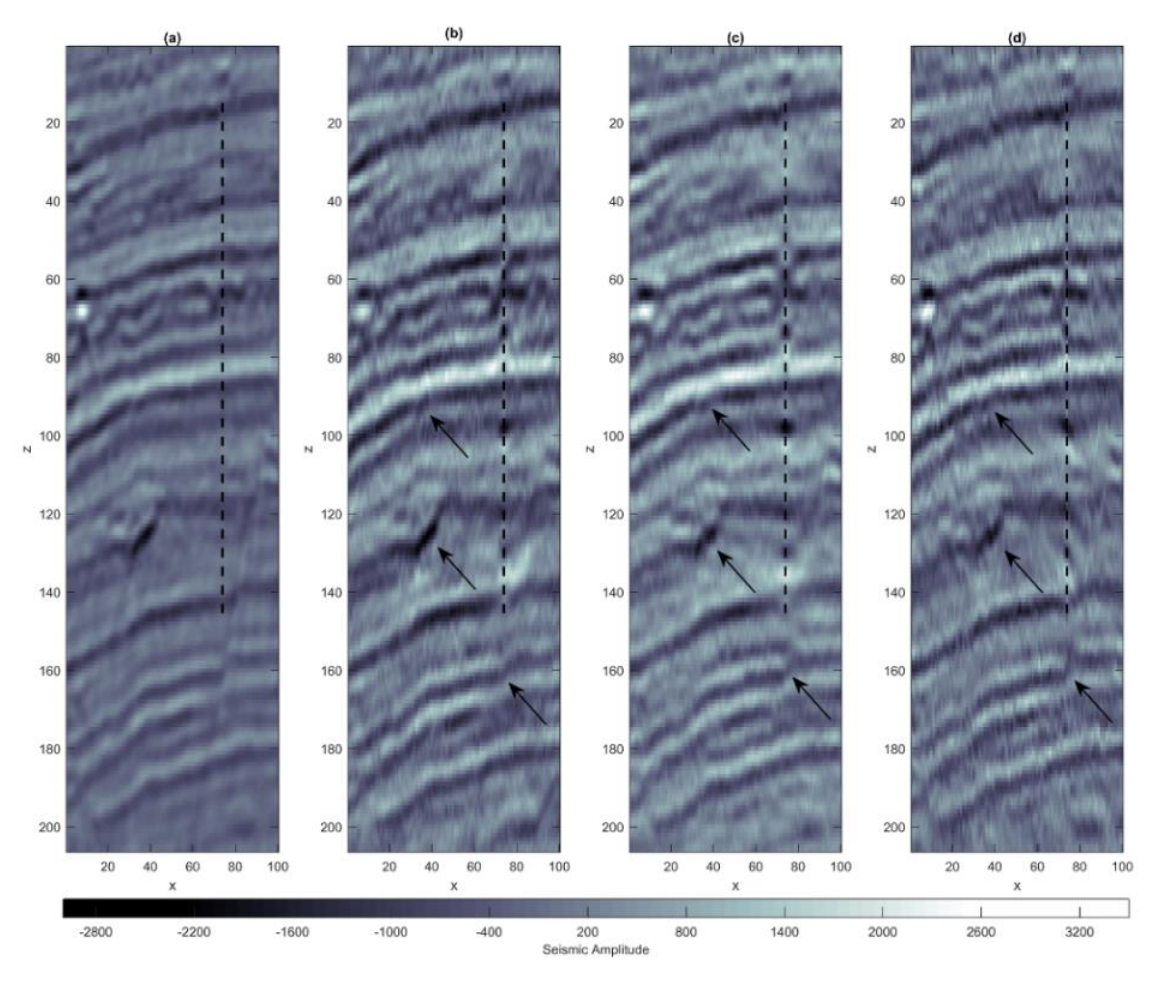


Figure $44 - \mathbf{a}$ Vertical section of the true seismic data with well position (black dashed line); **b** Synthetics seismic calculated from Ip mean models of the 6^{th} iteration GSI-LA-Self-Update; **c** GSI; **d** GSI-LA. Black arrows point to areas where it is possible to verify the similarity between the real seismic and the synthetics from all tested methods.

Comparing the proposed method with the synthetic seismic resulting from the other geostatistical seismic inversion methods (Figure 44), there is an improvement on the reproduction of seismic reflectors and their discontinuities, providing a more consistent and realistic geological meaning, either sedimentary or tectonic, to the seismic patterns.

Nevertheless, there is some random residual noise, in areas of lower similarity (Figure 46). The residuals are mainly related to high seismic amplitude values at well-log location, which are associated to a poor seismic-to-well tie (Figure 46). The residuals away from the well location are most likely linked to the representativeness of the wavelet in those locations, and to the fact that the data is broadband seismic, introducing some additional uncertainty during wavelet extraction.

The predicted Ip models obtained with the proposed method have some aspects worthwhile to discuss in detail (Figure 45). The use of local and more informative spatial models allows to highlight the presence of tectonic features, such as normal faults, when compared with the results obtained with GSI considering a global variogram model. Also, the detritical sedimentary patterns, such as turbidite channels, are better identified, characterizing and revealing the location of potential targets. Figure 45c shows a vertical section of the predicted Ip with a fixed local anisotropy model. This model is greatly discontinuous, indicating the poor a priori estimation of the local spatial continuity patterns, and illustrating the drawbacks of such approach. If the a prior estimation is not reliable, the quality of the inverted models will be poor.

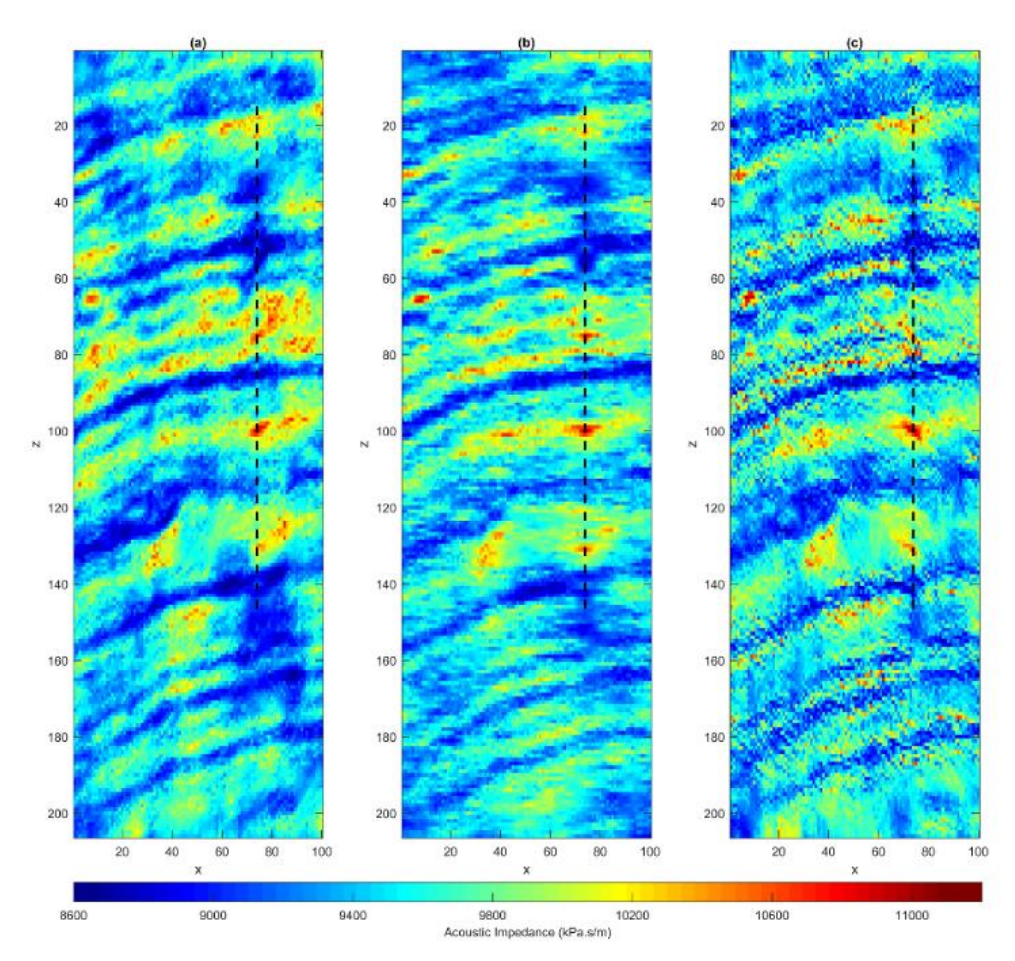


Figure 45 – Vertical sections of Ip mean model computed from the 6th iteration from: **a** GSI-LA-Self-Update; **b** GSI; **c** GSI-LA.

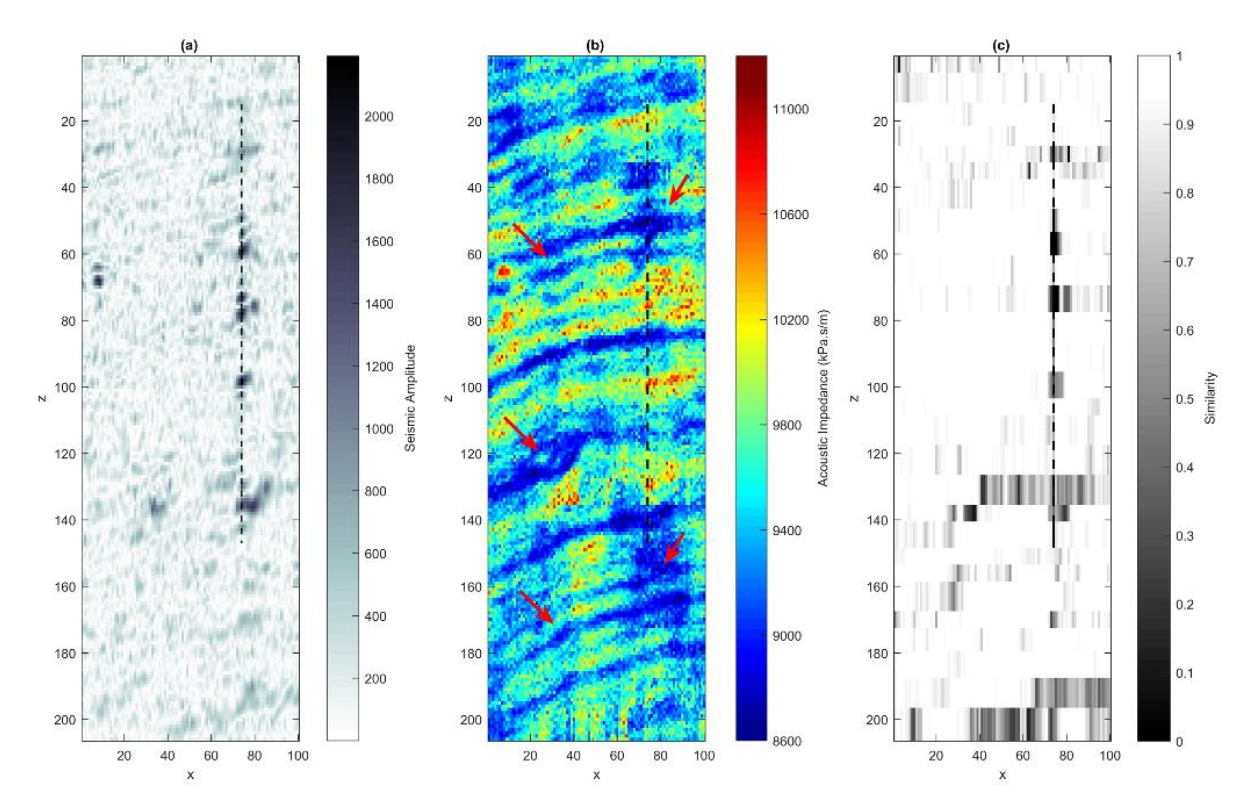


Figure 46 – Vertical section extracted from the: **a** residuals between synthetic and real seismic; **b** best-fit lp; **c** best-fit similarity models from 6^{th} iteration, with the proposed method. Red arrows point to low lp values related to turbidite channels or faults.

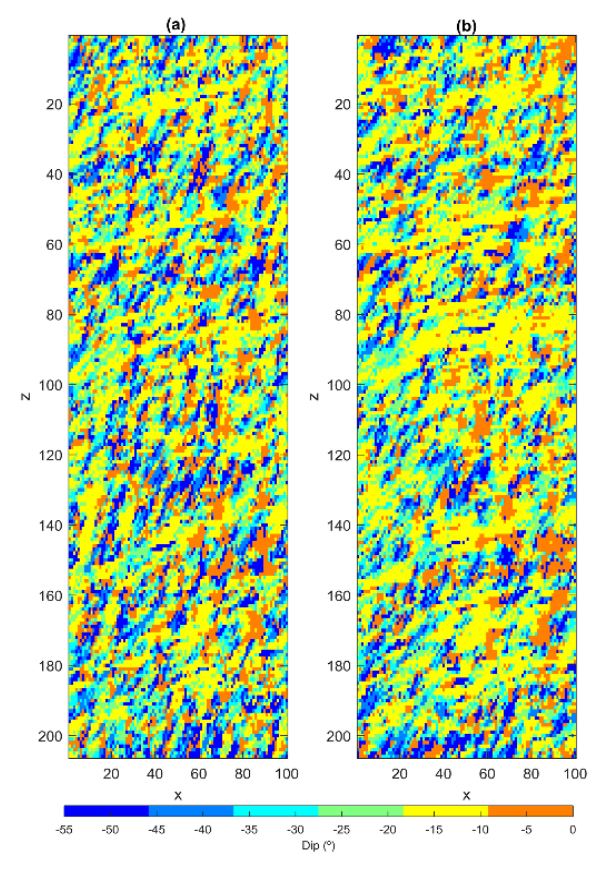


Figure 47 – Vertical section of local spatial patterns - Dip azimuth (°) for the 2nd iteration; **b** Vertical section of local spatial patterns - Dip azimuth (°) for the 5th iteration, with the proposed method.

An important issue is related with the ability of the proposed method to update the local spatial patterns (Figure 47) while keeping the reproduction of the statistics of the true Ip-log data. Figure 42b shows a comparison between both histograms. In Figure 47, showing the evolution of the local spatial patterns, it is possible to see the update and improvement of the Dip azimuth model between iterations with the proposed method, using template matching.

5.5. Discussion

The application examples of this study illustrate the improvements obtained in the inverted models with the self-updating of the local spatial continuity pattern of Ip. In such examples, the local continuity models was estimated with template matching, but alternative methods could be used. For example, Pereira et al. (2020) used automatic variogram fitting at each cell of the inversion grid to estimate a priori local variogram models. However, this is a very computational expensive estimation method when compared to with the template matching proposed here. Template matching proved to be an efficient and easy way to estimate the local variogram models.

The proposed seismic inversion method presents a clear advantage over the alternative methods that use a fixed spatial continuity model. The application examples show that iteratively updating the local spatial continuity models, particularly when the available seismic does not allow to extract reliable local models of anisotropy, results in better predictions in terms of elastic and rock properties. The proposed method improved the geological consistency and plausibility of the inverted models. The local information highlights the presence of geological discontinuities such as faults, folding or tilting of sedimentary sequences, and improves the spatial continuity in the presence of anisotropic depositional features, such as the meandriform channels typical of fluvial-deltaical sedimentary environments or deep-water turbidite systems.

The proposed method was tested in a challenging two-dimensional synthetic data set characterized by sinuous channels built with object modelling. An alternative approach to the proposed seismic inversion method would be the direct inversion of seismic data for facies and the integration of geostatistical simulation conditioned to multi-point geostatistics (e.g., González et al. 2008). These techniques have proven their value in these kinds of geological environments. However, they present additional difficulties related to the need of a reliable training image. The synthetic case application is noise free. However, the proposed method was also applied to a real data set that has noise associated with the measurement data and the predicted wavelet. This application example aim at showing the performance of the method under real noise conditions.

Both examples used the inversion method in fullstack seismic for acoustic impedance (Ip), but its extension to the elastic domain (e.g., geostatistical seismic AVA inversion; Azevedo et al. 2018) is straightforward.

Despite all the advantages of GSI-LA-Self-Update, it is important to discuss some limitations. To avoid unnecessary computational costs and to better estimate the local variogram model parameters, it is utmost importance to choose the most relevant templates combinations at the beginning. To optimize this choice, it is important to start by analyzing the shape, dimension and direction of main geological features in seismic data. This will indicate the best azimuthal ranges and anisotropy ratios to begin with. It is also important to start with bigger step sizes for azimuthal ranges and with very different anisotropy ratios, and then adjust parameters. It is recommended to use a relatively small, but representative area, to fine-tune the parameters before applying to the full seismic volume. Comparing time consumptions for the synthetic case as an example, the cost of one iteration to compute thirty-two realizations was 115min using GSI-LA and 93min using GSI-LA-Self-Update. Both inversion methods ran in a Core i7 workstation with 32GB of RAM. Two-dimensional examples were shown here, to facilitate the interpretation of the results, as well as the comparison with the other methods. However, the method can be applied directly to any three-dimensional volume.

5.6. Conclusion

This paper proposes an update of the GSI algorithm through a sequential updating of models based on new experimental data. Local spatial covariances are updated by conditioning the seismic inversion process to experimental data – seismic reflection data and local anisotropy models inferred directly from the data.

The new iterative geostatistical seismic inversion method is based on global stochastic seismic inversion, and uses an updatable local spatial continuity model, expressed by a local variogram model, self-updated at the end of each iteration to improve the petro-elastic properties estimation, and thus retrieve more consistent and realistic geological models with less artifacts, particularly for complex tectonic and detrital sedimentary environments.

The method was successfully applied to a synthetic and a real case, with acceptable computational costs. In the examples presented, there is a clear improvement when using not only a local variogram model, but also a self-updatable one, based on the data and during the seismic inversion procedure; this benefits the estimation of local anisotropies of complex geological environments, leading to more robust predictions of the subsurface geology.

Acknowledgments

The authors gratefully acknowledge the support of the CERENA, the University of Lisbon and the FCT - Fundação para a Ciência e Tecnologia (FCT SFRH/BD/136316/2018). The authors also thank Partex Oil and Gas for making the dataset of the real case application available and permission to publish it. We acknowledge anonymous reviewers for their comments that helped to improve the final version of the document.

6. Seismic inversion integrating seismic attributes to enhance geological models

Presented at 79th EAGE Conference & Exhibition, Paris, France 2017.

6.1. Introduction

Seismic attributes are quantitative information derived from seismic reflection data (Taner 2001). They are important interpretation tools used to support seismic interpreters to better understand the subsurface geology, by helping enhance geological structures, highlighting discontinuities, edges and hidden patterns, improving signal-to-noise ratio, used as filters or lithology classifiers. There is a vast number of seismic attributes, which quantify different properties associated to seismic data (e.g. stratigraphic, structural) (Chopra and Marfurt 2005, Barnes 2016). Some of the key seismic properties quantified by seismic attributes are: amplitude, frequency, phase, slope, dip, azimuth and curvature of seismic reflectors (Barnes 2016). In 1994 Taner (Taner et al. 1994) divided seismic attributes into two main categories: geometrical and physical attributes. Since then, seismic attributes classification has been change with the rise of different methods. Currently, seismic attributes may be classified into three main categories: geological, geophysical and mathematical. Seismic attributes can be derived from seismic pre-stack or post-stack seismic data, and can be computed in a seismic trace, a seismic horizon or in a seismic volume. Furthermore, seismic attributes can be interpreted individually or in a multi-attribute analysis (Chopra and Marfurt 2005, Barnes 2016).

Seismic inversion methods are used in reservoir modelling and characterization to infer the subsurface geological petro-elastic properties. This is due to the physical relation between the seismic wave propagation and the elastic response of the subsurface geology, depending on the type of lithology or facies. In reservoir modelling it is important to infer the spatial distribution of the subsurface rock properties, and understand the internal reservoir architecture. The resulting subsurface rock property models, must be geological reliable and accurate to reduce uncertainties. Hence, these models must reproduce the seismic stratigraphic patterns or the structural features, observed in the seismic reflection data, what in same cases can be a challenging assignment (Azevedo and Soares 2017).

One of the advantages of seismic attributes is to enhance the geological structures. Therefore, we propose to combine seismic inversion and seismic attributes in the same framework, to improve seismic patterns reproduction in the petro-elastic subsurface models,

resulting from seismic inversion procedure. Thus, we propose the integration of seismic attributes into the objective function (OF) of the geostatistical seismic inversion procedure (e.g. GSI, Soares et al. 2007). The classic Global Stochastic Inversion (GSI) uses the direct stochastic sequential simulation procedure (DSS, Soares 2001) as model perturbation technique. The convergence of the method is made by a global optimizer, based on genetic cross-over algorithm, driven by the match between the observed seismic reflection data and the resulting synthetic seismic (Soares et al. 2007, Caetano 2009). We propose the integration of seismic attributes, which highlights stratigraphic or structural features, by adding the match between seismic attributes computed from observed seismic reflection data and synthetic seismic, in the objective function. The GSI with different seismic attributes and multi-attributes were first tested, in a synthetic case. The methodology was also applied to challenging real case application example, where the variance and first derivative seismic attribute was integrated in the objective function of the proposed geostatistical seismic inversion procedure.

6.2. Methodology

The proposed methodology (Figure 48) follows the Global Stochastic Inversion algorithm (GSI, Soares et al. 2007), where seismic attributes are integrated into the objective function (OF), to improve the resulting models. Different types or combinations of seismic attributes (e.g. structural, stratigraphic) may be used and added to the objective function. Furthermore, the seismic attributes should enhance the geometries of the geological features. In the objective function, the mismatch between the reference seismic and the synthetic seismic is given by an extension of Equation 16 (see Section 3.3.2 for Equation 16 details), which combines the comparison of seismic and the comparison of seismic attributes in each iteration (Equation 20).

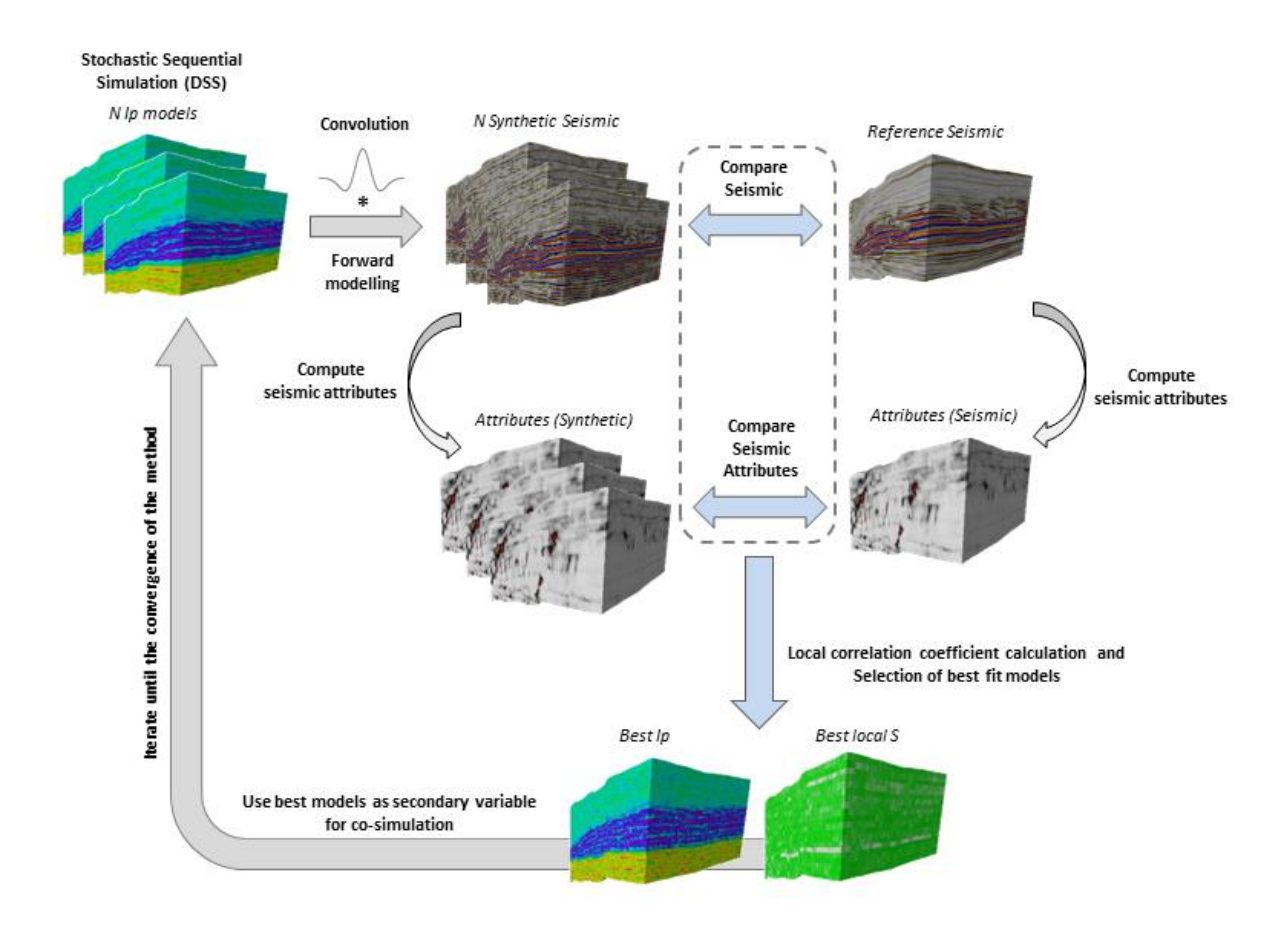


Figure 48 – Schematic representation of the iterative geostatistical seismic inversion integrating seismic attributes into the objective function.

The geostatistical seismic inversion method integrating seismic attributes into the objective function can be summarized by the following steps:

- Stochastic sequential simulation (e.g. DSS Soares 2001) of N realizations of Ip models from well-log data and conditioned to a spatial continuity pattern, imposed by a variogram model;
- 2. Computation of *N* synthetic seismic by convolving the reflection coefficients, obtained from the previous simulated Ip models with a wavelet;
- 3. Computation of seismic attributes (e.g. structural or stratigraphic seismic attributes) over the reference seismic and the synthetic seismic;
- 4. Comparison on a trace-by-trace basis of similarity ($S_{seismic}$) between the synthetic seismic trace (x_s) and the reference seismic trace (y_s). Simultaneously, comparison of similarity ($S_{attribute}$) between seismic attribute from synthetic seismic trace (x_a) and seismic attribute from reference seismic trace (y_a). The objective function (S_{OF}) is computed by the weighted sum of the different similarity components as follows (Equation 20),

Equation 20
$$S_{OF} = \alpha_s (S_{seismic}) + \alpha_a (S_{attribute})$$

$$S_{OF} = \alpha_s \left(\frac{2*\sum_{s=1}^{N} (x_s*y_s)}{\sum_{s=1}^{N} (x_s)^2 + \sum_{s=1}^{N} (y_s)^2} \right) + \alpha_a \left(\frac{2*\sum_{a=1}^{N} (x_a*y_a)}{\sum_{s=1}^{N} (x_a)^2 + \sum_{s=1}^{N} (y_s)^2} \right),$$

where α_s and α_a are weights between [0 1] assigned to the seismic and to the seismic attributes components respectively. The sum of the all weights must be equal to 1;

- 5. Selection of the Ip traces with the highest S_{OF} at a given iteration. These Ip traces along with the corresponding S_{OF} value, are stored in two auxiliary volumes;
- In the next iteration the two auxiliary volumes are used as secondary variable in the stochastic sequential co-simulation (e.g., Soares 2001) of a new set of N realizations of Ip models;
- 7. Return to step 1) and iterate until the global mismatch between the reference seismic and the synthetic seismic is above a given threshold.

6.3. Application Examples

6.3.1. Synthetic Case Application

The proposed geostatistical seismic inversion method integrating seismic attributes was applied to the synthetic application example presented in Section 5.4.1. This application example corresponds to curvilinear channels, which try to mimic a deep-water sedimentary environment. The reference seismic reflection data corresponds to a two-dimensional fullstack seismic section, with a grid dimension of 200 by 200 cells in i- and k- directions, respectively (Figure 49). For simplification, the seismic data is noise free and there is no uncertainty related about the wavelet used in the application example. The true subsurface rock property model is represented by the acoustic impedance (Ip) model in Figure 49, where the sand-rich channels are associated to low Ip values and the mud-rich background facies to high Ip values. The application example was conditioned to two wells with Ip log data. The wells are located at positions i = 25 and i = 185 and the Ip logs from 50 to 180 ms and 60 to 170 ms, respectively. A spatial distribution pattern was imposed by a variogram model, with 20 grid cells in the main direction and 5 grid cells in the vertical direction. The iterative inversion procedure was performed with six iterations, each one with thirty-two realizations of Ip models.

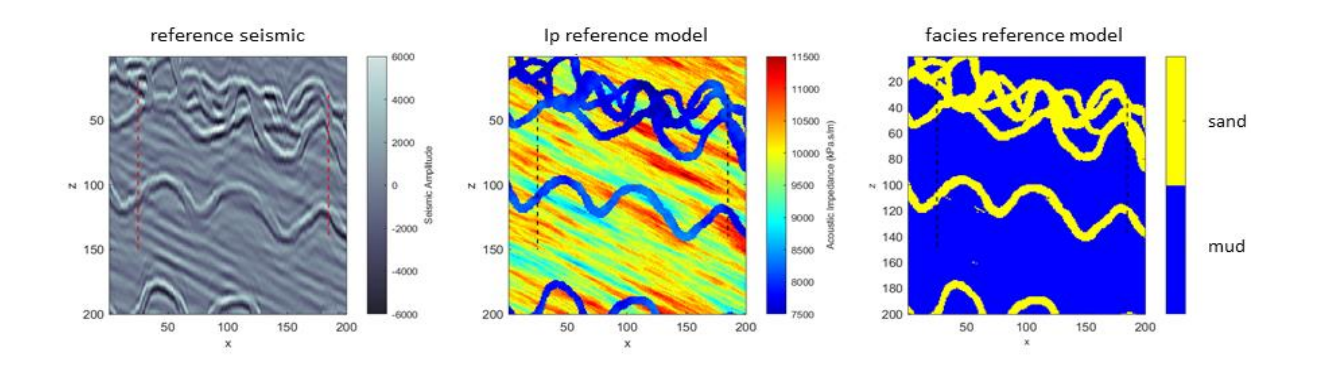


Figure 49 – (left) Vertical section of the reference seismic reflection data; (center) Vertical section of the reference acoustic impedance model; (right) Vertical section of the reference facies model. The vertical black lines represent the location of the wells used as conditioning data in the geostatistical seismic inversion.

To evaluate the integration of seismic attributes into the objective function, used to enhance the seismic stratigraphic patterns and structural features, different types of attribute were tested. Structural attributes such as variance and first derivative, along with stratigraphic attributes like the root-mean-square (RMS), were tested. Some seismic attributes were tested individually (e.g. RMS and variance) in addition, multi-attributes were also tested (e.g. RMS with variance, first derivative). The seismic attributes were computed during the inversion procedure from the reference seismic and from the synthetic seismograms. Some were computed considering the values of the adjacent cells (e.g. first derivative) and others were computed over a moving window, considering the neighboring values (e.g. RMS, variance). Different size window and weights were tested. The different tests were performed with the same parameterization, regarding the conditioning data and spatial distribution pattern, given by a global variogram model.

The results were compared with the classic Global Stochastic Seismic Inversion (GSI, Soares et al. 2007), with the same parameterization. Furthermore, the proposed method was also tested in Global Stochastic Seismic Inversion algorithm with local anisotropies (GSI-LA) and it was applied to a real case.

6.3.1.1 GSI with seismic attributes

The proposed method converges after six iterations (Figure 50). In Table 2 are listed the different performed tests. The global similarity (S) between the synthetic and the reference seismic, ranges from 0.82 to 0.85. The majority of the tests of GSI with seismic attributes show an improvement on the global convergence. The highest value of global similarity is associated to the integration of multi-attributes in the objective function, namely RMS

combined with first derivative (1st D) and RMS combined with variance (var), in both cases reaching a global similarity of 0.85 (Table 2). For the GSI classic approach, the global similarity decreases to 0.82. Globally the results show advantages in using seismic attributes in the inversion procedure.

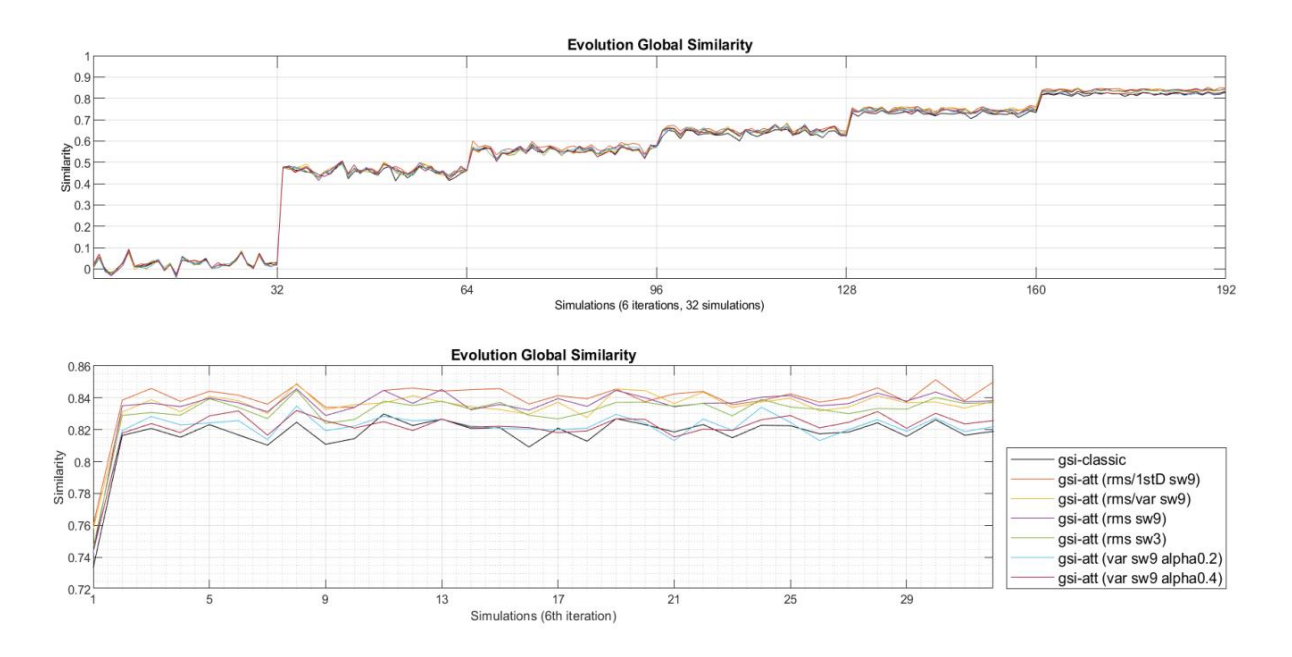


Figure 50 – [top] Evolution of global similarity (S) over iterations for GSI with attributes and classic GSI. [bottom] Detail of the evolution of global similarity (S) during 6^{th} iteration, for different tests of GSI with attributes compared to classic GSI.

Table 2 – Global Similarity for different tests with GSI.

Seismic Attributes	Global CC	Seismic Attributes	Global CC
gsi-classic	0.82	gsi-att (rms [sw=3])	0.84
gsi-att (rms/1stD)	0.85	gsi-att (var [sw=9, w=0.2])	0.83
gsi-att (rms/var)	0.85	gsi-att (var [sw=9, w=0.4])	0.83
gsi-att (rms [sw=9])	0.84		

The predicted synthetic seismic reproduced the reference seismic reflection data, regarding the amplitude content and the main seismic stratigraphic patterns (Figure 51). Comparing to the classic GSI, the GSI with seismic attributes, particularly with variance and RMS combined with other structural attributes (i.e. variance and first derivative), better reproduces the reference seismic, where it is possible to observe more continuous and better defined seismic reflectors (Figure 51). However, some areas remain with higher uncertainty, corresponding to lower local similarity (*S*) areas, associated to high heterogeneous spatial seismic patterns, such as intercrossed curvilinear channels in the upper area of the seismic section, where the local continuity patterns of the seismic reflectors are worse reproduced.

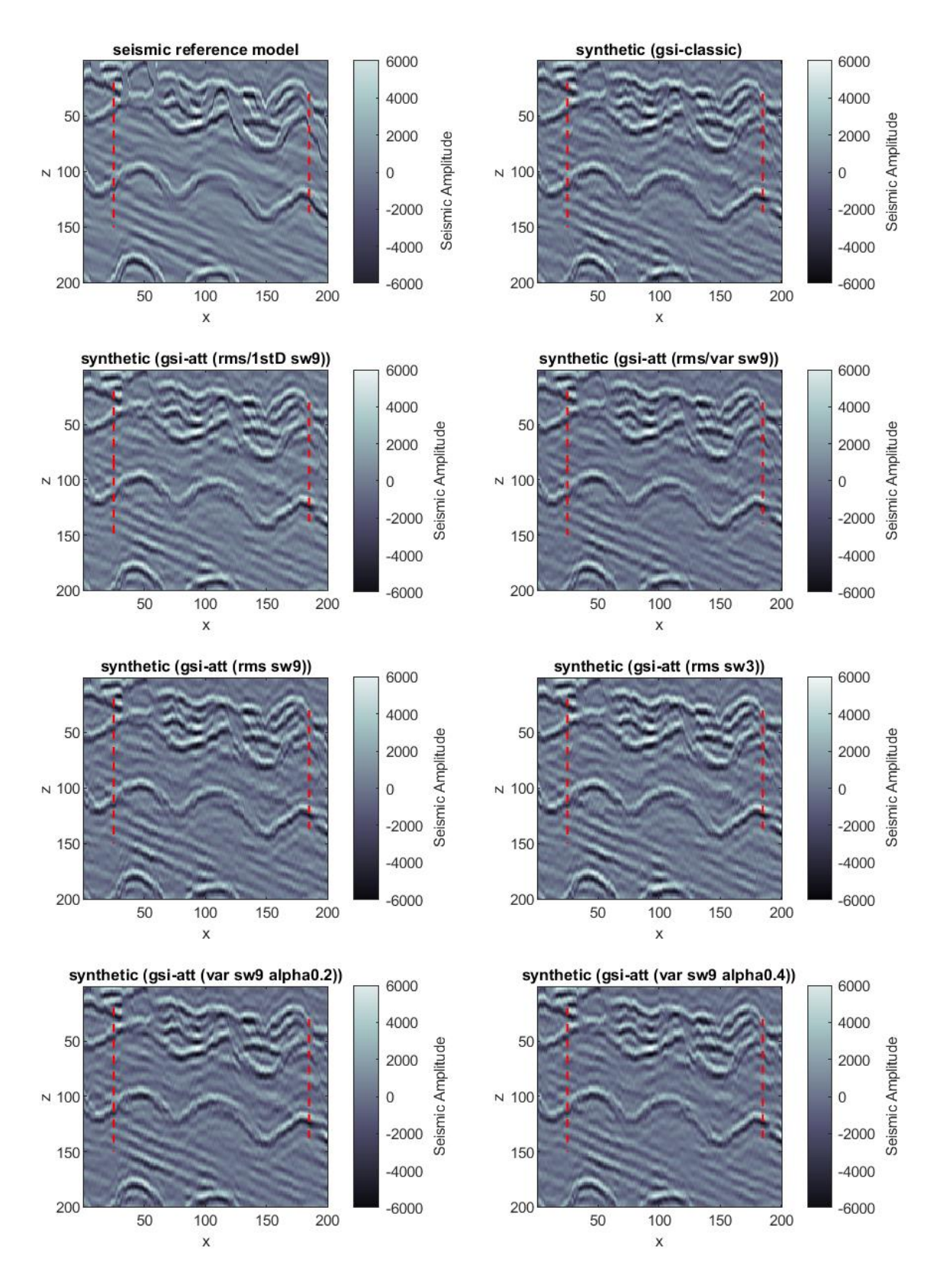


Figure 51 - Vertical section of synthetic seismic computed from the Ip mean model of 6th iteration from classic GSI and GSI with attributes.

In Figure 52 are shown the seismic attributes used in the objective function of the proposed method. The images refer to the test of GSI with RMS combined with variance attribute. For both seismic attributes, the main geometries and spatial continuity patterns from the seismic are correctly reproduced in the synthetic, including some smaller local details. This shows the convergence of the proposed method also in the seismic attribute domain.

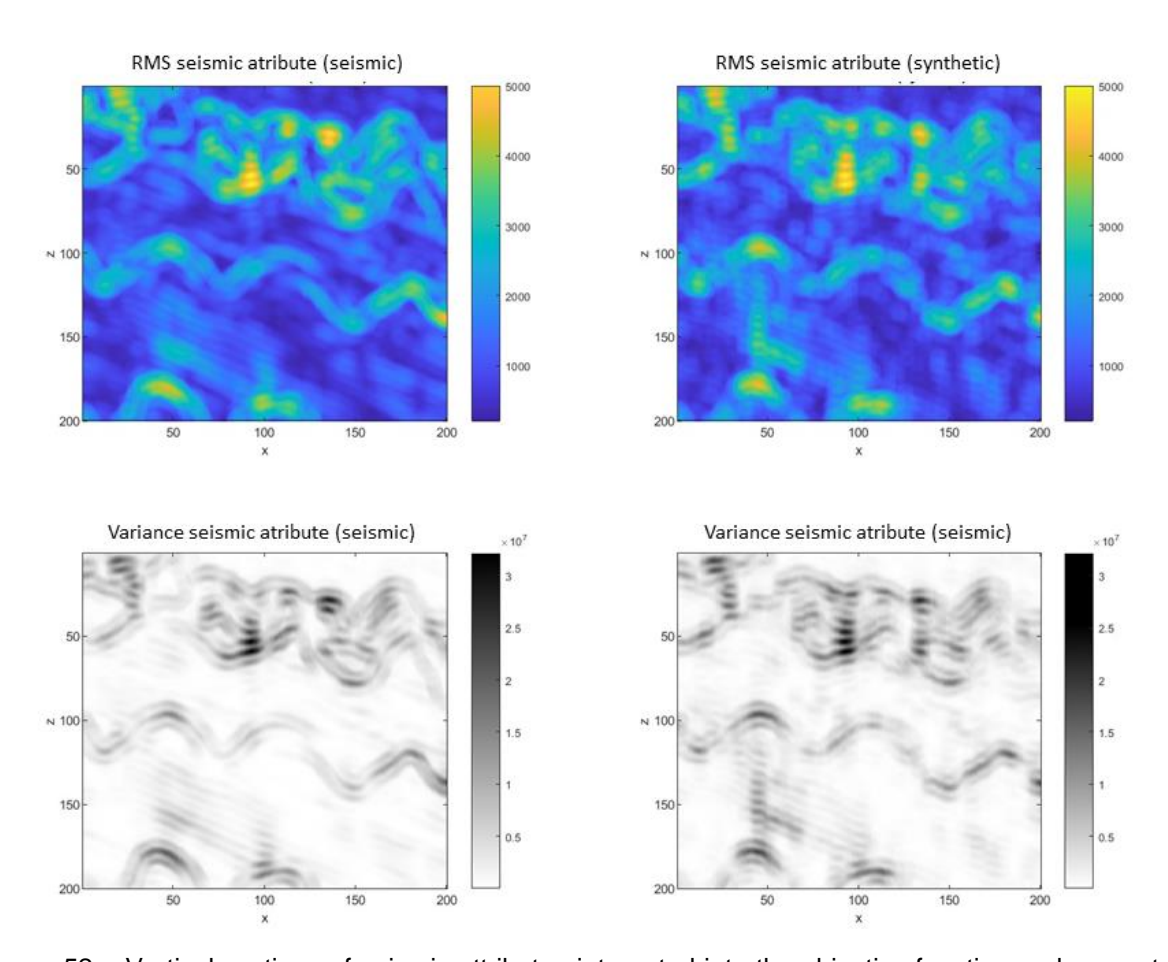


Figure 52 – Vertical sections of seismic attributes integrated into the objective function and computed from reference seismic and synthetic seismic in the last iteration of the seismic inversion procedure.

The Ip mean models computed from the 32 realizations, co-simulated during the last iteration, for each presented seismic inversion test, are shown in Figure 53. The mean Ip models reproduce the main spatial continuity patterns of the reference Ip model (Figure 49), namely the sedimentary patterns associated to the curvilinear channels and lower acoustic impedance values. The sedimentary sequences are also reproduced and the Ip mean models are geological consistent, regarding the reference Ip model. Nevertheless, comparing to the classic GSI, the integration of seismic attributes like variance, or multi-attributes like RMS combined with variance, improved the prediction of the spatial continuity and connectivity of the curvilinear channels. Additionally, the spatial continuity pattern of the

background sedimentary sequences (higher Ip values) is also more continuous, showing improvements on adding seismic attributes to the inversion procedure, comparing to classic GSI (Figure 53).

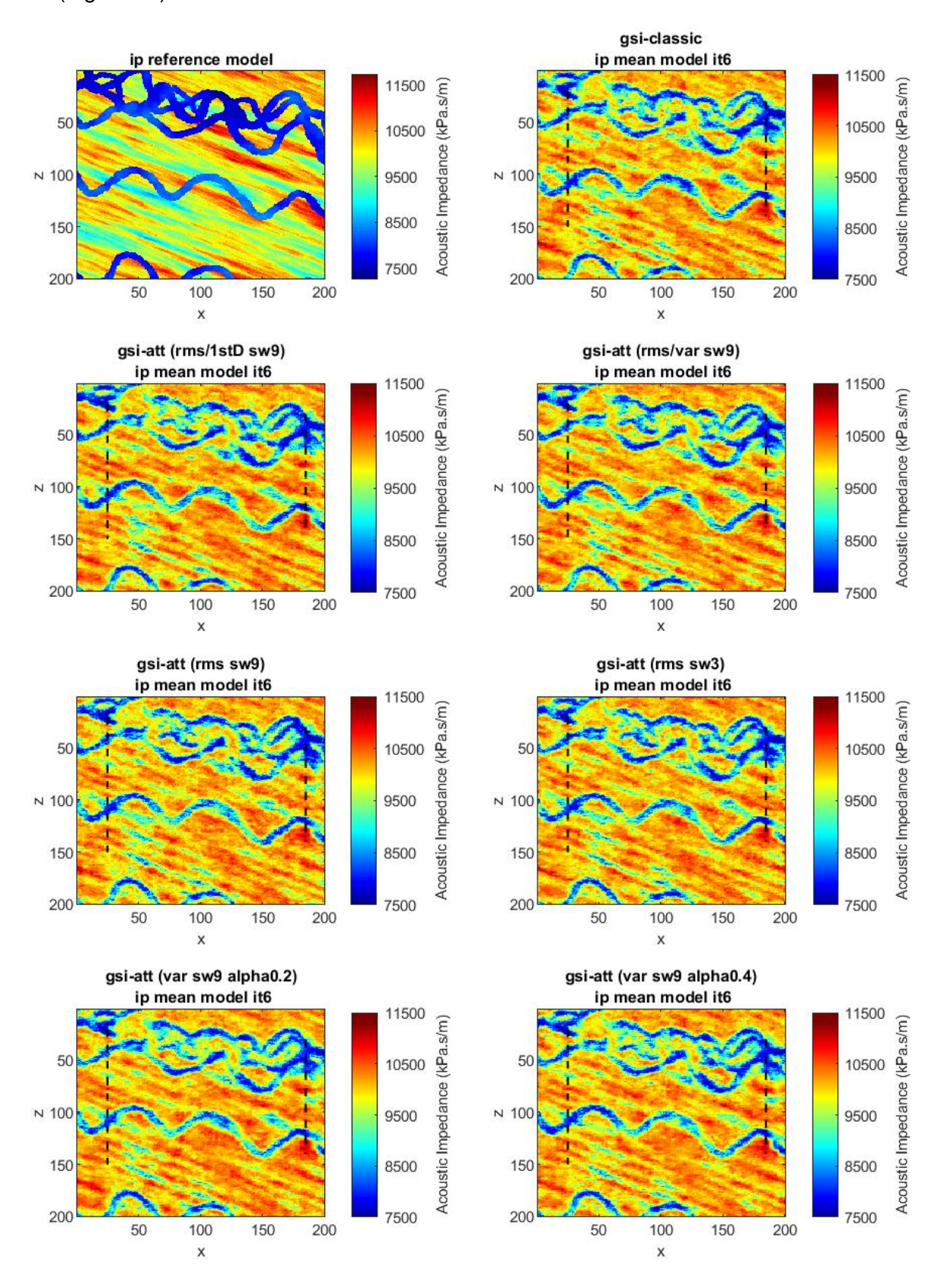


Figure 53 – Vertical section of Ip mean model of 6th iteration from classic GSI and GSI with attributes.

The set of Ip models from the last iteration, were classified into two facies and compared to the reference facies model (Figure 49), to evaluate the spatial continuity and connectivity, particularly of the sand channels, among the different tests. The reference facies model, was established based on a lp value threshold, where lp values below or equal to 8 500 kPa.s/m were classified as sand, corresponding to channel facies, and Ip values above 8 500 kPa.s/m were classified as mud, corresponding to muddy background facies. From the set of facies models, were computed the most likely facies models for the tests here studied. In Figure 54 are compared the most likely facies models with the reference model (Figure 49). The facies models highlight what was previously said about the elastic models. The integration of single seismic attributes or multi-attributes into the objective function of the inversion procedure, improves the spatial continuity and connectivity of the sedimentary patterns, particularly of curvilinear channels associated to sand facies (Figure 54). There is also a reduction on the artifacts. Among the different tests with the proposed method, the integration of RMS combined with first derivative, seems to provide the best result regarding these issues, showing more continuous spatial patterns, higher connectivity within the curvilinear channels and less number of artifacts. The facies model with variance attribute and the facies model with RMS combined with variance, have similar results. The differences are more evident, regarding the classic GSI approach.

In addition to evaluating the global similarity (S), were quantified the differences between the predicted Ip models from the last iteration and corresponding facies model, to the reference elastic and facies models respectively. The differences were computed with the Haussdorf distance, since it is sensitive to the shapes of the geobodies within the models (e.g., Scheidt and Caers 2009). The results were plotted in a three-dimensional MDS space, where in Figure 55 a two-dimensional top view of the models projection is shown. The Euclidean distance between the realizations ensemble and the reference Ip and facies models was also computed, to simplify the interpretation of the results (Figure 56).

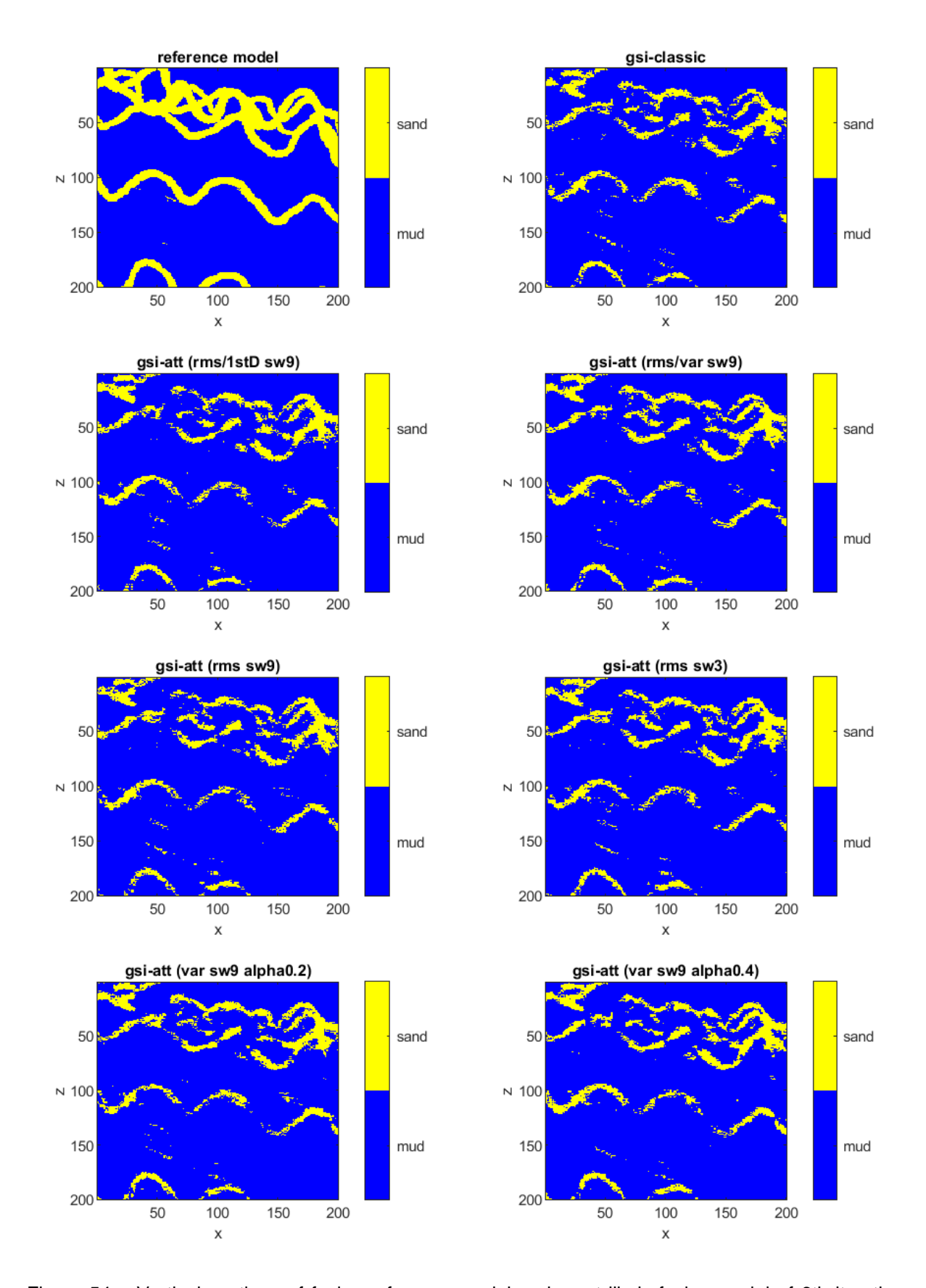


Figure 54 – Vertical sections of facies reference model and most likely facies model of 6th iteration from classic GSI and GSI with attributes. Sand (Ip <= 8500, in yellow) and mud (Ip > 8500, in blue).

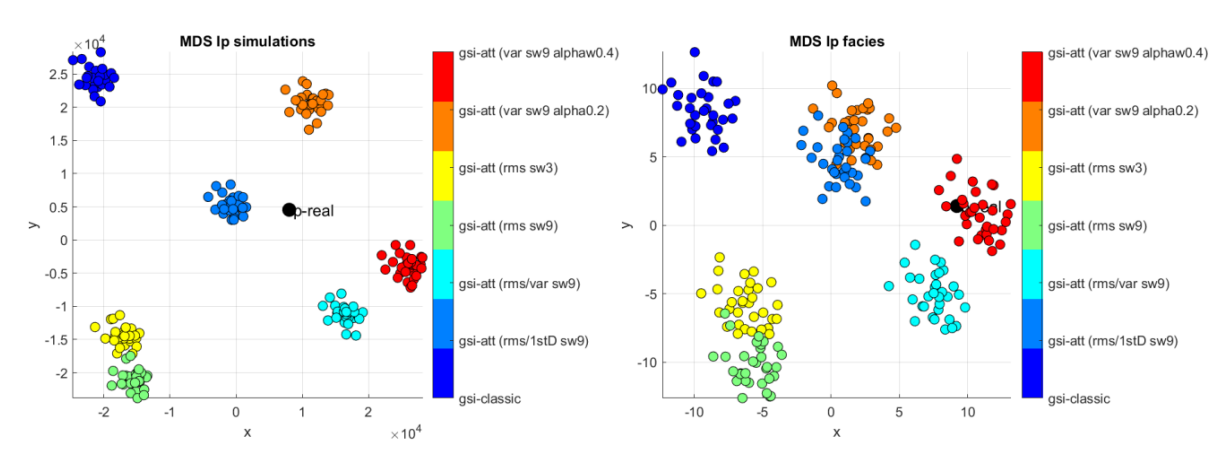


Figure 55 – Projection in the MDS space (2D top view) of the Ip and facies models, from last iteration, for the different seismic attributes and comparison with the reference models. It is possible to observe the distance to the reference models and the dispersion within the ensembles. The reference models are represented by a black dot.

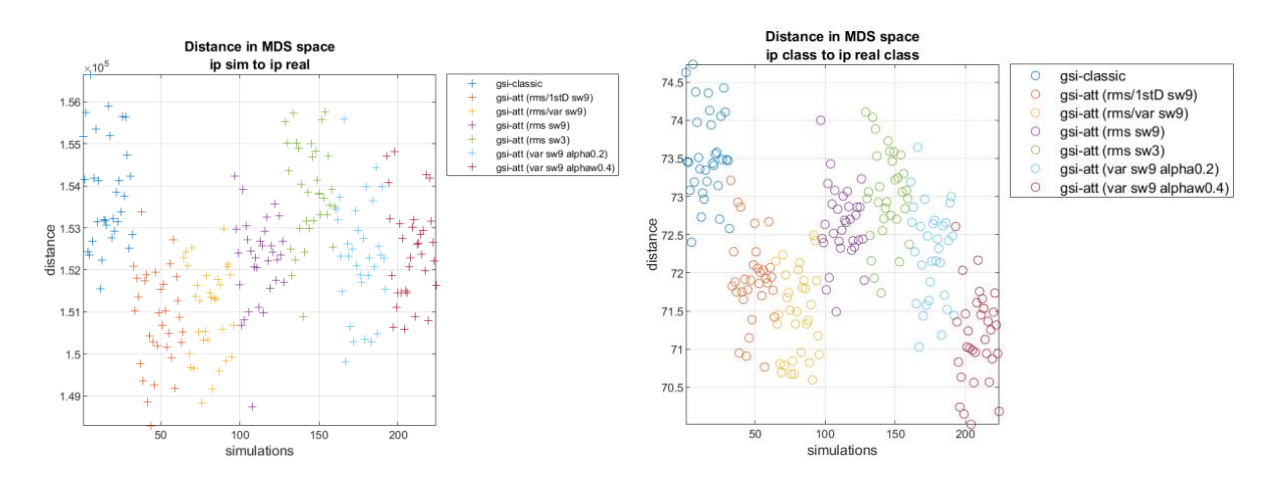


Figure 56 – Distance in MDS space for Ip and facies models, between the true model and the realization models from last iteration, for GSI with attributes and classic GSI.

In Figure 56, it is highlighted the advantage of the proposed method, comparing to the classic GSI. The Ip models predicted with seismic attributes, particularly with structural seismic attributes, or combining structural and stratigraphic seismic attributes, are closer to the true reference model (Ip and facies). For the Ip models, the GSI with the multi-attribute RMS combined with first derivative or combined with variance, present the best results, followed by GSI with variance attribute, which presents similar results. However, regarding the facies model GSI with variance attribute has the best result, closely followed by the GSI with multi-attribute RMS combined with first derivative or variance attribute (Figure 56). It is also important to mention, that the variability within the ensemble of the predicted models is preserved, comparing the proposed approach to the classic GSI (Figure 51, Figure 52).

6.3.1.2 GSI-LA with seismic attributes

The proposed method was also tested in global stochastic seismic inversion with local anisotropies (GSI-LA), where the inversion procedure is constrained by a local spatial continuity pattern, helping improving the subsurface geological models. In addition, the intent was to evaluate the influence of integrating seismic attributes in this case. Thus, was tested the integration in the objective function of the variance seismic attribute and the RMS combined with first derivative. The results were compared to the classic GSI-LA. The iterative geostatistical seismic inversion procedure converged after six iterations for the three tests (Figure 57), where the global similarity *S* between the reference seismic reflection data and the predicted synthetic seismic, was 0.89 for classic GSI-LA, 0.91 for GSI-LA with variance seismic attribute and 0.92 for GSI-LA with RMS combined with first derivative (Figure 57).

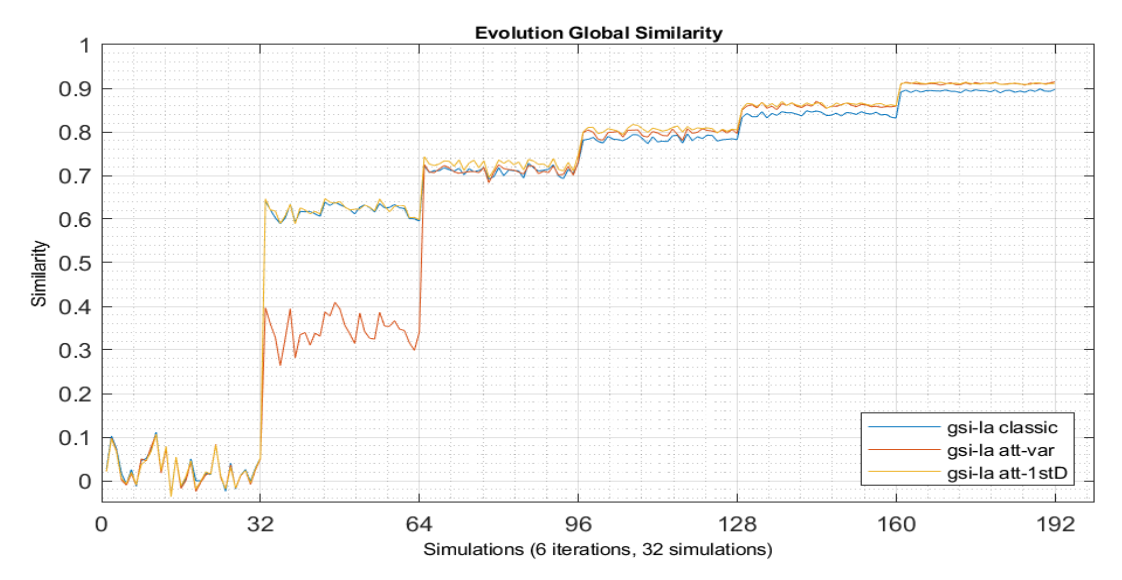


Figure 57 – Evolution of global similarity (S) over iterations in GSI-LA classic and GSI-LA with attributes. The global similarity (S) for: (blue) GSI-LA classic = 0.89; (orange) GSI-LA variance = 0.91; (yellow) GSI-LA RMS with 1st derivative = 0.92.

The projection in the MDS space of the predicted Ip and corresponding facies models, followed by the distance evaluation to the reference Ip and facies models respectively, is shown in Figure 58, where the predicted models from GSI with attributes is closer to the reference models.

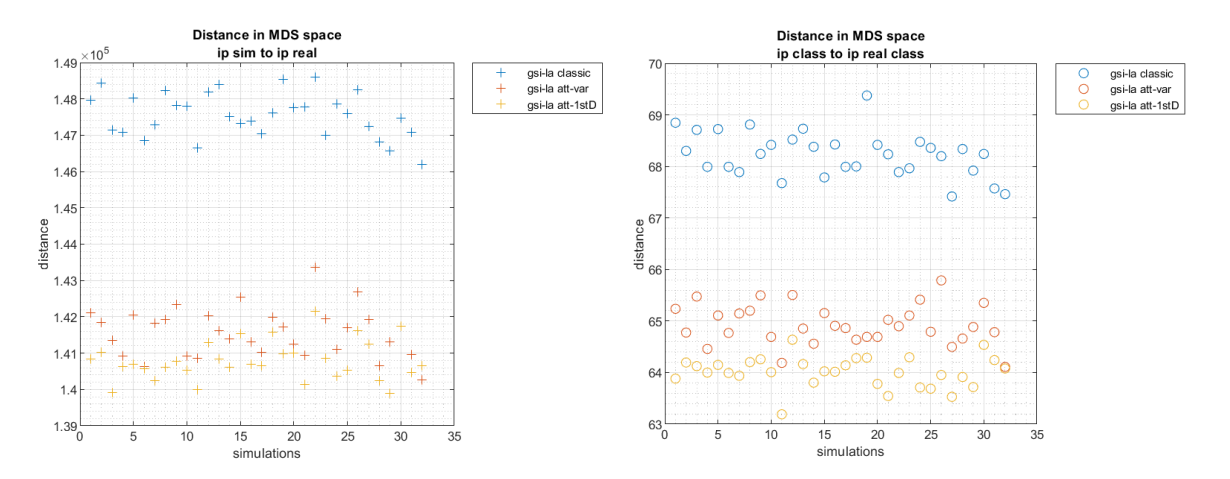


Figure 58 – Distance in MDS space for Ip and facies, between the true model and the retrieved models from last iteration for GSI-LA classic and GSI-LA with attributes.

The results for GSI-LA confirm the previously obtained for GSI. The integration of seismic attributes or multi-attributes in the objective function, to help evaluate the misfit between the predicted synthetic seismic and the observed seismic reflection data, during the geostatistical seismic inversion procedure, has a clear advantages over the classic approaches, improving predicting the subsurface geological models and the reproduction of the spatial continuity patterns and connectivity within the curvilinear channels. As is shown in the Ip mean models (Figure 59), computed from last iteration and in the corresponding synthetic seismic (Figure 60).

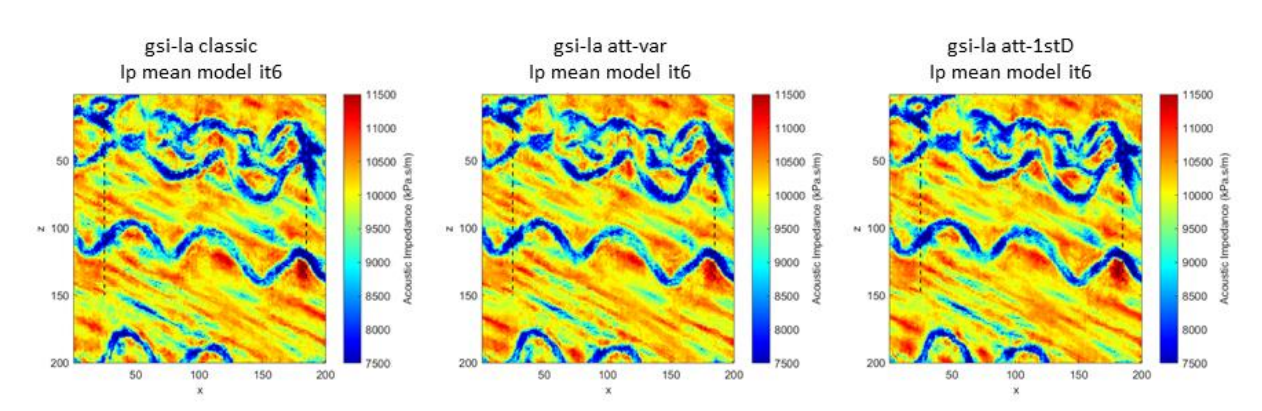


Figure 59 – Vertical section of Ip mean model of 6th iteration from GSI-LA classic and GSI-LA attributes.

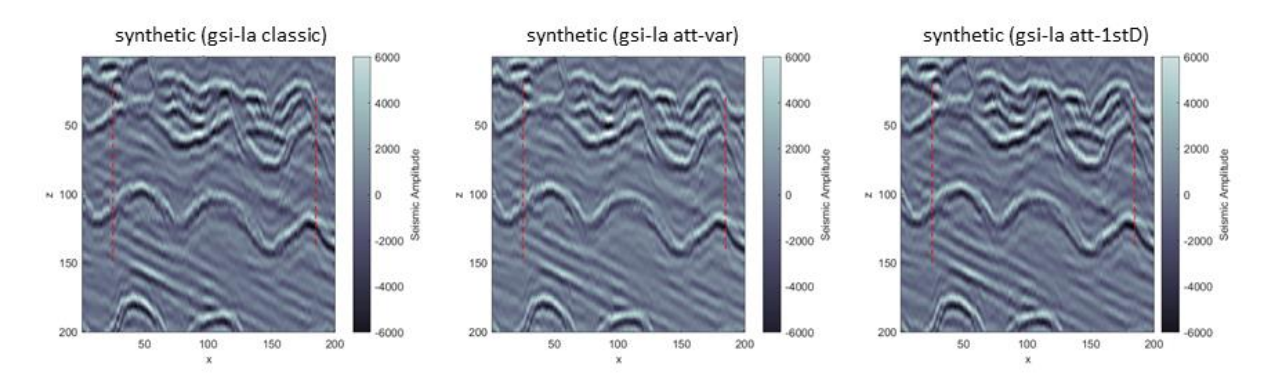


Figure 60 – Vertical section of synthetic seismic computed from the Ip mean model of 6th iteration from GSI-LA classic and GSI-LA attributes.

6.3.2. Real Case Application

The integration of seismic attributes in the objective function of the geostatistical seismic inversion procedure was tested in a real dataset, from a complex geological environment, characterized by the presence of sedimentary sequences and tectonic structures (e.g. faults), and which was previously introduced in Chapter 5. The dataset comprises a two-dimensional fullstack seismic reflection data (Figure 62), an Ip well-log (Figure 42b) and a 101 ms wavelet (Figure 42a). The inversion grid dimensions are 100 by 1 by 206 cells in i-, j- and k- directions. The well-log is located at the cell i = 74, with a length between cell k = 55 and cell k = 187. To run this real application example, the integration of seismic attributes in objective function was tested with the classic version of GSI-LA, aiming to improve the prediction of subsurface acoustic impedance models. The seismic attributes integrated in the objective function were the first derivative (1st D) and variance (var). The seismic inversion was performed with six iterations, each one with thirty-two realizations of elastic models (i.e. lp). In the last iteration (6th iteration), the global correlation between the synthetic seismic and the observed seismic data reaches 0.81 with the proposed method (Figure 61).

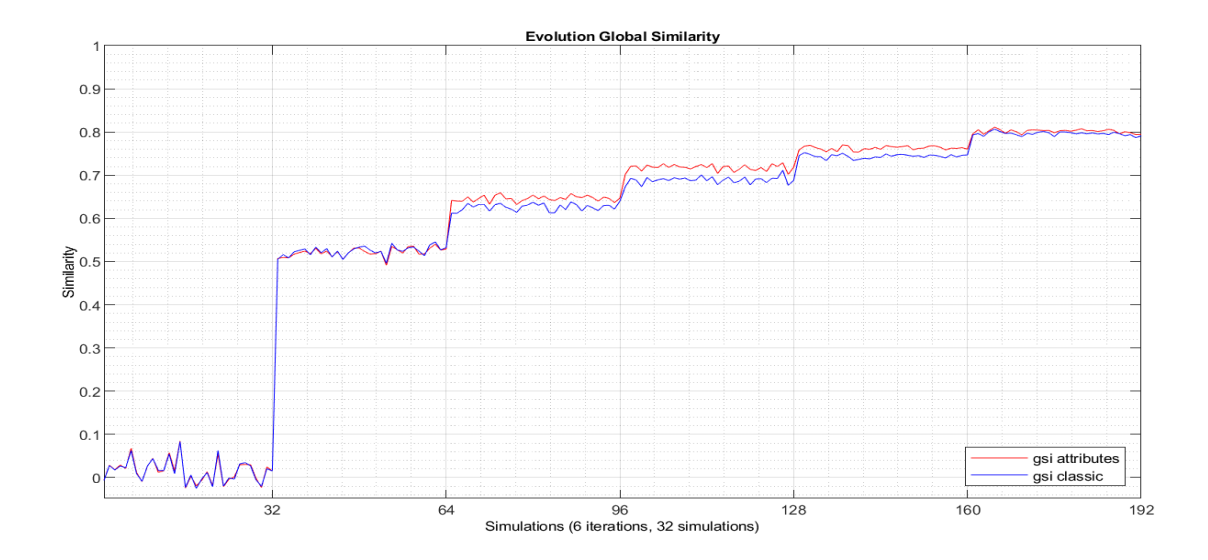


Figure 61 – Evolution of Global Similarity during the iterative seismic inversion.

The results from the inversion procedure are shown in Figure 62, were it is possible to see that the synthetic seismic computed from the Ip mean model, reproduce the main seismic patterns and main amplitude content. However, the residuals between the observed and the synthetic seismic, shows the areas were the proposed inversion procedure, struggle to converge and to reproduce the original spatial patterns (Figure 62).

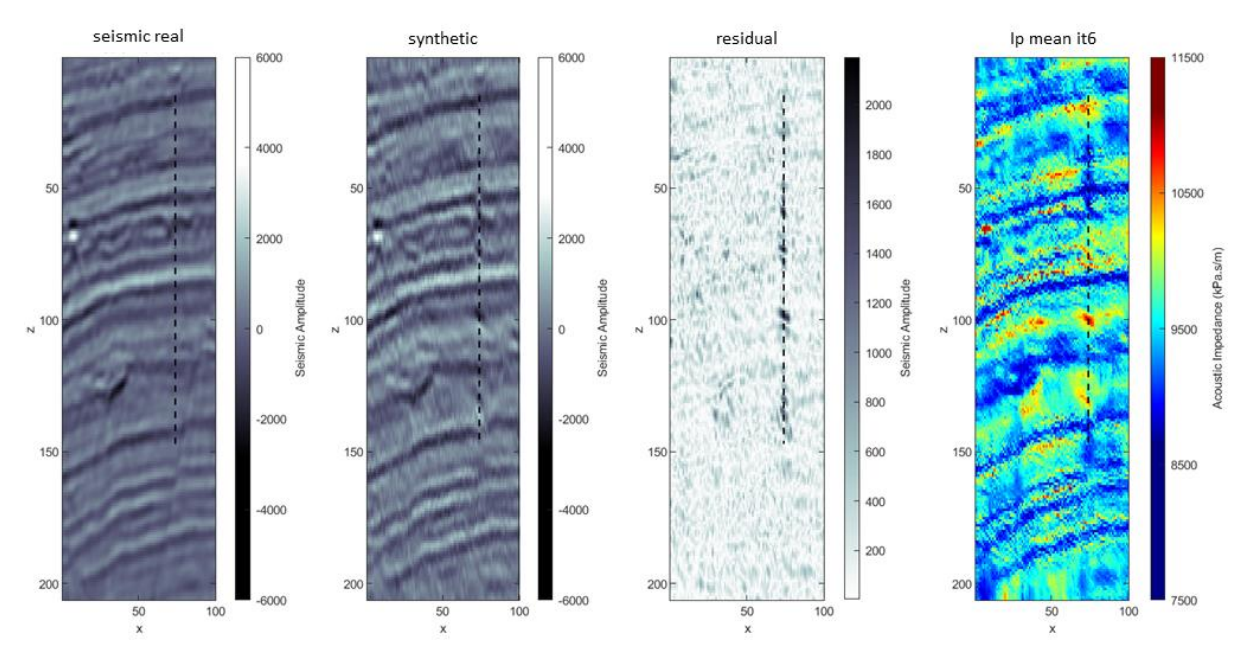


Figure 62 – (From left to right) Vertical section of the observed seismic reflection data, synthetic seismic, residuals and Ip mean model from the last iteration (6^{th} iteration).

Furthermore, the seismic attributes used in the objective function to improve the convergence of the proposed method, also reproduce the main geological patterns and the main seismic attribute content (Figure 63).

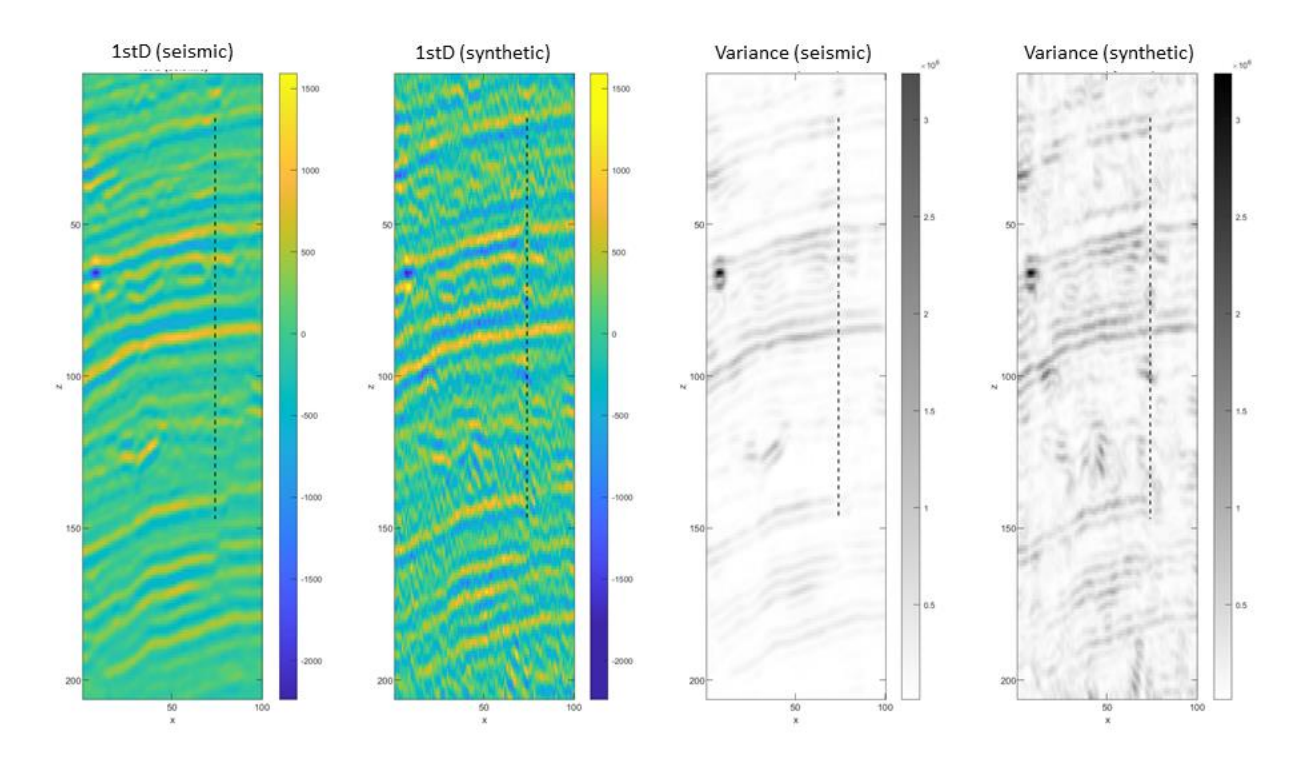


Figure 63 – [left] Vertical section of first derivative seismic attribute computed from observed seismic and synthetic seismic. [right] Vertical section of variance seismic attribute computed from observed seismic and synthetic seismic from last iteration (6th iteration).

6.4. Discussion

From the results of the synthetic example presented in Section 6.3.1, it is possible to see an improvement with the integration of seismic attributes into the objective function, of the seismic inversion procedure. Comparing to the classic approaches of GSI and GSI-LA, the integration of seismic attributes increases the global similarity in the iterative process (Figure 50, Figure 57). Nevertheless, although the global similarity, in some of the cases, is slightly lower than the highest one (Table 2), the use of multi-attributes brings the elastic models closer to the reference one, as shows the projection of the results in the MDS space (Figure 56, Figure 58). Namely, the combination of variance or first derivative with the RMS. In these cases the spatial continuity patterns are better reproduced, for instance in the curvilinear sand channels. It is important to mention, that the seismic attributes selection must be previously tested, considering the available data and the main goal.

The use of single seismic attributes, such as variance, which highlights discontinuities and edges, improved the elastic subsurface models. Moreover, combining stratigraphic and

structural seismic attributes shows to be a good option, since it may improve the reproduction of different seismic patterns. The weight assign to each seismic attribute, must be carefully considered, since it will have impact on the results. Same, for the number of neighboring points used to compute the seismic attributes.

The real case application shows promising results, since also increases the global similarity during the geostatistical seismic inversion, comparing to the classic approach (Figure 61). The real case application isn't noise free as the synthetic ones. This issue cannot be ignored, as it may have impact not only in the seismic inversion procedure, but also in the seismic attributes computation, which can lead to artefacts and uncertainty. Moreover, the uncertainty may also be associated with the predicted wavelet and poor well-tie, as it is possible to observe in the residuals (Figure 62) and from the non-reproduction of some amplitude and attribute content in the synthetic seismic (Figure 62, Figure 63). Nevertheless, from the presented application examples, the proposed method shows advantages over the classic approaches. Hence, the integration of seismic attributes or multi-attributes into the objective function, improved the global similarity between the synthetic and the observed seismic, helping to better reproduce the seismic patterns and consequently predict more reliable subsurface geological models.

6.5. Conclusion

The proposed methodology showed advantages on the integration of seismic attributes in the seismic inversion procedure for reservoir modelling and characterization. By comparing the match between the observed seismic and the synthetic seismic, and at the same time comparing the match between the associated seismic attributes, can improve the global Similarity. Furthermore, the resulting elastic subsurface models reproduce better the spatial continuity patterns of the subsurface rock properties. Therefore, the proposed geostatistical seismic inversion method integrating seismic attributes into de objective function, add more geological meaning and consistence to the subsurface geological models, helping reducing uncertainty.

7. Final remarks

This thesis proposes different methods, to improve the spatial continuity patterns of subsurface geological models and overcome the absence of well-log data, through the integration of geological information in geostatistical seismic inversion, for reservoir characterization and uncertainty assessment at early exploration stages.

To surpass the scarcity or absence of well-log data in frontier areas and at early exploration stages, in Chapter 4 was proposed and evaluated the integration of information from geological analogues and seismic interpretation to conditioning the geostatistical seismic inversion, for reservoir characterization and uncertainty assessment. The method was applied to a real case study, allowing predict subsurface rock property models and associated uncertainty. This is of great importance to quantify and reduce risk at early exploration stages. In Chapter 5, was presented the integration into geostatistical seismic inversion of the template matching technique, to infer and update local anisotropy patterns of surface geology. This methodology can be useful in complex geological environments and with scarcity of well-log data to improve subsurface geological models. Using template matching during the iterative process, allows inferring and self-update the local anisotropies, associated with geological spatial heterogeneous patterns (e.g. curvilinear channels), directly from seismic reflection data. By self-updating the local anisotropies, the proposed method, helps avoiding the propagation of errors associated to the local spatial continuity patterns. The prediction of spatial continuity patterns is very important for seismic reservoir characterization, to infer rock properties spatial distribution. In Chapter 6, was proposed the integration of seismic attributes and multi-attributes into the objective function of the geostatistical seismic inversion procedure. Where, the convergence of the iterative process is driven by a multi-objective function, based on the match in the seismic domain and in the seismic attribute domain. The use of stratigraphic and structural seismic attributes can be useful to improve the reproduction of seismic patterns, associated to sedimentary or tectonic structures, helping improving the subsurface geological models, particularly in complex geological environments.

As future work, it will be interesting to evaluate the integration of geological analogues combined with seismic attributes in geostatistical seismic inversion, for facies prediction at early exploration stages. Another possible future work is to explore other techniques to directly infer from seismic data the local anisotropies, to conditioning the geostatistical seismic inversion. Finally, it will be interesting as future work, to optimize the selection and combination of the seismic attributes, to be integrated into the objective function of the geostatistical seismic inversion procedure.

8. References

- Arpat G and Caers J (2007). Conditional simulation with patterns. Mathematical Geology, 39(2), 177–203.
- Aune E, Eidsvik J, Ursin B (2013) Three-dimensional non-stationary and non-linear isotropic AVA inversion. Geophysical Journal International 194(2): 787-803.
- Azevedo L, Nunes R, Correia P, Soares A, Guerreiro L, Neto GS (2014) Multidimensional scaling for the evaluation of a geostatistical seismic elastic inversion methodology. Geophysics 79:M1–M10.
- Azevedo L, Nunes R, Soares A, Mundin EC, Neto GS (2015) Integration of well data into geostatistical seismic amplitude variation with angle inversion for facies estimation. Geophysics 80(6):M113–M128.
- Azevedo L, Demyanov V and Soares A (2015). Integration of multi-scale uncertainty assessment into geostatistical seismic inversion: EAGE Petroleum Geostatistics Conference, Biarritz, France, 288-292.
- Azevedo L, Soares A (2017) Geostatistical methods for reservoir Geophysics. Springer, Berlin.
- Azevedo L, Nunes R, Soares A, Neto GS, Martins TS (2018) Geostatistical seismic Amplitude-versus-angle inversion. Geophysical Prospecting 66(S1):116–131
- Barnes A (2016) Handbook of Poststack Seismic Attributes. Geophysical References Series No. 21, Society of Exploration Geophysicists, Tulsa.
- Bongajum EL, Boisvert J, Sacchi MD (2013) Bayesian linearized seismic inversion with locally varying spatial anisotropy. Journal of Applied Geophysics 88: 31-41.
- Bortoli LJ, Alabert F, Haas A, Journel AG (1993) Constraining stochastic images to seismic data. In: Soares A (ed), Geostatistics Troia'92. Kluwer, Dordrecht, pp. 325–337.
- Bosch M, Mukerji T, González, EF (2010) Seismic inversion for reservoir properties combining statistical rock physics and geostatistics: a review. Geophysics 75(5):75A165–75A176.
- Boschetti F, Dentith MC, List RD (1996) Inversion of seismic refraction data using genetic algorithms. Geophysics 61:1715–1727.
- Brunelli R (2009) Template matching techniques in computer vision: Theory and practice. Wiley.
- Buland A, Omre H (2003) Bayesian linearized AVO inversion. Geophysics 68(1):185–198.

- Caeiro MH, Demyanov V, Soares A (2015) Optimized history matching with direct sequential image transforming for non-stationary reservoir. Math Geosci 47:975–994.
- Caers J (2001). Geostatistical reservoir modeling using statistical pattern recognition. Journal of Petroleum Science and Engineering, 29:177-188.
- Caers J (2005). Petroleum Geostatistics. Society of petroleum Engineers.
- Caers J & Zhang T (2004). Multi-Point Geostatistics: a quantitative vehicle for integrating geologic analogs into multiple reservoir models. Integration of outcrop and modern analogs in reservoir modeling: AAPG Memoir, 80, pp. 383-394.
- Caers J (2011). Modeling uncertainty in the Earth sciences. Wiley-Blackwell.
- Chilès JP, Desassis N (2018). Fifty Years of Kriging. In: Daya Sagar B, Cheng Q, Agterberg F (eds) Handbook of Mathematical Geosciences. Springer, Cham.
- Chopra S, Marfurt KJ (2005). Seismic attributes A historical perspective, Geophysics 70:3SO-28SO.
- Cox TF, Cox MAA (1994) Multidimensional scaling. Chapman & Hall, London
- Demyanov V, Arnold D (2018). Challenges and Solutions in Stochastic Reservoir Modelling Geostatistics, Machine Learning, Uncertainty Prediction. EAGE Publications bv.
- Deutsch CV, Journel AG (1992). GSLIB: Geostatistical Software Library and User's Guide. Oxford University Press, New York.
- Deutsch CV, Wang L (1996). Hierarchical Object-Based Stochastic Modeling of Fluvial Reservoirs. Mathematical Geology, 28(7):857-880.
- Deutsch CV (2002). Geostatistical Reservoir Modeling. University Press, Oxford.
- Dimitrakopoulos R, Mustapha H and Gloaguen E (2010). High-order statistics of spatial random fields: Exploring spatial cumulants for modeling complex non-Gaussian and non-linear phenomena. Mathematical Geosciences, 42:65–99.
- Doyen PM (2007). Seismic reservoir characterization. EAGE, Madrid.
- Drubule O (2003). Geostatistics for Seismic Data Integration in Earth Models. Society of Exploration Geophysicists, Tulsa.
- González, EF, Mukerji, T, Mavko, G (2008) Seismic inversion combining rock physics and multiple-point geostatistics. Geophysics, 73(1), R11–R21.
- Grammer GM, Harris PM and Eberli GP (2004). Integration of outcrop and modern analogues in reservoir modeling: AAPG Memoir 80: 1-22.

- Grana D, Della Rossa E (2010) Probabilistic petrophysical-properties estimation integrating statistical rock physics with seismic inversion. Geophysics 75(3):O21–O37.
- Grana D (2016) Bayesian linearized rock-physics inversion. Geophysics 81(6):D625–D641.
- Grana D, Fjeldstad T, Omre H (2017). Bayesian Gaussian mixture linear inversion for geophysical inverse problems. Math Geosci 49(4):493–515.
- Grijalba-Cuenca A, Torres-Verdin C (2000) Geostatistical inversion of 3D seismic data to extrapolate wireline petrophysical variables laterally away from the well. SPE 63283.
- Goovaerts P (1997). Geostatistics for natural resources evaluation. New York: Oxford University Press.
- Haas A, Dubrule O (1994) Geostatistical inversion—a sequential method of stochastic reservoir modeling constrained by seismic data. First Break 12:561–569.
- Holden L, Hauge R, Skare, Ø, Skorstad A (1998). Modeling of Fluvial Reservoirs with Object Models. Mathematical Geology 30:473–496.
- Horta A and Soares A (2010). Direct Sequential Co-simulation with Joint Probability Distributions. Math Geosci 42:269-292.
- Horta A, Caeiro M, Nunes R, Soares A (2010) Simulation of continuous variables at meander structures: application to contaminated sediments of a lagoon. In: Atkinson P, Lloyd C (eds.) GeoENV VII – Geostatistics for Environmental Applications. Springer, London, pp. 161–172.
- Howell JA, Martinius AW and Good TR (2014). The application of outcrop analogues in geological modelling: a review, present status and future outlook, in Martinius AW, Howell JA and Good TR, eds., Sediment-Body Geometry and Heterogeneity: Analogue Studies for Modelling the Subsurface: Geological Society, London, Special Publications, 387.
- Ferreirinha T, Nunes R, Azevedo L, Soares A, Pratas F, Tomás P, Roma N (2015) Acceleration of stochastic seismic inversion in OpenCL-based heterogeneous platforms. Computers & Geosciences (78):26–36.
- Filippova K, Kozhenkov A, Alabushin A (2011) Seismic inversion techniques: Choice and benefits. First Break 29:103–114.
- Francis AM (2006) Understanding stochastic inversion: Part 1. First Break 24:79–84.
- Lopes F, Cunha PP and Le Gall B (2006). Cenozoic seismic stratigraphy and tectonic evolution of the Algarve margin (offshore Portugal, southwest Iberian Peninsula). Marine Geology 231:1–36.

- Luis A, Almeida J (1997). Stochastic characterization of fluvial sand channels. In E. Baafi & N. Schofield (Edits.), Geostatistics Wollongong'96 (pp. 77-488). Netherlands: Kluwer Academic Publ.
- Ma X-Q (2002) Simultaneous inversion of prestack seismic data for rock properties using simulated annealing. Geophysics 67(6):1877–1885.
- Madsen RB, Hansen TM, Omre H (2020) Estimation of a non-stationary prior covariance from seismic data. Geophysical Prospecting 68(2): 393-410.
- Mallick S (1995) Model-based inversion of amplitude-variations-with-offset data using a genetic algorithm. Geophysics 60(4):939–954.
- Mallick S (1999). Some practical aspects of prestack waveform inversion using a genetic algorithm: An example from the east Texas Woodbine gas sand. Geophysics 64(2):326–336.
- Matheron G (1960). Krigeage d'un panneau rectangulaire par sa périphérie, Note géostatistique no 28, Centre de Géostatistique, Fontainebleau, France.
- Matias H (2007). Hydrocarbon potential of the offshore Algarve Basin: PhD Thesis, Faculdade de Ciências da Universidade Nova de Lisboa, pp 1–324.
- Matias H, Kress P, Terrinha P, Mohriak W, Menezes P, Matias L, Santos F and Sandnes F (2011) Salt tectonics in the western Gulf of Cadiz, southwest Iberia. AAPG Bull 95(10):1667–1698.
- Mariethoz G, Renard P and Straubhaar J (2010). The direct sampling method to perform multiple-point geostatistical simulations. Water Resources Research, 46(11):1–14.
- Martinius AW, Howell JA and. Good TR (2014). Sediment-Body Geometry and Heterogeneity: Analogue Studies for Modelling the Subsurface: Geological Society, London, Special Publications 387.
- Mavko G, Mukerji T and Dvorkin J (2009). The Rock Physics Handbook, Second Edition, Tools for Seismic Analysis of Porous Media, Cambridge University Press.
- Nunes R, and Almeida JA (2010). Parallelization of sequential gaussian, indicator and direct simulation algorithms: Computers & Geosciences 36:1042–105.
- Nunes R, Soares A, Neto GS, Dillon L, Guerreiro L, Caetano H, Maciel C, Leon F (2012) Geostatistical inversion of prestack seismic data. In: Ninth International Geostatistics Congress. Oslo, Norway, pp. 1–8.

- Nunes R, Soares A, Azevedo L and Pereira P (2017). Geostatistical Seismic Inversion with Direct Sequential Simulation and Co-simulation with Multi-local Distribution Functions: Mathematical Geosciences 49(5): 583-601.
- Nunes R, Azevedo L, Soares A (2019) Fast geostatistical seismic inversion coupling machine learning and Fourier decomposition. Computational Geosciences (23):1161–1172.
- Pereira P, Bordignon F, Azevedo L, Nunes R, Soares, A (2019) Strategies for integrating uncertainty in iterative geostatistical seismic inversion. Geophysics 84(2):R207–R219
- Pereira P, Calçôa I, Azevedo L, Nunes R, Soares A (2020) Iterative geostatistical seismic inversion incorporating local anisotropies. Computational Geosciences 24:1589–1604.
- Pringle JK, Howell JA, Hodgetts D, Westerman AR, Hodgson DM (2006) Virtual outcrop models of petroleum reservoir analogues: a review of the current state-of-the-art. First Break 24:33–44.
- Ramos A, Fernández O, Terrinha and Muñoz JA (2016). Extension and inversion structures in the Tethys–Atlantic linkage zone, Algarve Basin, Portugal. International Journal of Earth Sciences 105:1663–1679.
- Roque C. (2007). Tectonostratigrafia do Cenozóico das margens continentais sul e sudoeste portuguesas: Um modelo de correlação sismostratigráfica: Ph.D. thesis, Universidade de Lisboa, Faculdade de Ciências, Departamento de Geologia, Lisboa, 310 p.
- Russell B, Hampson D (1991) Comparison of poststack seismic inversion methods. In: 61st Annual International Meeting, SEG, Expanded Abstracts, pp. 876–878.
- Sambridge M (1999) Geophysical inversion with a neighborhood algorithm—I. Searching a parameter space. Geophys J Inte 138(2):479–494.
- Scheidt C, Caers J (2009) Representing spatial uncertainty using distances and kernels: Math Geosci 41:397–419.
- Sen MK, Stoffa PL (1991) Nonlinear one dimensional seismic waveform inversion using simulated annealing. Geophysics 56(10):1624–1638.
- Simm R, Bacon M. (2014). Seismic Amplitude: An Interpreter's Handbook. Cambridge University Press; 2014.
- Skorstad A, Hauge R, Holden L (1999). Well Conditioning in a Fluvial Reservoir Model. Mathematical Geology 31:857–872.
- Soares A (1990). Geostatistical Estimation of Orebody Geometry: Morphology Kriging. Journal Mathematical Geology, 22(7):787-802.

- Soares A (2001) Direct sequential simulation and cosimulation. Math Geol 33(8):911–926.
- Soares A, Diet JD, Guerreiro L (2007) Stochastic inversion with a global perturbation method. Petroleum Geostatistics. EAGE, Amsterdam, pp 10–14.
- Strebelle, S (2002). Conditional simulation of complex geological structures using multiple-point statistics. Mathematical Geology, 34(1):1–21.
- Strebelle, S and Zhang, T (2005). Non-stationary multiple-point geostatistical models. In O Leuangthong and CV Deutsch (Eds.), Geostatistics Banff 2004. Springer, Dordrecht, The Netherlands.
- Taner, M. (2001) Seismic Attributes. CSEG Recorder, 26(7):49-56.
- Tarantola A (2005) Inverse Problem Theory and Methods for Model Parameter Estimation, Society for Industrial and Applied Mathematics.
- Terrinha P, Ribeiro C, Kullberg JC, Rocha R and Ribeiro A (2002). Compression episodes during rifting and faunal isolation in the Algarve Basin, southwest Iberia. Journal of Geology110:101–113.
- Terrinha P, Rocha R, Rey J, Cachão M, Moura D, Roque C, Martins L, Valadares V, Cabral J, Azevedo MR, Barbero L, Clavijo E, Dias RP, Gafeira J, Matias H, Matias L, Madeira J, Marques da Silva C, Munhá J, Rebelo L, Ribeiro C, Vicente J and Youbi N (2006). A Bacia do Algarve: Estratigrafia, Paleogeografia e Tectónica. In Geologia de Portugal no contexto da Ibéria (Dias R, Araújo A, Terrinha P and Kullberg JC, Eds.). Univ. Évora, pp. 247-316.
- Tompkins MJ, Fernández Martínez JL, Alumbaugh DL, Mukerji T. (2011) Scalable uncertainty estimation for nonlinear inverse problems using parameter reduction, constraint mapping, and geometric sampling: Marine controlled-source. Geophysics, 76(4):263–281.
- Xu W (1996). Conditional Curvilinear Stochastic Simulation Using Pixel-Based Algorithms. Journal of Mathematical Geology, 28(7):937-949.